UNIVERSITY OF CALIFORNIA, SAN DIEGO

Small Molecule Control of HMG-CoA Reductase Degradation: The Dark Side of Allostery

A dissertation submitted in partial satisfaction of the requirements for the degree Doctor of Philosophy

in

Biology

by

Margaret A. Wangeline

Committee in charge:

Professor Randolph Y. Hampton, Chair
Professor Eric Bennett
Professor Partho Ghosh
Professor Gentry Patrick
Professor Lorraine Pillus

2017

The Dissertation of Margaret A. Wangeline is approved, and is acceptable in quality and form for publication on microfilm and electronically:

Chair

University of California, San Diego

2017

TABLE OF CONTENTS

Signature Page iii
Table of Contents iv
List of Figures vi
List of Tables viii
Acknowledgements ix
Vita xi
Abstract of the Dissertation xii

Chapter One: Proteostasis, protein quality control, and their intersection with the regulation of sterol biology 1
- Abstract 2
- Introduction 2
- Background 4
- Global regulation of sterol-related protein expression by the SREBP pathway. 9
- The sterol sensing domain, Insig, and lipid signals: The central dogma of sterol regulation 11
- Regulation of HMG-CoA Reducatase: ERADication of excess activity 15
- Regulated degradation of HMG-CoA Reductase in Saccharomyces Cerevisiae: Hrd behavior 19
- The necessary and autonomous sterol sensing domain 23
- A tale of two signals: The logic of Hmg2 regulation 24
- GGPP and ligand-regulated misfolding: The dark side of allostery 27
- Generalizing sterol sensing domain autonomy: Sterol-regulated SCAP in *Scizzosaccharomyces pombe* 30
- Viewing sterol-sensing domain function through proteostasis-tinted glasses .. 32
- MARCHing to the beat of a different ligase: sterol-regulated endoplasmic reticulum associated degradation of Squalene Monooxygenase 37
- Smith-Lemli-Opitz Syndrome 38
- Niemann-Pick Disease 39
- Final thoughts 42
- Acknowledgements 42

Chapter Two: Ligand-regulated entry into the Hrd ERAD pathway reveals the dark side of allostery 44
- Abstract 45
- Introduction 46
- Results 49
  - Specificity and potency of isoprenoids that trigger Hmg2 degradation in vivo 49
  - In vitro analysis of GGPP action on Hmg2 55
  - Antagonism of GGPP in vitro and in vivo 65
  - Testing GGPP as a ligand that promotes regulated misfolding 74

Discussion 85
Experimental Procedures 92
Reagents 92
Yeast strains and plasmids 93
Flow cytometry 93
Microsome preparation 94
Limited proteolysis 94
Thermal denaturation 95
Microsome preparation for co-immunoprecipitation 95
Co-immunoprecipitation 96
Acknowledgements 99

Chapter Three: The SSD: A Structure Shifting Domain required for ligand-mediated misfolding 100
Abstract 101
Introduction 102
Results 105
The SSD is required for Hmg2 regulated misfolding 105
Insig independence 106
Separate determinants for folding and degradation 114
Analysis of other regions of the transmembrane domain 116
Toxic subunits 139
The autonomous SSD 140
Discussion 149
Experimental Procedures 159
Reagents 159
Yeast strains and plasmids 161
Flow cytometry 161
Microsome preparation 162
Limited proteolysis 162
Thermal denaturation 163
Microsome preparation for co-immunoprecipitation 163
Co-immunoprecipitation 164
Acknowledgements 167

Chapter Four: Conclusions and future directions 168
Regulated misfolding of Hmg2: The story so far 169
Separation of binding and responding to ligands 171
This work as a platform for future studies 174
Ligand-mediated degradation in other systems 175

References 178

LIST OF FIGURES

Figure 1.1. The sterol or mevalonate pathway 8
Figure 1.2. Eukaryotic tactics of sterol pathway regulation 14
Figure 1.3. Geranylgeranyl pyrophosphate (GGPP)-mediated misfolding of Hmg2 ... 26
Figure 1.4. Mallostery, or a reversible, ligand-mediated misfolding model 33
Figure 2.1. The mevalonate pathway 50
Figure 2.2. Schematic of Hmg2-GFP 52
Figure 2.3. Selected structures of isoprenoids used in this study 53
Figure 2.4. Effects of GGPP and related molecules on Hmg2-GFP in vivo 54
Figure 2.5. Schematic of luminal myc Hmg2-GFP 56
Figure 2.6. Effect of GGPP on limited proteolysis assay 58
Figure 2.7. In vitro dose response of GGPP 60
Figure 2.7. In vitro dose response of other isoprenoids 62
Figure 2.9. Dose response curve of GGPP and other isoprenoids 63
Figure 2.10. Reversibility of GGPP treatment 64
Figure 2.11. Hmg2 responds to repeated GGPP treatment after reversal 64
Figure 2.12. Structurally similar analogs of GGPP 66
Figure 2.13. In vitro dose response of two inactive analogs of GGPP 67
Figure 2.14. Test of antagonism by structurally similar analogs of GGPP 68
Figure 2.15. In vivo antagonism by a structurally similar analog 69
Figure 2.16. The sensitized, rapidly degrading TDH3-Bts1 strain 70
Figure 2.17. In vivo antagonism by a structurally similar analog in the sensitized Bts1 strain 71
Figure 2.18. Glycerol stabilizes Hmg2-GFP in vivo 75
Figure 2.19. Glycerol reverses GGPP action in vivo and in vitro 76
Figure 2.20. Other chemical chaperons stabilize Hmg2-GFP in vivo 77
Figure 2.21. Other chemical chaperones reverse GGPP action in vitro 78
Figure 2.22. Effect of isoprenoids on thermal denaturation of Hmg2-GFP 80
Figure 2.23. Hmg2 forms multimers in vivo 83
Figure 2.24. GGPP does not affect multimerization state of Hmg2 84
Figure 3.1. Schematic of the SSD 107
Figure 3.2. SSD sequence alignment 108
Figure 3.3. The SSD mutation S215A stabilizes Hmg2 109
Figure 3.4. The SSD mutation S215A renders Hmg2 insensitive to isoprenoids 110
Figure 3.5. Sample limited proteolytic assay for structure of 1myc-Hmg2-GFP 111
Figure 3.6. The SSD mutation S215A blocks in vitro misfolding of Hmg2 112
Figure 3.7. The L219F mutation blocks in vitro misfolding of Hmg2 113
Figure 3.8. Insig deletion does not interfere with isoprenoid-induced misfolding of Hmg2 115
Figure 3.9. The K357R mutation, but not the K6R mutation, blocks in vitro misfolding of Hmg2 118
Figure 3.10. The S215A mutation is epistatic to K6R for misfolding in cis 119
Figure 3.11. Steady state level comparisons of other mutations made in this study .. 120

Figure 3.12. Comparison of response to GGPP by other mutations made in this study121
Figure 3.13. Comparison of response to GGPP and lovastatin by other mutations made in this study..... 122
Figure 3.14. N401A mutation behaves like an SSD mutation in vitro and blocks misfolding..... 123
Figure 3.15. Alignment of Hmg2 with the GGPP-binding proteins Ram2 and Bet2. 125
Figure 3.16. Schematic of Hmg2 with Loop 1 location 126
Figure 3.17. Schematic of loop 1 overexpression constructs 128
Figure 3.18. Co-expression of TM1-Loop1 and TM1-Loop1-TM2 but not Loop1-only blunts GGPP regulation..... 129
Figure 3.19. Co-expression of TM1-Loop1 does not affect NR1 TFYSA Hmg2-GFP84
Figure 3.20. Loop 1 constructs are expressed at low levels and degraded..... 131
Figure 3.21. Cycloheximide chases with GGPP and lovastatin on WT and S215A Hmg2-GFP for comparison 133
Figure 3.22. Cycloheximide chases with GGPP and lovastatin on RYL and epistasis mutations 134
Figure 3.23. Cycloheximide chases with GGPP and lovastatin on KRR and epistasis mutations 135
Figure 3.24. The RYL mutation causes constitutive misfolding in vitro 136
Figure 3.25. The KRR mutation but not K153A alone causes constitutive misfolding in vitro 137
Figure 3.26. D165A is stable and does not respond to GGPP in vivo 138
Figure 3.27. Mutated SSDs act as toxic subunits for Hmg2 degradation..... 141
Figure 3.28. Mutated SSDs act as toxic subunits for Hmg2 misfolding 142
Figure 3.29. Hmg2 proteolytic pattern and misfolding are preserved in some weak detergents..... 144
Figure 3.30. GGPP does not affect the non-responding TFYSA Hmg2 in digitonin. 145
Figure 3.31. GGPP enhances Hmg2 solubility in digitonin 146
Figure 3.32. GGPP solubility enhancement is specific for active isoprenoid and the intact SSD..... 150
Figure 3.33. S215A Hmg2 undergoes regulated misfolding after overnight treatment with GGPP..... 151
Figure 3.34. S215A misfolding is specific for active isoprenoid 152
Figure 3.35. S215A misfolding is dose dependent..... 153
Figure 3.36. Time course of S215A misfolding..... 154

LIST OF TABLES

Table 2.1. Yeast strains used in chapter 2 97
Table 2.2 Plasmids used in chapter 2 98
Table 3.1. Hmg2 mutations examined chapter 3 117
Table 3.2 Yeast strains used in chapter 3 165
Table 3.3 Plasmids used in chapter 3 166

ACKNOWLEDGEMENTS

Chapter One, in part, is a reprint of material accepted for publication, which will appear in: Wangeline, M.A., Vashistha, N. and Hampton R.Y. "Proteostatic Tactics in the Strategy of Sterol Regulation," Annual Review of Cell and Developmental Biology, Vol 33, 2017. I was the principal author of this paper.

Chapter Two, in full, is currently in preparation for submission for publication as: Wangeline, MA and Hampton, RY, "Ligand-regulated entry into the HRD ERAD pathway reveals the dark side of allostery." I was the principal researcher/author of this work.

Chapter Three, in part, is currently in preparation for submission for publication of the material as: Wangeline, MA and Hampton, RY, "The SSD: A Structure Shifting Domain required for ligand-mediated misfolding." I was the principal researcher/author of this work.

I want to thank Randy for being a fantastic mentor. I really appreciate all the scientific guidance, career advice, teaching advice, and writing help (and books!).

I want to thank the whole Hampton lab—Matt Flagg and Sonya Neal especially—for all of their help, ideas, support, friendship, and fun over the years. I especially want to thank former lab members Chandra Theesfeld and Nidhi Vashistha for helping me get started in the lab and being great friends (and Chandra for teaching me so much about yeast genetics). I also want to thank Amanjot Singh for being incredibly patient, helping me with cloning, and knowing everything about

chaperones, Xin Tang for making the lab a great place to be, and Alex Shearer for his troubleshooting help.

Last but not least, thank you so much to my friends and family, especially my parents and my brother, Cory, for their love and support.

VITA

EDUCATION:

University of California, San Diego, La Jolla, CA
Ph.D. in Biology. December 2017.

Massachusetts Institute of Technology, Cambridge, MA
B.S. in Biology and Chemical Engineering. June 2010.

ABSTRACT OF THE DISSERTATION

Small Molecule Control of HMG-CoA Reductase Degradation: The Dark Side of Allostery

by

Margaret A. Wangeline

Doctor of Philosophy in Biology

University of California, San Diego 2017

Professor Randolph Y. Hampton, Chair

Protein quality control is an essential set of processes which allow cells to detect and mange misfolded proteins. Deficits in protein quality control increase with aging and are associated with disease, from inborn disorders to neurodegeneration and

cancer. One arm of quality control is endoplasmic reticulum (ER) associated degradation (ERAD) a pathway which identifies and ubiquitinates ER and secretory pathway proteins. The conserved E3 ligase Hrd1 catalyzes the ubiquitination of a variety of misfolded substrates, but was discovered for the regulated degradation of HMG-CoA reductase, a critical sterol pathway enzyme, in yeast. The yeast isozyme Hmg2 is degraded when flux through the sterol pathway is high and stabilized when levels of pathway molecules fall. Work in our laboratory found that under degradation conditions, Hmg2 takes on some of the features of a misfolded protein, including becoming more susceptible to proteolysis in vitro. Because of the clinical importance of sterols and protein quality control in general, and because of questions about how quality control pathways distinguish misfolded proteins from the structural diversity in the cell, we are interested in learning more about how Hmg2 transitions between its normal and misfolded states. In this work, we found that the isoprenoid GGPP causes direct, reversible misfolding of Hmg2. This action is potent, specific for GGPP's structure, and antagonizable with a similar molecule. In response to GGPP, Hmg2 takes on the features of a misfolded protein. Its structure becomes more accessible to proteases and detergents, it is degraded by ERAD, and these effects are reversible by treatment with chemical chaperones. Hmg2 is a multimer, and its multimerization is unchanged by GGPP treatment. These actions require the sterol sensing domain (SSD), a domain found in many human disease proteins. SSD mutations prevent Hmg2 misfolding in cis and even in wild type Hmg2 in trans. Taking these findings together, we liken Hmg2 misfolding to allostery, with an output of misfolding.

CHAPTER ONE:

Proteostasis, protein quality control, and their intersection with the regulation of sterol biology

Abstract

In eukaryotes, the synthesis and uptake of sterols undergo stringent multivalent regulation. Both individual enzymes and transcriptional networks are controlled to meet changing needs of the many sterol pathway products. Regulation is tailored by evolution to match regulatory constraints, which can be very different in distinct species. Nevertheless, a broadly conserved feature of many aspects of sterol regulation is employment of proteostasis mechanisms to bring about control of individual proteins. Proteostasis is the set of processes that maintain homeostasis of a dynamic proteome. Proteostasis includes protein quality control pathways for the detection, and then the correction or destruction, of the many misfolded proteins that arise as an unavoidable feature of protein-based life. Protein quality control displays not only the remarkable breadth needed to manage the wide variety of client molecules, but also extreme specificity toward the misfolded variants of a given protein. These features are amenable to evolutionary usurpation as a means to regulate proteins, and this approach has been used in sterol regulation. We describe both well-trod and less familiar versions of the interface between proteostasis and sterol regulation and suggest some underlying ideas with broad biological and clinical applicability.

Introduction

Proteostasis is the set of processes that maintain homeostasis of a dynamic proteome. Proteostasis includes protein maturation and trafficking pathways for the delivery of proteins to the correct cellular compartments and protein quality control

pathways for the detection—and then the correction or destruction—of the many misfolded proteins that arise as an unavoidable feature of protein-based life. Protein quality control displays not only the remarkable breadth needed to manage the wide variety of client molecules, but also extreme specificity toward the misfolded variants of a given protein.

The features of astonishing breadth and specificity make proteostasis pathways amenable to evolutionary hijacking or usurpation for the regulation of specific processes within the cell. This approach has been used extensively to regulate sterol biology in a variety of different organisms.

In eukaryotes, the synthesis and uptake of sterols undergo stringent multivalent regulation. Both individual enzymes and transcriptional networks are controlled to meet changing needs of the many sterol pathway products. Regulation is tailored by evolution to match regulatory constraints, which can be very different in distinct species. Nevertheless, a broadly conserved feature of many aspects of sterol regulation is employment of proteostasis mechanisms to bring about control of individual proteins.

The continuous requirement for sterols and related molecules, either produced by the sterol-synthesizing mevalonate pathway or taken up from the extracellular world, raises a biochemical double-edged sword. The sterol synthetic pathway is metabolically costly, and later stages are heavily oxygen dependent. Furthermore, pathway intermediates can cause toxicity in a variety of biophysical and pharmacological ways. Sterols and related molecules also act as ligands in signaling

and development. As a result, concentrations of sterol pathway molecules must be tightly regulated in space and time. Regulation involves simultaneous control of synthesis, uptake, and cellular efflux of a variety of molecules that are all made by this highly branched metabolic pathway.

A surprising number of sterol regulatory mechanisms pertain to protein quality control. Proteostasis pathways have been around since the dawn of proteins, and evolution has apparently capitalized on the specificity and alacrity of these mechanisms in many facets of sterol regulation. This introduction will describe both long-known and newly-discovered points of interest at the interface of proteostasis and ssterol biology. It will also point out long-standing questions in the field and underlying themes that have broad biological and clinical applicability. This introduction will not be comprehensive, but fortunately many current examples exist (Brown & Goldstein 2008, Jiang & Song 2014, Jo & DeBose-Boyd 2010, Raychaudhuri et al. 2012, Sharpe et al. 2014, Ye & DeBose-Boyd 2011, Zhang et al. 2012). This introduction tells a particular set of stories about using protein quality control to regulate metabolism to provide a new framework for thinking about the intersection of these two indispensable sets of pathways.

Background

The sterol pathway produces a dazzling variety of lipid molecules (Figure 1). The breadth of products includes not only cholesterol and other sterols, but also a massive collection of isoprenoids (based on the 2-methyl butyl carbon skeleton) and

derivatives used in all walks of organismal life. This highly branched sequence of reactions—also termed the mevalonate pathway—includes essential molecules in nearly every cellular process. Approximations for the number of distinct natural isoprenoids top 30,000 (Lange et al. 2000). Accordingly, in a sense the sterol/mevalonate pathway can be viewed as a Darwinian combinatoric library. Regulation of sterol synthesis occurs at several levels, including coordinated feedback regulation of multiple gene groups. In addition, several key enzymes are controlled. The prevailing theme in all these layers is modification of protein levels rather than activity per se, through the use of protein synthesis, trafficking, quality control, and degradation.

Sterol synthesis in eukaryotes occurs by the conversion of acetate in the greater-than-30-step mevalonate pathway (Figure 1). The pathway proceeds by sequential addition of 2-carbon acetate groups from acetyl-CoA to produce 3-hydroxy-3-methyl-glutaryl-CoA (HMG-CoA). The reduction of HMG-CoA to mevalonic acid by HMG-CoA reductase (HMGR) is considered a rate-controlling step in many circumstances (Geelen et al. 1986). Mevalonate then undergoes phosphorylation and loss of CO_2 to produce isopentanoid building blocks, which are used to assemble the remarkable variety of molecules seen in the biosphere. The sterol pathway condenses these first molecules into the 15-carbon farnesyl pyrophosphate and then the 30-carbon squalene, which is then oxidized and rearranged to produce the first sterol shape, lanosterol. Next, a variety of reactions produce the main sterol of a given organism (mammals: cholesterol; yeast: ergosterol, plants: phytosterol) used to create

both biologically amenable membranes and a variety of high-potency sterol-based mediators and hormones (Bloch 1965). Numerous enzymes of the mainstream sterol pathway show highly conserved regulation. They are introduced as the examples relevant to our story arise below, along with the pertinent sterol-regulatory proteins. A motif parts list emerges that will be useful to frame our destructive and "misfolded" view of sterol regulation.

Mammalian sterol uptake is a whole-organism affair that starts with dietary sterols and ends with cellular uptake and distribution of sterols and other lipids. Sterols are given safe and soluble passage through the bloodstream as passengers in a variety of lipoprotein particles.

The most famous and best-studied example is the receptor-mediated uptake of plasma low-density lipoprotein (LDL) by the LDL receptor (LDLR). More recent additions to the uptake story include elucidation of the Niemann-Pick cholesterol intracellular transport proteins (Infante et al. 2008a, Ohgami et al. 2004, Vanier 2015) and the intestinal transport factor NPC1L1 (Niemann-Pick type C like), which allows for movement of dietary sterol molecules from the digestive tract to the intestinal cells that package them into chylomicrons (Abumrad & Davidson 2012, Altmann et al. 2004, Davies et al. 2000, Hussain 2014, Wang & Song 2012). Finally, sterol removal and excretion are parts of the entire balance. It is now clear that LDLRs mediate an important component of sterol removal due to catabolism and excretion after uptake (Favari et al. 2015, Jakulj et al. 2016). Furthermore, the reactions that break down sterols to foster their exit as bile acids, as well as the machinery for reuptake of bile

acids from the gut, constitute another regulated component of sterol flux through mammals.

This chapter connects a number of sterol regulatory mechanisms to the seemingly separate field of proteostasis. Proteostasis includes the production, folding, delivery, and destruction of proteins and occurs constantly in all cells. A critical branch of proteostasis involves management of misfolded proteins. The folded integrity of the proteome is under constant challenge by the conditions of life. It has been eloquently noted that the typical cell operates in almost diametric opposition to the best practices of a biochemist (Goldberg 2003). A good biochemist keeps proteins isolated, at approximately 1 mg/ml concentrations, in the cold and away from reactive chemicals. A good cell keeps its proteins in complex mixtures; at approximately 200--300 mg/ml concentrations; often at 37°C; and in the presence of oxygen, reactive oxygen species, light of many wavelengths, and numerous reactive metabolic intermediates. So protein-based life is a compromise between the good kinetics of action and the unfortunate kinetics of misfolding. The ongoing struggle to maintain a functional, folded proteome requires a network of corrective processes collectively termed protein quality control. Protein quality control is a beautiful example of

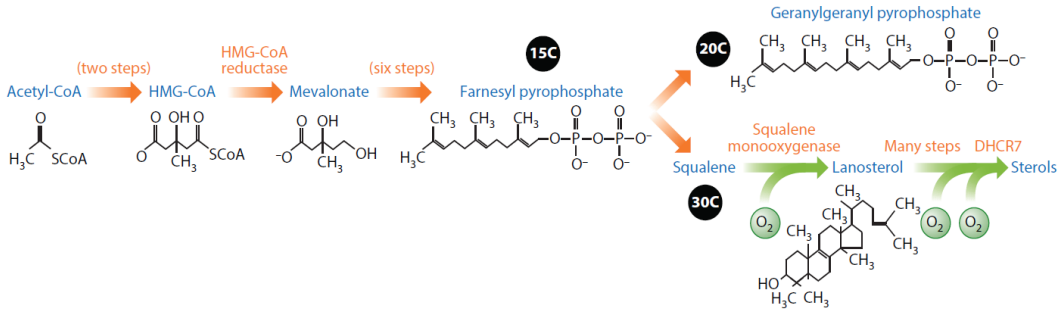

Figure 1.1. The sterol or mevalonate pathway
Only the salient features of this widely conserved and essential biosynthetic pathway are shown. The carbon number for some intermediates is shown in black circles (because carbon is black). Brown arrows indicate the early, oxygen-independent section of the pathway. Green arrows indicate the later, sterol-synthesizing, oxygen-dependent section of the pathway.

evolution's ability to adapt cellular specificity—in this case the high selectivity that protein quality control pathways display for misfolded versions of their normally folded clients—to effect regulation.

Global regulation of sterol-related protein expression by the SREBP pathway

Study of the molecular mechanisms of sterol regulation has a rich history. A key turning point came with a focus on the cellular mechanisms of LDL more than 40 years ago by the Brown and Goldstein group (Brown & Goldstein 1974, Goldstein & Brown 1973, Schneider et al. 1982). These researchers' discovery of, and studies on, the LDLR launched a multidecade endeavor that brought the physiological significance and the biochemical beauty of sterol regulation into wide view (Brown & Goldstein 2008; Goldstein & Brown 2009, 2015). In the course of unraveling familial hypercholesterolemia, they discovered that normal receptor-mediated LDL (and thus sterol) uptake causes marked downregulation of both sterol synthesis and LDL uptake. Feedback inhibition of sterol synthesis was profound, showing a more-than-100-fold decrease in the activity of the rate-limiting enzyme HMGR in some cases (Brown et al. 1973). These observations set the stage for deep mechanistic studies, leading to rich lines of inquiry and new biological fields that continue today. The basic model can be stated as global coordinated transcriptional control of synthesis and uptake, overlaid by posttranslational control of individual proteins. Many of the underlying mechanisms involve surprising adaptations of both synthetic and degradative aspects of proteostasis. Although the global transcriptional control is both very important and

beautifully efficient, it has been reviewed numerous times in high detail (Horton et al. 2002, Osborne & Espenshade 2009, Ye & DeBose-Boyd 2011). This topic will be treated here more briefly because the involved molecules define a useful parts list in exploration of the sterol-proteostasis interface.

Transcriptional control of sterol uptake and synthesis involves the transcription factor SREBP (sterol response element–binding protein). This classic bHLH-zip transcription factor is the soluble N terminus of a larger two-spanning membrane protein that resides in the endoplasmic reticulum (ER). The membrane anchor allows the SREBP to be regulated by the classic ER vesicle trafficking pathway used to process and deliver approximately 30% of all cellular proteins to various destinations in the secretory pathway. Cleavage and hence activation of SREBP rely on a protein termed SCAP (SREBP cleavage-activating protein), which is required for liberating the soluble N-terminal transcription factor from its membrane anchor. SCAP normally traffics between the ER and the Golgi complex by binding to one of the coat proteins from an ER transport vesicle. SCAP also binds to the C terminus of SREBP, and SCAP thus serves as a driver for SREBP, taking it to the Golgi complex to be sequentially cleaved by two separate Golgi-resident proteases that liberate the active, soluble SREBP N terminus. Cholesterol regulates SREBP activation through this SCAP-based transport (Figure 2). When cellular cholesterol levels are high, SCAP binds to an ER-localized multispanning membrane protein termed INSIG (insulin-induced gene 1; Insig in mammals) that retains it in the ER, thus preventing activation by prohibiting SREBP trafficking to the Golgi complex. Put simply, high cholesterol

blocks SREBP trafficking to its cleavage site, and low cholesterol allows SREBP trafficking to its cleavage site. Because active SREBP brings about expression of sterol synthetic enzymes and the LDLR, this scenario makes homeostatic sense. When cholesterol is low, both sterol synthesis and uptake are increased, and when cholesterol is abundant, both are curtailed. It is worth remembering that the ER-to-Golgi trafficking pathway is a major conduit of protein processing and transport, and so the theme of proteostasis looms large in the mechanism of regulation that evolution has chosen for this multigene portion of sterol regulation. Furthermore, the SCAP regulatory mechanism reveals a number of cis and trans components that are employed in a variety of other sterol regulation events. Accordingly, there is a revealing unity in several of the independent processes of sterol regulation and an interesting consistency to the idea that proteostasis has been harnessed to effect highly specific regulation.

The sterol sensing domain, Insig, and lipid signals: The central dogma of sterol regulation

SCAP is an eight-spanning membrane protein. Embedded in the SCAP sequence is an intriguing motif termed the sterol-sensing domain (SSD). The SSD was first noted by aligning the sequences of a variety of integral membrane proteins that have something to do with sterols (Kuwabara & Labouesse 2002, Nohturfft et al. 1998, Osborne & Rosenfeld 1998). Although this description may sound glib, the breadth of SSD protein actions renders it fairly accurate. SSD is found in proteins with

diverse functions in sterol regulation, including enzymes, trafficking components, signaling devices, and degradation factors. Thus, an ongoing goal of sterol regulation is to decide whether there is an underlying common function of the SSD. The SSD consists of highly conserved residues within or near transmembrane spans 2--6 of SCAP. The SSD was originally speculated to bind cholesterol and to thus allow an overlay of regulation or sensing (Goldstein et al. 2006, Radhakrishnan et al. 2004). However, further studies on SCAP indicate that SSD function is distinct from sterol binding (Motamed et al. 2011). Nevertheless, the extreme conservation of this motif over two billion years of evolution demands focus on its function. The highly conserved residues of the SSD are consistently demonstrable as important in a variety of regulatory actions, indicating the phenotypic importance of the SSD. Through the lens of proteostasis, an interesting hypothesis about an SSD function emerges. This view also depends on another key player in the sterol regulatory arena: INSIG proteins.

The INSIG proteins (Insig1 and -2 in mammals) reside in the ER, where they anchor SCAP in a cholesterol-dependent manner (Yang et al. 2002). The INSIG proteins are highly conserved in both sequence and function from yeast to mammals (Burg et al. 2008, Flury et al. 2005). The ability of cholesterol and other sterols to regulate the trafficking of SCAP—and thus the processing of SREBP—is due to a cholesterol-dependent change in the conformation of SCAP that allows binding to Insig and thus precludes trafficking (Adams et al. 2003, Brown et al. 2002). Direct biochemical assays on purified SCAP demonstrated that cholesterol binds to SCAP

with a nanomolar K_d, causing a structural change in the pure protein. The original idea that the SSD was responsible for sterol binding was supplanted by studies showing that the first luminal loop of the protein (outside the SSD) was necessary and sufficient for high-affinity binding of sterols (Motamed et al. 2011). The model from a variety of studies is that the SSD is responsible for engaging INSIG; it has even been proposed that the SSD designation be changed to IBD (INSIG binding domain) to emphasize this function (Motamed et al. 2011). However, in the context of SSD action outside of the mammalian arena, the SSD has autonomous on-pathway functions that suggest that the IBD moniker is too narrow.

The story of these parts is further complicated by the observation that INSIGs also have affinity for a distinct class of sterols, and INSIG binding of sterols can similarly restrict SCAP to the ER. The structure activity of INSIG-sterol binding is distinct from that of SCAP, as far as has been measured, with the strongest ligands being oxidized species (Adams et al. 2004, Radhakrishnan et al. 2007). Thus, there may be in this regulatory axis an ability to monitor a number of facets of sterol anabolism, catabolism, and transport. A variety of studies show that both the SSD and INSIGs have long and separate evolutionary histories that came together in eukaryotes (Hausmann et al. 2009, Kuwabara & Labouesse 2002, Ren et al. 2015). What is clear is that the functional relationship between SSD and INSIG proteins is often but not always intertwined; with this parts list now in hand, we turn to examples that employ these components in revealing ways in mammals and other eukaryotes.

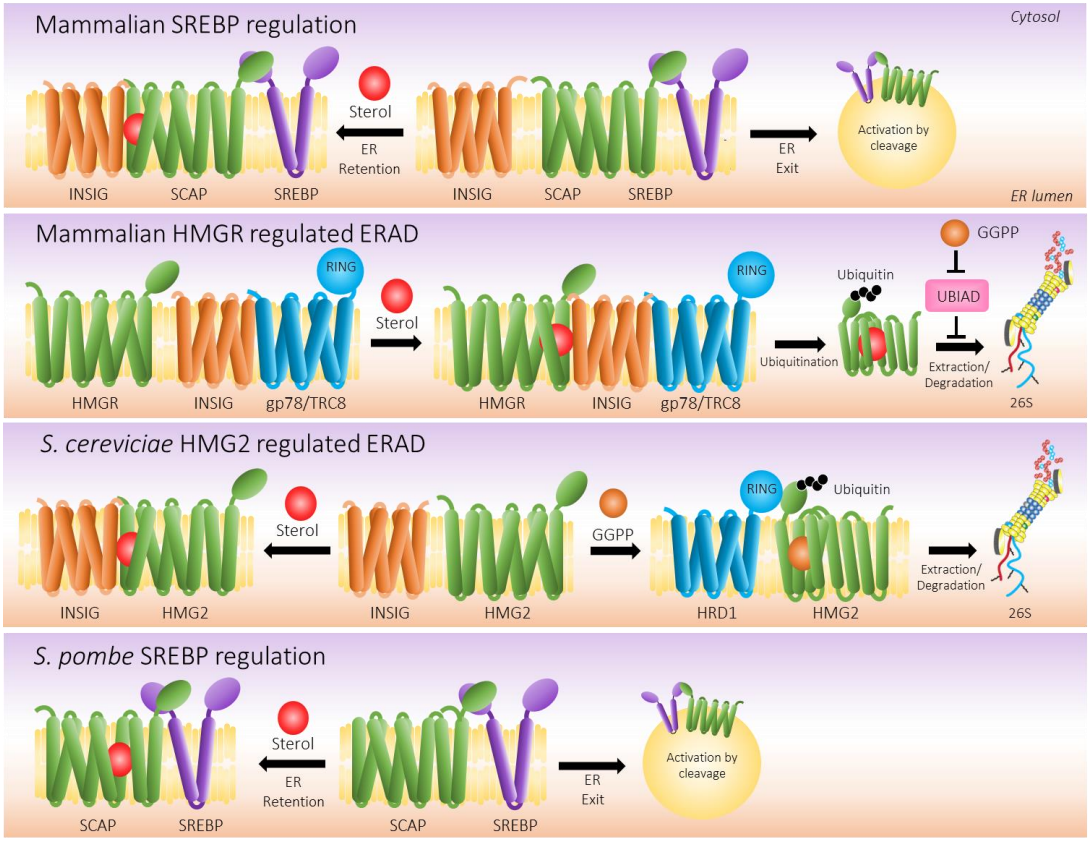

Figure 1.2. Eukaryotic tactics of sterol pathway regulation
A highly stylized cartoon showing the basic features and a parts list of the proteins involved in control of the sterol pathway. (a) Mammalian regulated ER retention of SCAP (and bound SREBP). (b) Mammalian regulated ER-associated degradation (ERAD) of HMG-CoA reductase (HMGR). (c) Saccharomyces cerevisiae regulated ERAD of the Hmg2 HMGR isozyme. (d) Schizosaccharomyces pombe regulated ER retention of SCAP (and bound SREBP). Sterol-sensing domain proteins are shown in green, INSIGs in blue, SREBP cargo in purple, and the ER membrane in yellow (the lumen is down, and the cytosol is up). Ligands are ball shaped. GGPP denotes geranylgeranyl pyrophosphate.

Regulation of HMG-CoA Reducatase: ERADication of excess activity

HMGR undergoes feedback-regulated degradation as a part of pathway control. In cell culture, the activity of HMGR varies up to 200 fold, depending on sterol abundance and availability. Similarly, in vivo in animals, liver levels of the enzyme can oscillate more than two orders of magnitude during a typical diurnal cycle (Hwang et al. 2016). This impressive range appears to be entirely due to altering the amount of HMGR protein. Although the cytosolic HMGR catalytic domain undergoes control by phosphorylation (Beg et al. 1985, Omkumar et al. 1994), this modification is reserved for switching between catabolic and anabolic states. Accordingly, HMGR production and degradation are used to regulate the activity of this enzyme. Synthesis is controlled en bloc by the SREBP pathway described above, and this mechanism accounts for approximately 10 to 20-fold variation. The remainder of the variation is due to regulated degradation of the HMGR enzyme, which responds in the expected way to flux through the sterol pathway: When levels of sterol pathway products are abundant, HMGR undergoes rapid degradation (Edwards et al. 1983). When pathway flux is slowed, HMGR becomes stable, and the difference in half-life is on the order of 30 minutes in the rapidly degraded state to more than 6 hours when stable.

Regulated degradation of HMGR is a highly selective process, targeting only this protein. The high specificity makes this branch of sterol regulation particularly interesting as a novel clinical target and has engendered much research (Ravid et al. 2000, Roitelman & Simoni 1992, Sever et al. 2003a,b). HMGR is an ER-resident integral membrane protein, with an N-terminal eight-spanning membrane anchor

followed by a linker and a highly conserved cytoplasmic catalytic domain that catalyzes the rate-limiting production of mevalonic acid. The large transmembrane anchor is necessary and sufficient for regulated degradation by ubiquitination. The ubiquitin pathway involves a cascade of enzymatic reactions that result in construction of a multiubiquitin chain on a substrate, which targets that protein for destruction by the 26S proteasome. Ubiquitination is brought about by transfer of ubiquitin from one of a small number (10 in yeast, ~50 in mammals) of E2 ubiquitin-conjugating enzymes (UBCs) to the substrate or substrate-bound growing multiubiquitin chain (Amm et al. 2014, Kleiger & Mayor 2014). Transfer of ubiquitin from the UBC to the substrate is catalyzed by an E3 ubiquitin ligase, which is responsible for the specificity of ubiquitination. HMGR degradation is accomplished by regulated ubiquitination, in which the enzyme is tagged with multiple copies of the ubiquitin, followed by its extraction from the ER membrane and proteolysis by the cytosolic 26S proteasome. Our understanding of mammalian HMGR ubiquitination owes much to the elegant work of the DeBose-Boyd group (Jo et al. 2011a; Song et al. 2005a,b). The initial model involved a single E3 ubiquitin ligase and some of the familiar components from the SREBP story: Like SCAP, the HMGR transmembrane anchor has an SSD, and this domain is required for regulated degradation. When sterol levels are high, HMGR associates with Insig. Insig binding brings an ER-resident E3 ubiquitin ligase known as gp78 into close proximity with HMGR, causing its ubiquitination and eventual degradation by the cytosolic proteasome. gp78 is one of a number of E3 ubiquitin ligases involved in ER-associated protein degradation (ERAD), by which misfolded

proteins of the ER are selectively detected and destroyed (Brodsky 2012, Hirsch et al. 2009, Needham & Brodsky 2013). A variety of highly conserved pathways participate in ERAD. Because many of the maladies of aging involve pathologies associated with misfolded proteins, degradative quality control is an active field of endeavor. Although the regulated recruitment of gp78 to HMGR is highly specific, the range of substrates that are removed by ERAD pathways is very broad. Thus, in this aspect of sterol regulation, again a highly general proteostatic process is adapted to bring about a highly specific regulatory outcome. For SREBP, the high-throughput conveyor belt of ER-to-Golgi transport is involved, and in this context, one of the broad-specificity ERAD quality control pathways operates in conjunction with protein synthesis and folding to ensure a well-folded proteome.

Since those initial studies, it has become clear that mammalian HMGR degradation is more complex than this initial understanding. Another multispanning ER-resident E3 ubiquitin ligase termed TRC8 is also capable of supporting regulated degradation of HMGR (Jo et al. 2011a). Moreover, gp78 can apparently degrade TRC8. Furthermore, TRC8 has its own SSD and can interact with INSIGs, allowing for a fairly complex interplay of these factors (Jo et al. 2011a, Lee et al. 2010a). Significantly, even this more nuanced two-E3 view has been challenged using gp78$^{-/-}$ null cells (Tsai et al. 2012); evidence from those studies indicates that the model of E3 participation in HMGR degradation may be incomplete. Finally, the individual regulatory proteins that mediate HMGR and SREBP regulation clearly undergo ERAD by a variety of mechanisms. For example, TRC8 is a substrate of gp78, and the Insig

proteins are also subject to degradation when they are not bound to a client (Lee et al. 2006, 2010b). The final understanding of the true complexity of these intertwined systems may be resolvable only by newer gene editing methods, perhaps using systems biology approaches.

The principal sterol that brokers the gp78-INSIG association with HMGR is derived from lanosterol, rather than cholesterol (Lange et al. 2008; Song et al. 2005a,b). Lanosterol is produced only by the sterol pathway. Thus, regulated degradation of HMGR is keyed to sterol synthesis rather than simple sterol abundance, appropriate for HMGR's rate-limiting status in this pathway. The HMGR presumably has a binding site for 24,25-dihydrolanosterol, although this has not been demonstrated. HMGR stability is also controlled by the 20-carbon isoprenoid geranylgeranyl pyrophosphate (GGPP). The original observation was that addition of the 20-carbon isoprene geranylgeraniol (GGOH, the unphosphorylated form of GGPP) accelerated sterol-mediated degradation of HMGR (Sever et al. 2003a,b). Recent studies have implicated the multispanning integral membrane prenyltransferase UBIAD1 (UbiA prenyltransferase domain–containing 1) by the following mechanism: UBIAD1 binds to HMGR during its sterol-dependent ubiquitination and prohibits the extraction of ubiquitinated HMGR from the ER membrane for degradation. Added GGOH is converted into the pathway intermediate GGPP, which then binds to UBIAD1, promoting its liberation from HMGR and thus allowing the steps downstream of its degradation to proceed (Schumacher et al. 2015, 2016). Thus,

mammalian HMGR stability is keyed to two biosynthetic signals: GGPP and lanosterol (Figure 1).

The highly conserved sterol/mevalonate pathway is found in all eukaryotes. We next discuss two examples of sterol pathway regulation separated from mammals by one billion years of evolution; regulated degradation of HMGR in *Saccharomyces cerevisiae* (which we term yeast) and the SREBP pathway in *Schizosaccharomyces pombe*. Study of common regulatory components such as INSIGs and SSDs in these model citizens of the biosphere reveals core functions and novel insights applicable to all examples.

Regulated degradation of HMG-CoA Reductase in *Saccharomyces Cerevisiae*: Hrd behavior

Regulated ubiquitination of HMGR was first discovered and studied in *S. cerevisiae* (Hampton & Bhakta 1997, Hampton et al. 1996), and its study continues to provide insights into both sterol regulation and ERAD (Neal et al. 2017, Sato et al. 2009, Vashistha et al. 2016). HMGR is essential for life in yeast, allowing synthesis of many isoprenoids and ergosterol, which is the principal sterol. Yeast HMGR has a body plan very similar to that of mammalian HMGR: an eight-spanning N-terminal ER membrane anchor and a C-terminal cytosolic catalytic domain connected by a linker to the membrane anchor. The mammalian catalytic domain, which is ~60% identical to the yeast catalytic region, can provide the needed HMGR activity to yeast. In contrast, the eight-spanning N-terminal transmembrane region has far more limited

homology but nevertheless has a clear SSD that is critical for regulated degradation of HMGR. There are two isozymes of HMGR in yeast: Hmg1 and Hmg2. Either isozyme can supply the essential enzyme activity, but only Hmg2 undergoes regulated degradation.

Regulated degradation of Hmg2 follows the dictates of feedback regulation: High flux through the mevalonate pathway promotes degradation, whereas lowered flux causes stabilization. In this way, Hmg2 half-life can vary between 15 min and 6 h (Gardner et al. 1998, Shearer & Hampton 2004). Genetic analysis of Hmg2 degradation led to the discovery of the HRD genes (which are responsible for Hmg-CoA reductase degradation), along with many other substrates. The HRD1 and HRD3 genes encode a pair of ER-resident proteins that form the core subunits of a highly conserved E3 ubiquitin ligase, which is responsible for ubiquitination of Hmg2, leading to proteasome-mediated degradation (Bays et al. 2001, Gardner et al. 2000, Garza et al. 2009a, Hampton et al. 1996, Vashistha et al. 2016). The Hrd1 protein is a multispanning E3 ubiquitin ligase with an N-terminal transmembrane region and a C-terminal E3 ubiquitin ligase domain. A canonical RING-H2 domain in this E3 domain is responsible for brokering the transfer of ubiquitin, primarily from the E2 Ubc7, to Hmg2. Hrd3 (Sel1L in mammals) has a large luminal domain and is found in stoichiometric association with Hrd1. Loss of either protein causes complete removal of the HRD pathway and full stabilization of Hmg2 and all other HRD degradation substrates. Surprisingly, in addition to a role in Hmg2 degradation, the HRD pathway is central to eukaryotic ERAD. As mentioned above, ERAD is conserved in

eukaryotes and is instrumental in alleviating potentially lethal ER stress (Brodsky & Skach 2011, Koenig & Ploegh 2014, Travers et al. 2000, Walter & Ron 2011). Hrd1 is a clear homolog of gp78, the main E3 ubiquitin ligase used in mammalian HMGR degradation, with a similar layout, sequence identities throughout the protein, and similar E2 requirements (Fang et al. 2001; Song et al. 2005a,b). Thus, the theme of regulation by use of protein quality control is extant across the impressive evolutionary gap that separates yeast from hepatocytes. However, unlike the complex involvement of other E3 ubiquitin ligases in addition to gp78 in mammals, Hrd1 appears to be the sole E3 ubiquitin ligase required for HMGR degradation.

The HRD pathway is responsible for the degradation of many misfolded ER proteins, including both luminal and integral membrane substrates (Bordallo et al. 1998, Hampton et al. 1996, Vashist & Ng 2004). All misfolded model substrates examined are constitutively degraded by the HRD pathway. By contrast, pathway signals regulate the entry of wild-type Hmg2 into the always operating HRD pathway (Hampton & Rine 1994). Use of drugs and molecular biological approaches indicated that the 15-carbon isoprenoid farnesyl pyrophosphate (FPP) was the source of a signal for enhanced degradation (Figure 1) (Gardner & Hampton 1999a, Shearer & Hampton 2005). Subsequent work revealed that the de facto signal is in fact GGPP—the same molecule that enhances degradation of mammalian HMGR. However, unlike the mechanism proposed in mammals, in which GGPP enhances sterol-regulated ERAD of HMGR, in yeast GGPP is the primary signal for HRD-dependent Hmg2

degradation (Garza et al. 2009a). Our ongoing studies suggest a simple model for GGPP action with the possibility of broad utility and possible clinical application. The conundrum of normally folded Hmg2 undergoing regulated degradation by the constitutive HRD quality control pathway is resolved with a misfolding step as part of the regulatory circuit. It appears that GGPP causes reversible misfolding of Hmg2, allowing for enhanced degradation by the HRD machinery. This idea emerged from our initial studies with the chemical chaperone glycerol, in which Hmg2 undergoing rapid regulated degradation was immediately and strongly stabilized by the addition of glycerol, indicating that Hmg2 undergoing regulated degradation behaved like a misfolded protein (Gardner et al. 2001b). An in vitro limited proteolysis assay was developed to explore this idea and is depicted in Figure 3. Hmg2 with a protected epitope tag in isolated ER microsomes undergoes a characteristic time-dependent proteolysis pattern when treated with trypsin. In vitro Hmg2 trypsinolysis is greatly slowed by the direct addition of glycerol or other chemical chaperones (Shearer & Hampton 2004) and is accelerated by the direct addition of GGPP (Garza et al. 2009a). Our first studies of this in vitro structural regulation were with the neutral isoprenoid farnesol (FOH; FPP without phosphates), which showed a similar specific alteration in Hmg2 structure (Shearer & Hampton 2005). However, the effect of FOH was seen only at millimolar concentrations of FOH. By contrast, the effects of GGPP in vitro were observed with an EC_{50} in the low-nanomolar (approximately 50 nM) range (Figure 3) This finding is consistent with the clear role of GGPP as the bona fide physiological regulator of Hmg2 stability in vivo (Garza et al. 2009a). The effect of

GGPP on Hmg2 structure is fully reversible, and GGPP does not result in wholesale misfolding of Hmg2, because the thermal denaturation curve is unaffected at any concentration (Wangeline & Hampton). Importantly, the effects of GGPP on Hmg2 stability in vivo or on Hmg2 structure in vitro are reversed by the addition of chemical chaperones such as glycerol, indicating that GGPP causes Hmg2 misfolding. The microsomal limited trypsinolysis assay has provided a simple, powerful approach to understanding GGPP-mediated regulated misfolding and the Hmg2 SSD.

The necessary and autonomous sterol sensing domain

The ongoing work on Hmg2 has allowed us to study a critical and autonomous function for the SSD. The Hmg2 N-terminal transmembrane domain has a clearly defined SSD, with residues found in transmembrane spans 2—6 (Kuwabara & Labouesse 2002, Theesfeld et al. 2011). The simplicity of the in vitro Hmg2 regulatory readout provides a unique opportunity to move toward understanding SSD function. Deeply conserved residues are shared in SSDs spread over billions of years of evolution. We found in our initial studies of the Hmg2 SSD that many of these highly conserved residues are critical for regulated degradation of Hmg2 (Theesfeld et al. 2011). A typical example is serine 215 (S215). The S215A mutant is completely stable in vivo at all levels of GGPP, whether added exogenously or by forced production with enzymes. The limited proteolysis assay revealed that the S215A mutant of Hm2 no longer undergoes the characteristic GGPP-stimulated structural transition. An alanine scan of all Hmg2 conserved SSD residues resulted in a simple

binning of residue functions: Either alanine substitution had no effect on GGPP-stimulated degradation, or a replacement caused strong stabilization of Hmg2. In no case did replacement of a highly conserved SSD residue cause destabilization of Hmg2. Thus, the SSD apparently allows for GGPP-regulated misfolding. Taken alone, this observation leads to the conclusion that SSD mediates either GGPP recognition or misfolding mediated by GGPP bound to a different site. We are currently involved in resolving these two scenarios but favor the transmission role for the reasons described below.

Whatever the molecular function of the SSD, a key general feature emerges from these studies: The SSD has a bona fide regulatory function independent of the INSIG proteins known to be intimately involved in SSD protein action in mammals. Importantly, yeast has two INSIG proteins, Nsg1 and Nsg2; they interact with Hmg2 and participate in sterol regulation. However, removal of both Nsg1 and Nsg2 has no effect on GGPP-stimulated Hmg2 degradation. Thus, the Hmg2 SSD is autonomously required for permission to enter the HRD pathway, and alteration of many of the highly conserved residues---often to amino acids that are more suited to be within a lipid bilayer---results in a version of Hmg2 that can no longer undergo feedback regulation.

A tale of two signals: the logic of Hmg2 regulation

The independence of Hmg2 SSD–dependent function from INSIGs is not due to an absence of these proteins in yeast sterol regulation. In fact, yeast INSIGs provide

an additional layer of regulation to regulated degradation of Hmg2. In striking contrast to the mammalian situation, Nsg1 inhibits Hmg2 degradation, so sufficient levels of Nsg1 will block the GGPP-dependent degradation of Hmg2. Nsg-mediated stabilization of Hmg2 apparently occurs at the level of regulated misfolding as well: The presence of stoichiometric levels of Nsg1 slows the in vitro limited proteolysis of Hmg2 in a manner very similar to that of other stabilizing influences such as chemical chaperones (Flury et al. 2005).

This action of Nsg1 occurs at native levels of both Hmg2 and Nsg1 and was initially perplexing. Why would Hmg2 have elaborate stability regulation only to be blocked by Nsg1? The logic of this extra layer of regulation came from the realization that, as in the mammal, the Hmg2-Nsg1 interaction is sterol dependent. Nsg1 inhibits Hmg2 degradation by interacting with the Hmg2 transmembrane region, and this interaction requires lanosterol. When lanosterol is present, Nsg1 binds to Hmg2, prohibiting GGPP-mediated regulated degradation (Theesfeld & Hampton 2013). Why have this extra layer of regulation? We think the action of Nsg1 allows an oxygen contingency to Hmg2-regulated degradation. The first part of the sterol pathway up to the 30-carbon squalene is oxygen independent (Figure 1). Later steps are strongly oxygen dependent (Figure 1). Accordingly, GGPP can be made in the absence of oxygen, whereas production of the first bona fide sterol, lanosterol, requires oxygen. Because of the interplay of GGPP-stimulated Hmg2 degradation and lanosterol/Nsg1-mediated stabilization, Hmg2 will undergo regulated degradation only when GGPP is abundant and lanosterol is not. These are exactly the biochemical conditions of

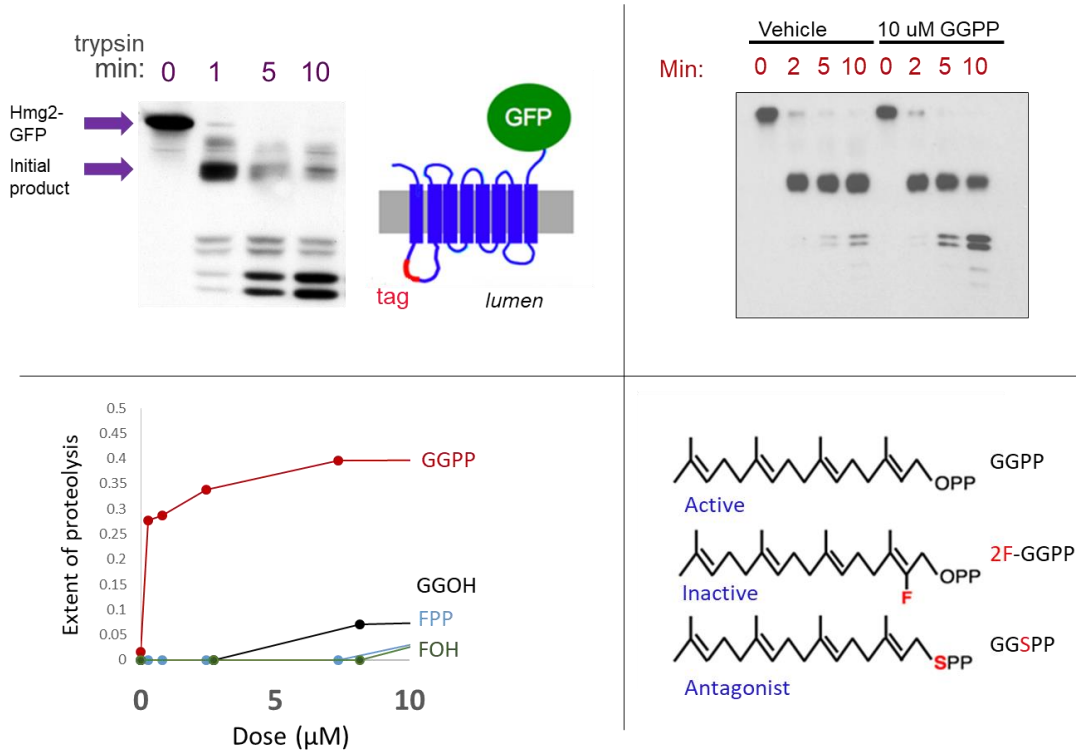

Figure 1.3. Geranylgeranyl pyrophosphate (GGPP)-mediated reversible misfolding of Hmg2

(a) An example of the trypsinolysis assay used to explore Hmg2-GFP structure. The time course of the trypsinolysis using a high concentration of trypsin, measured by SDS-PAGE and epitope tag blotting. Initial product is generated by rapid removal of GFP at the start of the assay. Hmg2-GFP with a luminal epitope is also depicted. (b) Effect of added GGPP on the rate of Hmg2 cleavage in the limiting trypsinolysis assay. Abbreviations: FOH, farnesol; FPP, farnesyl pyrophosphate; GGOH, geranylgeraniol. (c) Concentration dependence of GGPP in altering Hmg2-GFP structure in the trypsinolysis assay, along with several other isoprenoids. GGPP EC50 ~ 50 nM. Extent of proteolysis is defined as the fraction of the major fragment degraded. Adapted from Wangeline & Hampton 2017. (d) The GGPP effect is highly specific; 2F-GGPP has no effect on Hmg2 trypsinolysis, whereas GGSPP is an antagonist of GGPP in vitro and in vivo.

anaerobiosis, and this model is detailed in (Theesfeld & Hampton 2013). Whatever the purpose of this two-signal control, it is interesting that both yeast and mammals measure GGPP and lanosterol to regulate HMGR activity. Mammalian HMGR is degraded when lanosterol is abundant, and degradation is further enhanced when GGPP is also abundant (Sever et al. 2003a,b). Yeast has evolved a distinct response to the same two signals, using the same core molecular devices. Although our model pertains to anaerobiosis, Hmg2-regulated degradation occurs in all growth conditions, allowing for easy study in any circumstance in which Hmg2 levels surpass those of Nsg1 (Flury et al. 2005).

GGPP and ligand-regulated misfolding: the dark side of allostery

The key observation from Hmg2-regulated degradation is that GGPP-mediated Hmg2 degradation is dependent on the SSD, and this dependence represents an autonomous function of this motif. INSIG-mediated, sterol-dependent regulation of Hmg2 stability inhibits the action of GGPP, but GGPP-regulated Hmg2 degradation is completely INSIG independent. Accordingly, Hmg2 regulation presents an unparalleled opportunity to learn about the conserved function of the SSD motif and its involvement in many independent signaling axes.

We have more recently focused on the nature of the GGPP- and SSD-dependent misfolding of Hmg2. Our recent work indicates that GGPP-stimulated ERAD of Hmg2 may be a form of allosteric regulation, with many of the hallmarks of this classic mode of enzyme control but with ligand-dependent misfolding as the

structural readout. Using both the in vitro limited proteolysis assay (Flury et al. 2005, Shearer & Hampton 2004) and in vivo Hmg2 degradation, a variety of experiments point to an allosteric model of induced Hmg2 misfolding. The allosteric misfolding model arose from in vitro studies of the GGPP regulator, which by every criterion behaves like an allosteric ligand. The in vitro structural effects of GGPP are rapid and fully reversible. Washing Hmg2 microsomes treated with even 100 times the GGPP needed for the maximal change in Hmg2 structure restores Hmg2 to its untreated state. As mentioned above, GGPP is potent in this assay, with an EC_{50} in the 50 nM range—a concentration that is below the typical K_m for yeast enzymes that process this normal isoprenoid. The most revealing data emerge from structure-activity studies. Because GGPP is a substrate of the prenyltransferases needed to activate the RAS oncogene and other signaling proteins, many analogs have been produced in the study of prenylation. Subtle changes in the GGPP structure render the analogs unable to cause any changes in the limited proteolysis assay or any change in Hmg2 stability in vivo. GGPP consists of the 20-carbon alcohol gernanylgeraniol in phosphoester linkage with a pyrophosphate group (Figure 1). Substitution of the alcohol O with an S, or replacement of a 2C methylene H with F, completely removes the ability of these analogs to affect Hmg2 structure in vitro. Furthermore, the GGSPP analog, but not the 2F version, is a GGPP antagonist of GGPP, reversing the GGPP-mediated changes in Hmg2 structure in vitro and GGPP-stimulated degradation of Hmg2 in vivo (Figure 3). The existence of an antagonist is strong, if indirect, evidence for a specific GGPP binding site required for reversible misfolding of Hmg2.

The action of GGPP sounds similar to that of an allosteric regulator, which are generally reversible binding ligands for the regulated protein. We further explored this idea by examining features of the Hmg2 protein itself. We found that the Hmg2 transmembrane domain forms multimers, as is often the case for allosteric proteins. Neither the interaction with GGPP, nor the presence of conservative SSD mutants that remove the effects of GGPP, affects Hmg2 multimerization. Importantly, these highly ligand-specific effects of GGPP are reversed by a variety of chemical chaperones in vitro, indicating that folding state is the susceptible feature of Hmg2 being controlled by the ligand. Our current view is that reversible high-affinity binding of GGPP to a specific binding site on the Hmg2 quaternary structure causes a transition to a misfolded state that is more susceptible to ERAD-based quality control.

The idea that a small-molecule ligand can trigger the entry of a specific, normal protein to enter a degradative quality control pathway has interesting implications. Because quality control is highly specific to subtle changes in folding and is widely used in all kingdoms of life, the possibility exists for the inherent specificity of quality control to be similarly controlled by a small molecule in cases of natural protein regulation. Two examples include ligand-triggered degradation of the ER-bound IP_3 receptor in mammals (Wojcikiewicz et al. 1994, 2009) and regulated destruction of an early enzyme of the LPS biosynthetic pathway in *Escherichia coli* (Fuhrer et al. 2006). Whatever the extent of such regulation in nature, developing molecules that can bring about ligand-regulated misfolding might allow for selective pharmaceutical manipulation of previously undruggable targets. This novel approach

to drug development is being actively explored in a variety of ways (Lai & Crews 2016), and harnessing the power of allosteric misfolding could be a distinct approach that mimics natural modes of regulation. There are many known cases of pharmacological chaperones, that is, ligands that improve the folding and stability of their protein binding partners, allowing more of the protein to be accumulated by skirting destruction by quality control (Bernier et al. 2004, Leidenheimer & Ryder 2014). In contrast, we posit that GGPP is a so-called pharmacological chaotrope, causing selective misfolding of its binding partner. Because GGPP-regulated degradation of Hmg2 has many parallels to allosteric regulation but results in detectable misfolding, we suggest the term mallostery to refer to this potentially pervasive ligand-mediated alteration of a protein's folding state (Figure 4).

Generalizing sterol sensing domain autonomy: Sterol-regulated SCAP in *Schizosaccharomyces pombe*

Our studies on Hmg2 reveal an example in which the SSD is absolutely required for a regulatory function but operates autonomously. This is in contrast to the mammalian examples, in which the INSIGs are intimately involved in the sterol-mediated regulation of SSD-containing proteins HMGR and SCAP. How often is SSD function divorced from INSIGs? The autonomy of the SSD is also evident in another fruitful nonmammal, *S. pombe*, as revealed by the beautiful work from the Espenshade group on sterol-regulated SREBP cleavage (Hughes et al. 2005, Porter et al. 2010, Ravid et al. 2000). This example is particularly intriguing; the main function of

SREBP (Sre1 in *S. pombe*) regulation is apparently to employ the sterol pathway as a biochemical indicator of oxygen status (Hughes et al. 2005, Todd et al. 2006). Because sterol synthesis is strongly dependent on oxygen (Figure 1) biosynthesis of sterols is a hallmark of oxygen abundance. As in the mammal, when sterol levels drop in *S. pombe*, SREBP processing by cleavage to an active transcription factor increases, and transcripts are produced. But in *S. pombe*, the majority of these transcripts encode proteins needed for life at low oxygen, and removal of SREBP results in poor survival following hypoxia. The regulation of SREBP is similar to that in mammals: SCAP (Scp1 in *S. pombe*) mediates the trafficking of SREBP from the ER to the Golgi complex, where SREBP is cleaved into its soluble, transcriptionally active form. As in the mammal, in *S. pombe* the presence of sterol regulates SREBP processing: High sterols preclude SCAP exit from the ER, and thus SREBP processing ceases. Low sterols allow for exit and processing of SCAP and bound SREBP. However, an important difference is in the complete lack of a role for INSIG (Ins1 in *S. pombe*) proteins in this process. Indeed, they are present and mediate regulatory phosphorylation of HMGR (Burg et al. 2008), but the sterol-dependent retention of SCAP (with bound SREBP) is completely INSIG independent (Hughes et al. 2005). As with Hmg2, the ability of *S. pombe* SCAP to respond to its sterol pathway signal requires a number of conserved residues of the SSD (Hughes et al. 2008). The SSD point mutants that alter SCAP function do so by allowing SCAP to cycle constitutively at all levels of sterol. Thus, as in Hmg2, the SSD is needed for a sterol pathway molecule to alter the regulated protein. Significantly, the cleavage

mechanism of *S. pombe* SREBP is quite different from that in mammals, revealing an intriguing new mechanism of protein processing in the Golgi compartment (Lloyd et al. 2013; Stewart et al. 2011, 2012). Nevertheless, the use of SCAP to ferry SREBP out of the ER in a sterol-regulated manner is very similar to what is seen in mammals and *S. pombe* and is thus revealing in comparison.

Viewing sterol-sensing domain function through proteostasis-tinted glasses

Is there an underlying consistency to the varied actions of this widely conserved motif? The two principal perplexing features are (*a*) the varied number of sterol pathway ligands or signals that seem to promote regulation through SSD-bearing clients and (*b*) the varied role of INSIG proteins in SSD-dependent regulation. We posit that the unifying function of the SSD in these cases is to allow ligand-mediated misfolding as a path to regulation. In the simplest case, *S. pombe* SCAP normally cycles between the Golgi complex and the ER with the bound SREBP cargo. When ergosterol (the *S. pombe* main sterol) binds to SCAP, SCAP is retained in the ER and no longer assists in trafficking of SREBP to its activation site. One of the primary responses to misfolded ER proteins is retention in the ER, as happens when ergosterol is elevated and presumably binds to *S. pombe* SCAP. Consistent with this idea, mutations of many of the highly conserved SSD residues in *S. pombe* SCAP produce a version that still exits the ER and transports SREBP but no longer shows sterol-dependent ER retention. This scenario sounds very similar to that of Hmg2,

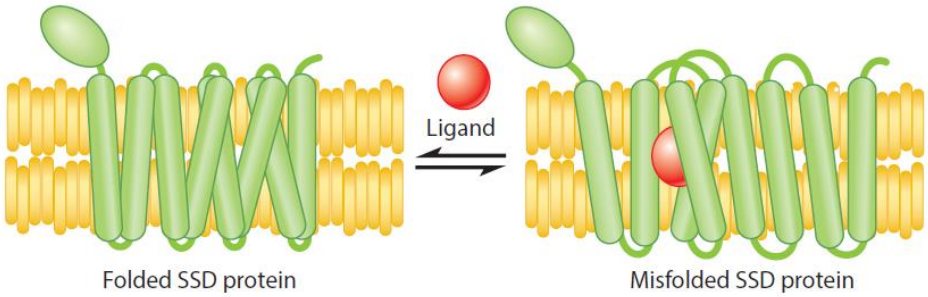

Figure 1.4. Mallostery, or a reversible, ligand-mediated misfolding model
Mallostery, or a reversible, ligand-mediated misfolding model for sterol-sensing domain (SSD) proteins, in which the SSD motif imparts the ability to undergo reversible misfolding. We posit that the SSD protein functions as a multimer and effects a variant of allosteric regulation, allowing for ligand-mediated misfolding as a regulatory tactic.

which undergoes ligand-dependent misfolding in the presence of GGPP, a totally distinct signal.

The role of INSIGs in Hmg2 regulation may fit a model of regulated quality control as well. The function of yeast INSIGs is to thwart Hrd1-dependent degradation of Hmg2. We have posited that the INSIGs represent a family of sterol-dependent chaperones for the misfolded SSD state (Flury et al. 2005, Theesfeld & Hampton 2013). Thus, GGPP-engaged Hmg2 is susceptible to INSIG binding, which stabilizes it or protects it from Hrd1-mediated ubiquitination. Stabilization of misfolded proteins is certainly one function of traditional chaperones and may be how INSIGs stabilize Hmg2 in the presence of abundant GGPP. Similarly, mammalian SCAP undergoes a structural transition in the presence of a third signal, cholesterol, and is retained in the ER by virtue of a now-permitted interaction with INSIG. If the response to sterol by mammalian SCAP were similar to that in *S. pombe*, then this response would be consistent with INSIG stabilizing the misfolded state and causing retention, also a function of traditional chaperones (Araki & Nagata 2011, Gidalevitz et al. 2013, Kim et al. 2013). Finally, mammalian HMGR responds to a fourth signal, lanosterol or a related metabolite (Lange et al. 2008; Song et al. 2005a,b), to undergo degradation by an ERAD quality control E3 ubiquitin ligase, gp78, that is a Hrd1 homolog. This interaction requires INSIG engagement of HMGR when sterols are abundant. Because there are numerous cases of more traditional chaperones or protein trafficking factors recruiting ubiquitin E3 ligases to degrade misfolded clients (Chen et al. 2011, Guerriero & Brodsky 2012), this embellishment would again be consistent with

INSIGs serving as SSD-specific chaperones. Although this view is probably too simplistic, it creates an interesting framework for useful hypothesis generation, which would include a plethora of powerful tools and models not normally accessed in sterol biology.

If the SSD is required for programmed misfolding, it could have at least two roles: binding of the mallosteric ligand and a more structural role that allows ligand-mediated misfolding to occur. The number of distinct ligands in the four examples above implies that the SSD may be a motif that permits alteration of the protein's folding state rather than binding per se. Consistent with this idea, the recent work on mammalian SCAP has clearly implicated a luminal loop, and not the SSD, of SCAP as a nanomolar-affinity sterol binding site (Motamed et al. 2011). This modularity would result in the SSD permitting regulated misfolding for a variety of distinct ligands. Whatever the model, it will be important and interesting to parse these two models with molecular biological and structural approaches. Recent structures of the NPC1 SSD region indicate that a new mechanistic era in understanding the SSD is now beginning (Li et al. 2016, Zhao et al. 2016).

An example of the utility of a quality control view of sterol regulation may be found in the complexities of regulated degradation of mammalian HMGR. As described above, there is some disagreement about the E3 ubiquitin ligases that are required for mammalian HMGR degradation. The explanation may lie in the nature of protein quality control. It is clear that quality control E3 ubiquitin ligases have broad and overlapping substrate ranges, as is also the case for the folding branches of

proteostatic quality control (Gidalevitz et al. 2013, Vembar & Brodsky 2008). Accordingly, removal of one quality control factor will often unveil or induce another (Hirsch et al. 2009, Stolz et al. 2013). A telling example of ERAD flexibility for HMGR arose when hamster HMGR and its cognate INSIG were co-expressed in *Drosophila* cells. Indeed, sterol-regulated degradation of the mammalian HMGR occurred in this heterologous system. However, the E3 ubiquitin ligase required for regulated ubiquitination was none other than the endogenous *Drosophila* Hrd1 (dHrd1), the prototype ERAD quality control E3 ubiquitin ligase (Faulkner et al. 2013, Nguyen et al. 2009). This finding indicates that the transplanted mammalian HMGR can undergo sterol-regulated entry into a canonical ER quality control pathway in the correct circumstances. Another implication is that INSIG SSD–dependent sterol regulation of mammalian HMGR degradation may also involve regulated misfolding and may thus be susceptible to the known flexibility of ERAD E3 ubiquitin ligases. This feature could provide an explanation for, or at least a mechanistic framework with which to resolve, the varied roles of E3 ubiquitin ligases involved in mammalian HMGR ERAD.

Whether or not there is an underlying unitary explanation for SSD-mediated sterol regulation based on quality control degradation, this approach to modulation is widely employed in sterol regulation and in many other niches of biology. Below are some briefly described examples to illustrate this point and to hopefully inspire ideas and experiments.

MARCHing to the beat of a different ligase: sterol-regulated endoplasmic reticulum-associated degradation of Squalene Monooxygenase

Squalene monooxygenase (SM, or Erg1 in yeast) is the first oxygen-dependent step in the sterol pathway, creating an epoxide from the 30-carbon isoprenoid squalene, which is next rearranged to lanosterol, the first sterol of the pathway (Figure 1). SM is an integral ER membrane protein. It was first reported that SM undergoes cholesterol-regulated proteasome-mediated degradation in mammalian cells (Gill et al. 2011). High cholesterol levels cause increased degradation of SM, whereas low cholesterol levels decrease degradation rate. Subsequent proteomic studies in yeast indicated that SM regulation is highly conserved, and they implicated the yeast Doa10 RING-H2 E3 ubiquitin ligase (Foresti et al. 2013). This distinct ERAD pathway works alongside the HRD pathway in eukaryotes. The conserved involvement of this E3 ubiquitin ligase in SM regulation was confirmed by the finding that MARCH6 (a DOA10 homolog) is responsible for regulated SM degradation in mammals (Foresti et al. 2013, Zelcer et al. 2014). Curiously, yeast SM (Erg1) degradation is keyed to lanosterol rather than cholesterol (Foresti et al. 2013). Furthermore, the first 100 amino acids of mammalian SM is sufficient for cholesterol-regulated degradation, and although yeast lacks this region of the protein, it shows sterol-regulated degradation by the same ERAD pathway (Howe et al. 2015).

Cholesterol-regulated degradation of SM is thus another example of signal-regulated entry into an ERAD pathway. There is no SSD in SM, nor is its degradation dependent on INSIGs. However, the features of mammalian SM regulation bear many

similarities to those of yeast Hmg2. SM is stabilized in vivo by application of the chemical chaperone glycerol, implying that cholesterol is causing misfolding. Cysteine-based scanning and a PEGylation cysteine modification assay confirm that SM undergoes a cholesterol-dependent conformational change (Howe et al. 2015). Because there is a lack of known motifs, further analysis of the first 100 amino acids of mammalian SM, and its interaction with cholesterol, will be important for understanding this version of regulated misfolding.

Smith-Lemli-Opitz Syndrome

Smith-Lemli-Opitz syndrome is a single-gene metabolic disease with challenging and complex clinical symptoms (Kelley & Hennekam 2000, Nowaczyk & Irons 2012). The disease is caused by hypomorphic mutations in the single late sterol pathway enzyme 7-dehydrocholesterol reductase (DHCR7) (Fitzky et al. 1998, Wassif et al. 2002). Thus, clinical approaches for this currently incurable disease include ways to elevate DHCR7 levels in patients. Recent work (e.g., by (Prabhu et al. 2016)) indicated that DHCR7 is subject to cholesterol-regulated degradation. Elevating the level of cholesterol in cultured mammalian cells causes selective degradation by the proteasome. DHCR7 is a multispanning ER membrane protein with a highly diverged SSD. Thus, it is presumably a substrate for one (or more) of the several mammalian ERAD ubiquitin ligases. So far, MARCH6 has been shown to be not involved, leaving open a variety of other pathways that will be interesting to test. Importantly, the mammalian Insigs appear to be uninvolved in degradation. Because we now know that

SSDs are sufficient to promote ERAD and other ER-based quality control processes, it will be important to test the conserved residues for any role in DHCR7 stability or retention. Finally, DHCR7 loss of function causes buildup of intermediate sterols that are normally converted to cholesterol by the enzyme. Perhaps some of these serve as atypical degradation signals, and thus their buildup furthers disease severity by promoting degradation of the already compromised enzyme. Understanding the degradation of this critical enzyme will certainly reveal new aspects of regulated degradation and may pave the way to a novel proteostasis-based approach to this syndrome.

Niemann-Pick Disease

Other SSD-containing proteins are known to be involved in mammalian sterol regulation, including the highly similar Niemann-Pick Type C protein 1 (NPC1) and Niemann-Pick Type C1-Like 1 (NPC1L1).

NPC1L1 is a multispanning membrane protein and transports cholesterol from the intestinal lumen into the cells that line the intestine for uptake, packaging, and export into the bloodstream (Davies et al. 2000, Zhang et al. 2011). It is a critical part of human cholesterol homeostasis, and is a target of the cholesterol-lowering drug ezetimibe (Jakulj et al. 2016). The N-terminal domain of NPC1L1 has been shown to bind to cholesterol, and the protein traffics from the brush border membrane of intestinal epithelial cells to the endosomal compartment upon cholesterol binding, which is thought to regulate the rate of cholesterol uptake (Skov et al. 2011). This

cholesterol dependent trafficking is highly reminiscent of the trafficking of both mammalian and *S. pombe* SCAP, and also NPC1L1's closely related counterpart, NPC1.

Like NPC1L1, NPC1 is a multispanning membrane protein and binds cholesterol (Infante et al. 2008b). Mammalian NPC1 localizes primarily to the lysosome and late endosome, where it and its partner Niemann Pick Type C 2 (NPC2) function as a "tag team" for moving cholesterol from the lysosome and distributing it to the rest of the cell (Subramanian & Balch 2008). Cholesterol bound by NPC2 is passed to NPC1, where it is moved from the lumen of the endosomal compartment to the membrane. This process requires a cholesterol binding domain in NPC1 and also an intact SSD, and is critical for sterol, sphingolipid, and ceramide homeostasis. Mutations in NPC1 and NPC2 cause the deadly neurodegenerative lysosomal storage disorder, Niemann-Pick Type C (Liscum & Sturley 2004, Vanier 2015). Mutations in the cholesterol binding domain and in the SSD both negatively affect cholesterol trafficking. Moreover, while deletion of the *S. cerevisiae* homolog of NPC1, Ncr1, has no obvious phenotypes, mutations in the SSD cause dominant defects sphingolipid and ceramide metabolism. Similarly, mutations analogous to the SCAP activating SSD mutations also cause a gain of function phenotype in mammalian NPC1, resulting in an increase in cholesterol trafficking from the endosome to the ER and the plasma membrane (Loftus et al. 1997).

Until recently, there were no published structures of the SSD. There were several studies which published partial structures of SSD-containing proteins, but

always with the SSD removed. Potentially, the dynamic nature of the SSD made it less than ideal for structural methods. Recently, however, two structures have been published of the entire NPC1 protein (Li et al. 2016, Zhao et al. 2016). It was found that the NPC1 SSD has a pocket capable of accommodating cholesterol, which looks like it is open both to the endosomal lumen and to the inner leaflet of the membrane, potentially providing a mechanistic explanation for NPC1 cholesterol transfer, and explaining why mutations in the SSD affect cholesterol trafficking.

Strikingly, NPC1 also undergoes protein degradation (Nakasone et al. 2014). Like many membrane proteins, mutant and sometimes wild-type NPC1 undergo ERAD during maturation. The most common human disease mutant protein, I1061T, is rapidly degraded and was found to be stabilized by the expression of the Hsp70 and Hsp90 chaperones. When stabilized in this manner, the mutant protein correctly localizes to the endosome and appears to have some function, as it partially rescues the over-accumulation of cholesterol (Schultz et al. 2016). Even wild-type NPC1 associates with chaperones, including Hsp70, Hsp90, and calnexin, and has its half-life increased by proteasome inhibition. Ubiquitination of even the wild-type protein has been detected in cells.

Additionally and more intriguingly, mature NPC1 is specifically degraded upon cholesterol depletion (Schultz et al. 2016). When cholesterol is depleted from cells, NPC1 is ubiquitinated, associates with the SKD1/Vps4 endosomal sorting complex required for transport (ESCRT), and is degraded. Mutations in the ESCRT complex, which has been found to be involved in the regulated ubiquitin-mediated

degradation of a variety of proteins, including plasma membrane nutrient transporters, results in the accumulation of ubiquitinated NPC1. A mutation in the sterol sensing domain of NPC1 (P691S) prevented NPC1 from responding to cholesterol.
Like other SSD proteins, it appears that NPC1 undergoes regulated entry into a proteostasis pathway in response to sterol signal. (Or, in this case, a lack thereof.) Since many human disease mutations which cause Niemann-Pick Type C result in the translation of a partially functional but rapidly degraded protein, a greater understanding of how NPC1 interacts with the proteostasis machinery could open up new avenues for treating this deadly disorder.

Final thoughts

The high selectivity of proteostatic processes has been adapted in many ways to effect regulation. Elucidating these mechanisms of control will hopefully lead to new and creative ways to modify the sterol pathway in a variety of clinical circumstances. Imitating nature's tendency to employ ligand-mediated misfolding could usher in new approaches to protein targeting and new classes of drugs that work through proteostatic mechanisms.

Acknowledgements

This work was supported by NIH grants 5R37DK051996-18 (to R.Y.H.) and 5T32GM007240-40 (to CMG trainee M.A.W.). The authors wish to express their gratitude to members of the Hampton lab and numerous colleagues at the University

of California, San Diego, for oft-tapped input and vibrant discussions. We wish to dedicate this work to the memory of Susan Lindquist, who recently passed, far too soon. She was a remarkable leader in many aspects of proteostasis and an energetic and inspiring colleague. Her work was always creative and cutting edge, and her presence at conferences was an optimal fusion of high-level science and fun interaction. She will be deeply missed.

Chapter One, in part, is a reprint of material accepted for publication, which will appear in: Wangeline, M.A., Vashistha, N. and Hampton R.Y. “Proteostatic Tactics in the Strategy of Sterol Regulation,” Annual Review of Cell and Developmental Biology, Vol 33, 2017. I was the principal author of this paper.

CHAPTER TWO:

Ligand-regulated entry into the Hrd1 ERAD pathway reveals the dark side of allostery

Abstract

HMG-CoA reductase (HMGR) undergoes regulated degradation as part of feedback control of the sterol pathway. In yeast the Hmg2 isozyme of HMGR is keyed to levels of the 20 carbon pathway intermediate geranylgeranyl pyrophosphate (GGPP): increasing levels of GGPP causes more efficient degradation by the HRD pathway, thus bring about feedback regulation of HMGR in response to pathway flux. The HRD pathway is a conserved quality control pathway critical ER-associated degradation of a wide variety of misfolded ER proteins. To understand this regulatory axis, we have explored to role and action of GGPP in this process. We have found that GGPP is highly potent as a regulatory molecule. In an in vitro limited proteolysis assay, GGPP caused a change in Hmg2 folding state that is required for regulated degradation, and functions in this regard in the low to mid nanomolar region of concentration. The structural effect of GGPP is required for regulated degradation of Hmg2, and is absent in a variety of stabilized or non-regulated mutations of the protein. Consistent with its high potency, the effects of GGPP are highly specific; other closely related molecules are 100s of times less potent or completely ineffective in affecting Hmg2 structure. Strikingly, two close GGPP analogues, 2F-GGPP and GGSPP are completely inactive at all concentrations tested. Furthermore, the GGSPP molecule is in fact an antagonist of the GGPP effects on Hmg2 both in vivo and in vitro. The effects of GGPP on Hmg2 structure and degradation are reversed by a variety of chemical chaperones, indicating that GGPP causes selective misfolding of Hmg2. Taken together, these data indicate that GGPP functions in a manner analogous

to an allosteric ligand, causing Hmg2 misfolding through interaction with a reversible, specific binding site highly specific for the GGPP structure. Consistent with this, the Hmg2 protein forms mulitmers, and this association is not altered by the presence or absence of GGPP. We propose that this "allosteric misfolding" may be a widely used tactic of biological regulation, with potential for development of small molecules that similarly cause selective misfolding to bring about desired destruction of a pharmaceutical target. We suggest that this type of "misfolding by allostery" be called mallostery, to include both the ideas of misfolding and allosteric regulation in a single portmanteau.

Introduction

Protein quality control includes a variety of mechanisms to ensure tolerably low levels of misfolded proteins in the living cell. Among these, selective degradation of misfolded, damaged or un-partnered proteins is often employed for removal of these potentially toxic species. One of the best characterized pathways of degradative quality control is ER-associated degradation (ERAD), entailing a group of ubiquitin-mediated pathways that degrade both lumenal and integral membrane proteins of the endoplasmic reticulum (ER) (Hirsch et al. 2009, Mehnert et al. 2010, Needham & Brodsky 2013, Smith et al. 2011). All degradative quality control pathways show a remarkable juxtaposition in their action. They are all highly specific for misfolded versions of the substrate proteins, yet they recognize a wide variety of distinct and unrelated substrates (Amm et al. 2014, Brodsky & Wojcikiewicz 2009). This "broad

selectivity" is based on the ability of the ubiquitination enzymes to recognize or respond to specific structural hallmarks of misfolding shared by a wide variety of client substrates. The details and restrictions of these recognition features are still being discovered due to the apparently wide range of ways that E3 ligases can detect their clients (Brodsky & Wojcikiewicz 2009, Gardner et al. 1998, Rosenbaum & Gardner 2011, Sato et al. 2009).

The remarkable selectivity for misfolded proteins positions degradative quality control as a powerful tactic for physiological control of normal proteins. It is now clear that a number of cases exist where a normal protein can enter a bone fide quality control pathway to bring about its physiological regulation (Foresti et al. 2013, Gill et al. 2011, Hampton & Garza 2009, Hampton et al. 1996, Roitelman & Simoni 1992, Sever et al. 2003b, Wojcikiewicz et al. 2009). The best studied example of this sort of control is the regulated degradation of HMG-CoA reductase (HMGR), a rate limiting enzyme of the sterol synthetic pathway. In both mammals and yeast, this essential enzyme undergoes regulated degradation in response to molecular signals from the sterol pathway as a mode of feedback control of sterol synthesis. In both cases, ERAD pathways are employed to bring about the regulated degradation of the normal enzyme, allowing for a deep understanding of selectivity in ERAD, and holding the promise for development of new strategies to control the levels of individual protein targets.

Our studies of sterol regulation in S. cerevisiae show that the HRD ERAD pathway mediates the regulated degradation of the Hmg2 isozyme of HMGR. The

HRD pathway is centrally involved in mitigating ER stress through ubiquitin-mediated degradation of a wide variety of misfolded, ER resident lumenal and integral membrane proteins (Bays et al. 2001, Bordallo et al. 1998, Hampton et al. 1996, Hiller et al. 1996). The primary signal for Hmg2 degradation is the 20 carbon sterol pathway product geranylgeranyl pyrophosphate (GGPP) which is produced during normal cell anabolism and is thus a fiduciary indicator of sterol pathway activity (Garza et al. 2009b). When levels of GGPP are high, HRD dependent degradation of Hmg2 increases, and when GGPP levels are low, Hmg2 becomes more stable, thus effecting feedback control at the level of enzyme stability. It was initially surprising that this central quality control pathway is required for the precisely regulated degradation of normal Hmg2. Because the HRD pathway functions to remove misfolding proteins, we had previously posited that GGPP functions by promoting a change in the structure of Hmg2 to a better HRD pathway substrate, thus employing the selectivity of the HRD machinery for purposes of physiological regulation. The studies herein test and explore that idea.

We find that indeed GGPP directly influences the structure of the Hmg2 multispanning anchor, in the concentration range of low to mid nanomolar. These potent actions of GGPP are highly specific, and in fact can be antagonized by close GGPP analogues, both in vivo and in vitro. Furthermore, the effects of GGPP are blocked by a variety of chemical chaperones, indicating that this molecule causes remediable misfolding of the Hmg2 structure to promote HRD recognition. Taken together, these studies lead to a natural model of regulated quality control as a form of

allostery that may be widely employed in biology to harness the intrinsic specificity of the many branches of degradative quality control. Because this axis of ligand-dependent regulation appears to be based on reversible misfolding due to specific ligand binding, we have given it the name “mallostery: to reflect both the elements of misfolding implied by the prefix, and the action of a selective regulatory ligand that hallmarks allosteric control of many enzymes and other proteins.

Results

Specificity and potency of isoprenoids that stimulate Hmg2 degradation in vivo

In our earlier work, we tested the effects of a variety of sterol pathway molecules on Hmg2 stability (Gardner et al. 2001a, Garza et al. 2009b). We found that only the 20-carbon isoprenoid geranylgeranyl pyrophosphate (GGPP) caused Hmg2 degradation *in vivo* when added to culture medium (Garza *et al.,* 2009*)*. This surprising ability of exogenous GGPP to stimulate Hmg2 degradation has been a useful feature for study of this regulatory signal (Theesfeld & Hampton 2013, Theesfeld et al. 2011). Because this response is part of a selective negative feedback loop, we posited that the signal would be specific, physiologically relevant, and highly potent. To more systematically evaluate these ideas, we first performed dose response experiments on pathway isoprenoids alone and in combination.

We examined the effects of candidate isoprenoids on Hmg2 stability *in vivo* using flow cytometry on cells expressing Hmg2-GFP, which undergoes regulated degradation identical to the native enzyme (Gardner & Hampton 1999a), but provides

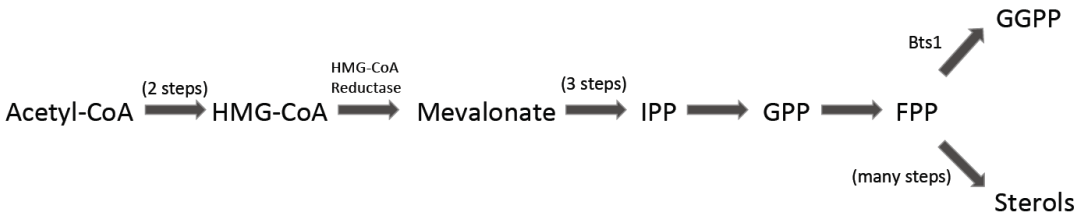

Figure 2.1. The mevalonate pathway
Schematic of the basic sterol synthetic pathway, showing relative positions of GGPP and other molecules mentioned in the studies.

no additional enzymatic contribution to signal production. Each was tested at a variety of concentrations by direct addition to yeast cultures, followed by a 1 hour incubation and flow cytometry. GGPP caused Hmg2-GFP degradation at culture concentrations as low as 1 μM, reaching a maximum at approximately 20 μM (Figure 2.4). The effect of GGPP on Hmg2-GFP was highly specific: the 15 carbon farnesyl pyrophosphate (FPP) and the non-phosphorylated 20 carbon geranylgeraniol (GGOH) had no effect *in vivo*. Similarly, neither of the earlier pathway isoprenoids, isopentenyl pyrophosphate (IPP) or geranyl pyrophosphate (GPP), had any effect on Hmg2-GFP at concentrations up to 27 μM. Because GGPP is synthesized by addition of the 5 carbon IPP (Figure 2.1 and 2.3) to FPP, we also tested if addition of both FPP and either of the interconvertible precursors might simulate direct addition of GGPP by allowing synthesis of this regulator from these precursors. Accordingly, we also treated cells simultaneously with the combinations IPP and FPP, or GPP and FPP. Neither of these co-additions had any effect.

These results indicated a clear structure-function relationship for GGPP as a degradation signal, since similar molecules did not act to stimulate Hmg2 degradation. We were curious how stringent the structural features of GGPP were, so we next tested two close analogues of GGPP: 2F-GGPP and GGSPP (Figure 2.12 and 2.15). Despite the striking similarity to GGPP, neither of these molecules stimulated Hmg2 degradation in vivo at even very high concentrations. Thus, the in vivo effect of GGPP on Hmg2 degradation appeared to be highly specific. The high specificity of GGPP the in vivo

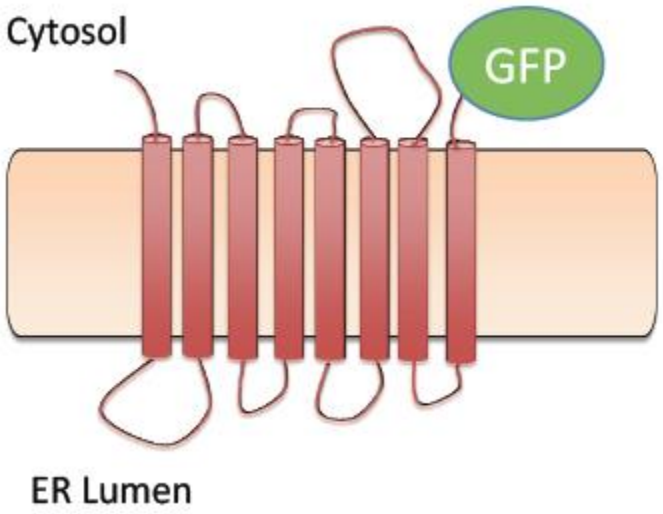

Figure 2.2. Schematic of Hmg2-GFP
Representation of Hmg2-GFP, a multispanning integral membrane ER protein and HRD pathway substrate. Hmg2-GFP undergoes normal regulated degradation, but has no catalytic activity. In this construct, GFP replaces the C-terminal cytoplasmic catalytic domain.

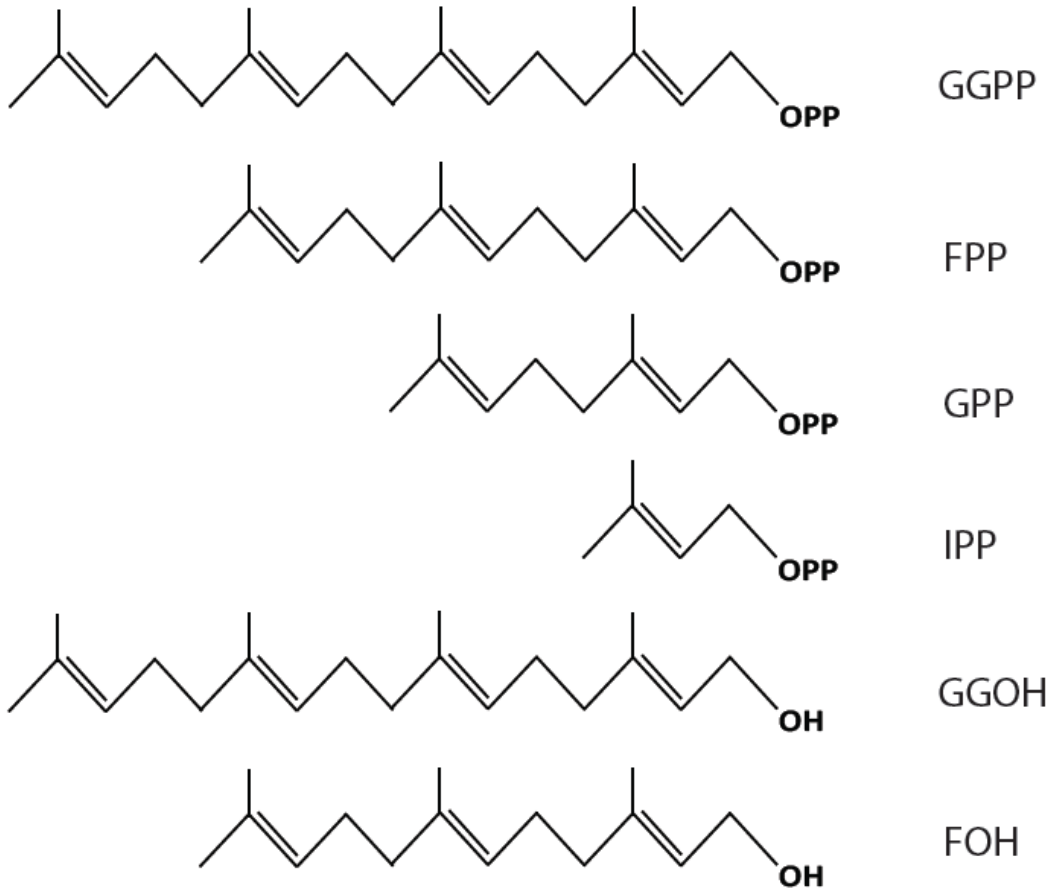

Figure 2.3. Selected structures of isoprenoids used in this study
Structures of key sterol pathway molecules studied in this work, including the potent biological regulator of Hmg2, GGPP.

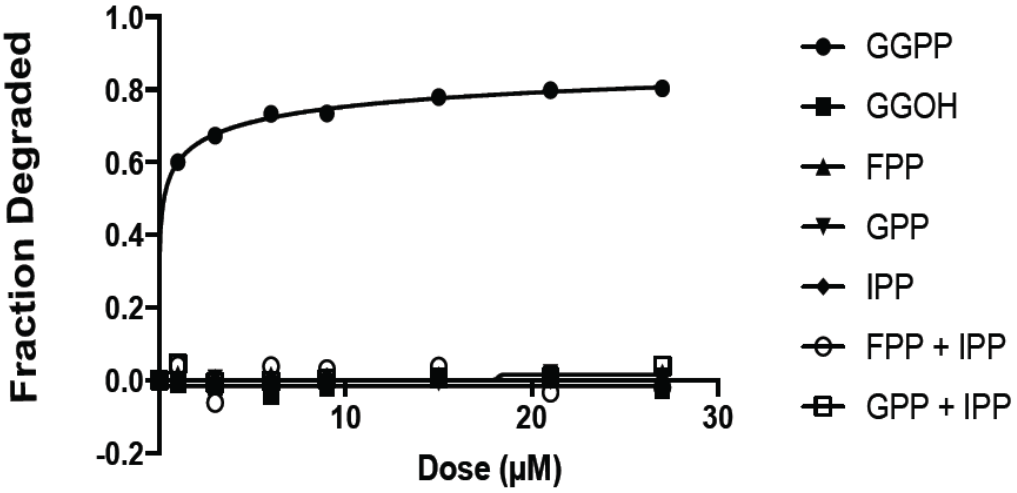

Figure 2.4. Effects of GGPP and related molecules on Hmg2-GFP in vivo
In vivo dose-response curve of the molecules pictured in 1c for loss of in vivo fluorescence after a 1 hour 30o C incubation after direct addition of indicated compounds to culture medium and flow cytometry, counting 10,000 cells. Fractional degradation is the difference in fluorescence initially versus 1 hour, as a fraction of initial fluorescence.

assay could have a variety of explanations so we turned to a previously employed in vitro approach to directly evaluate the action of GGPP on regulated stability of Hmg2.

In vitro analysis of GGPP action on Hmg2

Our early studies described a limited proteolysis assay for studying the effects of small molecules and expressed proteins on the structure of the Hmg2 transmembrane domain (Shearer & Hampton 2004, 2005). The assay uses myc_L-Hmg2-GFP, a version of Hmg2-GFP with an added single myc tag inserted into the first luminal loop of the transmembrane domain (Figure 2.5). The exact placement of lumenal tag along the Hmg2 sequence provides two key features: first, it does not perturb in vivo regulation of the resulting protein. Second, because the myc tag is present in the lumenal space, complete proteolysis of the tagged Hmg2 can be accomplished by addition of proteases to the cytoplasmic side of ER-derived microsomes without loss of myc signal (Shearer & Hampton 2004). Because ER microsomes from yeast are almost completely cytosol-side-out (Kreft et al. 2006), expression of myc_L-Hmg2-GFP allows facile analysis of structural features of microsomal Hmg2-GFP with a simple limited proteolysis assay (Flury et al. 2005; Shearer & Hampton 2004, 2005; Theesfeld et al. 2011).

When microsomes isolated from cells expressing myc_L-Hmg2-GFP are treated with a low concentration of trypsin, immunoblotting the protected myc eptope after SDS-PAGE reveals a characteristic time-dependent pattern of proteolyzed fragment production (Figure 2.6). Because the myc tag is protected, the total myc

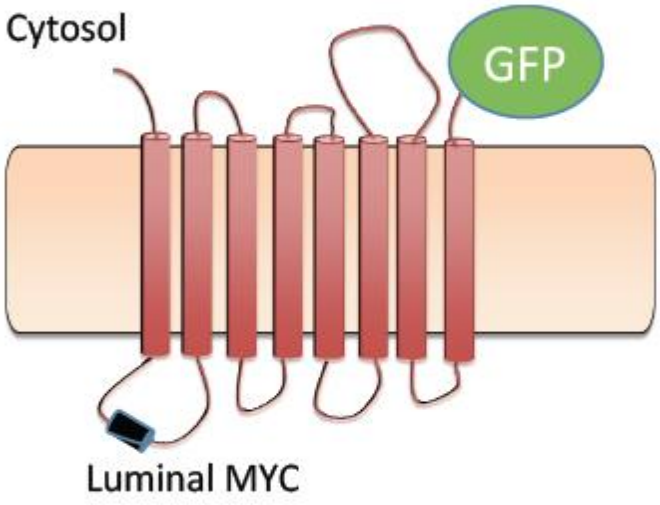

Figure 2.5. Schematic of luminal myc Hmg2-GFP
Cartoon of 1myc-Hmg2-GFP. Fully regulated Hmg2-GFP with protected lumenal 1myc epitope to allow limited proteolysis assay of Hmg2 stucture in isolated microsomes, as described below and in (Shearer & Hampton 2004)

immunoblotting signal intensity is unchanged by proteolysis. We developed this assay to explore how signals from the sterol pathway affect the structure of Hmg2 to render it more susceptible to the HRD quality control pathway (Shearer & Hampton 2005). In those early studies we found that the rate of myc_L-Hmg2-GFP proteolysis was altered by manipulations that affect the in vivo stability of the protein, such that in vitro proteolysis occurred more rapidly when microsomes were prepared from strains where the degradation signals are high (Shearer & Hampton 2005). In vivo, Hmg2 or Hmg2-GFP is strongly stabilized by chemical chaperones (Gardner et al. 2001b). Similarly, proteolysis of microsomal myc_L-Hmg2-GFP is drastically slowed by addition of the chemical chaperone glycerol, and this structural change is fully reversible (Shearer & Hampton 2004). We employed this in vitro structural assay to explore the possibility that sterol pathway signals directly affected the structure of Hmg2 to allow regulated degradation. In those studies, we showed that the 15 carbon neutral isoprenoid farnesol (FOH) caused significant acceleration of in vitro myc_L-Hmg2-GFP trypsinolysis, again preserving the cleavage pattern but altering the kinetics (Shearer & Hampton 2005). This effect of FOH was fully reversible. Furthermore, mutants of Hmg2-GFP that do not respond to in vivo degradation signals, including a substitution of a small number of amino acids known as “TYFSA”, or a single point S215A point mutant of a highly conserved residue of the sterol-sensing domain (SSD), do not respond to farnesol in the limited proteolysis assay (Shearer & Hampton 2005, Theesfeld et al. 2011). Although those results were

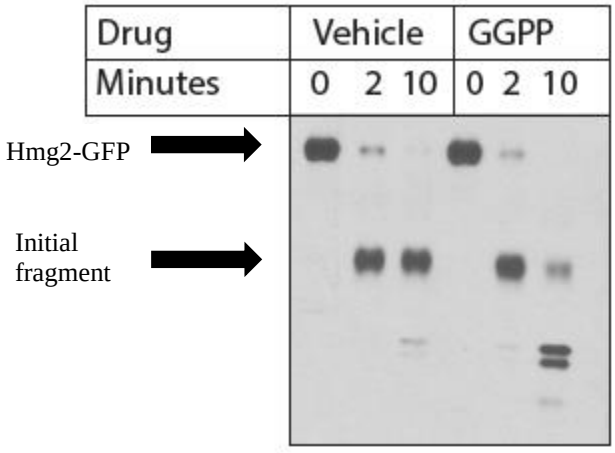

Figure 2.6. Effect of GGPP on limited proteolysis assay
Nine μM GGPP added to microsomes immediately before incubation with trypsin, followed by SDS-PAGE and myc immunoblotting as described. The initial size of 1myc-Hmg2-GFP before proteolysis is indicated with an arrow labeled "Hmg2-GFP." The size of the first fragment, which results from rapid and unregulated cleavage in the linker between the membrane domain and GFP is marked "initial fragment."

intriguing and biologically appropriate, the role of farnesol per se was unclear. Although there was a clear structure-activity relationship for farnesol in the proteolysis assay, the concentrations required to cause the in vitro effects were very high (EC_{50} ~ 100 uM), and farnesol is extremely toxic to yeast. In the times since these studies, we discovered that the bone fide physiological regulator was the normally made isoprenoid GGPP, which also caused the structural transition of Hmg2-GFP in the proteolysis assay (Garza et al. 2009b). Accordingly we returned to this assay to evaluate the specificity and potency of GGPP in this more controlled setting.

In striking contrast to FOH, we found that GGPP was a potent modifier of Hmg2 structure. GGPP accelerated in vitro trypsinolysis at concentrations as low as ~15 nM, with an apparent half-maximum concentration lower than 200 nM (Figure 2.7 and 2.9). Intriguingly, this concentration is in the range of the K_M of yeast enzymes that use GGPP as a substrate (Jiang et al. 1993, Stirtan & Poulter 1997, Witter & Poulter 1996), indicating that this concentration is likely physiologically relevant since the enzymes are "tuned" to concentrations of substrate that exist in their milieu. The maximal effect of GGPP was similar to that seen with the largest effects of FOH reported earlier, about a 5 fold increase in proteolysis rate. The highly stable mutant S215A, which previously did not respond to FOH in the in vitro assay, also did not respond to GGPP at any concentration tested (Figure 2.8 and 2.9).

To investigate the specificity of this potent effect of GGPP, we directly compared a variety of isoprenoid molecules, GGOH, FPP, and FOH all of which we have previously shown accelerate proteolysis to some degree. While all three had, to

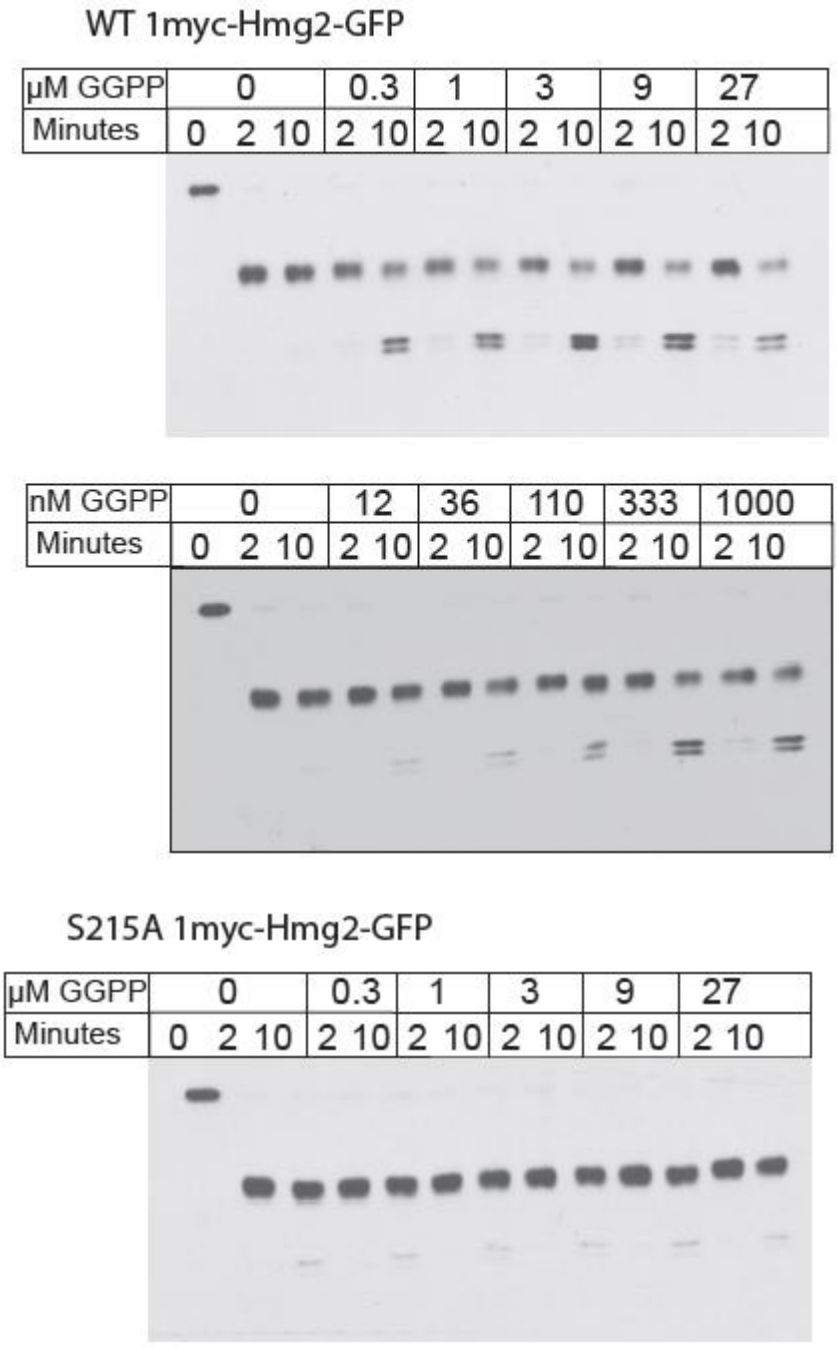

Figure 2.7. In vitro dose response of GGPP

Effect of various concentrations of GGPP on 1myc-Hmg2-GFP with normal transmembrane region or the highly stable S215A point mutation in the SSD. Concentrations of GGPP are listed in µM (top and bottom) or nM (middle). Note effect begins at approximately 12 nM GGPP.

varying degrees, altered Hmg2-GFP structure at very high concentrations, their effects occurred at half-maximum concentrations over 100 fold higher than GGPP (Figure 2.7-2.9). We next tested the close structural analogues of GGPP, 2-fluoro GGPP (2F-GGPP) and S-thiolo GGPP (GGSPP), since these were inactive in the in vivo assay. Even in the direct in vitro assay, neither analogue induced the structural transition at any concentration tested, over 40 μM (Figure 2.12 and 2.13).

The much higher potency of GGPP compared to isoprenoid alcohols and non-hydrolyzable analogs raised the question of whether GGPP was being used to covalently modify Hmg2 or another protein in the microsome extract. Though the yeast geranylgeranyl transferase machinery is cytosolic, and thus unlikely to have activity in our washed membranes, we addressed this possibility by testing whether the GGPP effect on Hmg2-GFP was readily reversible. Microsomes were prepared normally and then washed three times in reaction buffer either before or after treatment with vehicle and GGPP. When microsomes were washed before treatment with GGPP, Hmg2-GFP became more susceptible to proteolysis as usual. When microsomes were washed after treatment, GGPP's effect was reversed (Figure 2.10). Furthermore, the treated and then washed microsomes remained competent for the GGPP-induced structural transition: when GGPP was added back to the washed microsomes, Hmg2-GFP again became more susceptible to proteolysis, and to the same extent as the original exposure (Figure 2.11).

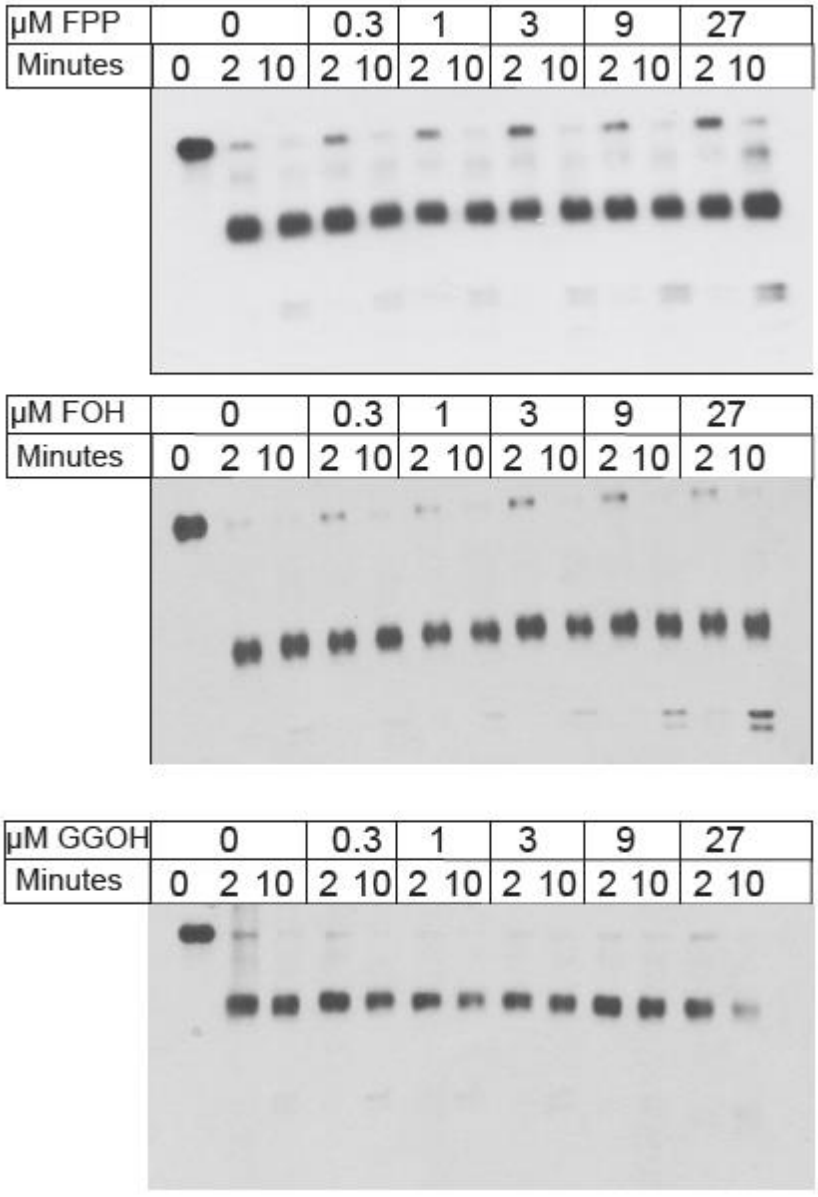

Figure 2.8. **In vitro dose response of other isoprenoids**
Effect of various concentrations of different isoprenoids on 1myc-Hmg2-GFP. Concentrations are listed in µM.

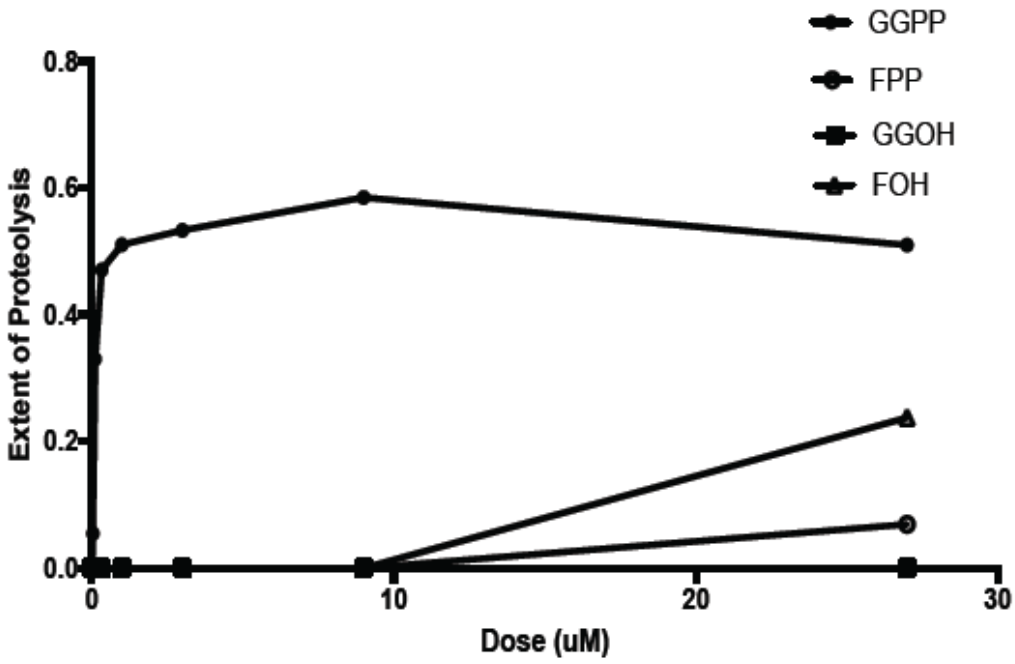

Figure 2.9. **Dose response curves of GGPP and other isoprenoids**
Graphical representation of results in Figures 2.7 and 2.8. Imunoblot films were scanned and pixel counted for total lane intensity and pixels in final doublets that result from extended incubation with trypsin. Extent of proteolysis is a measure of cleavage and calculated as doublet intensity divided by total lane intensity.

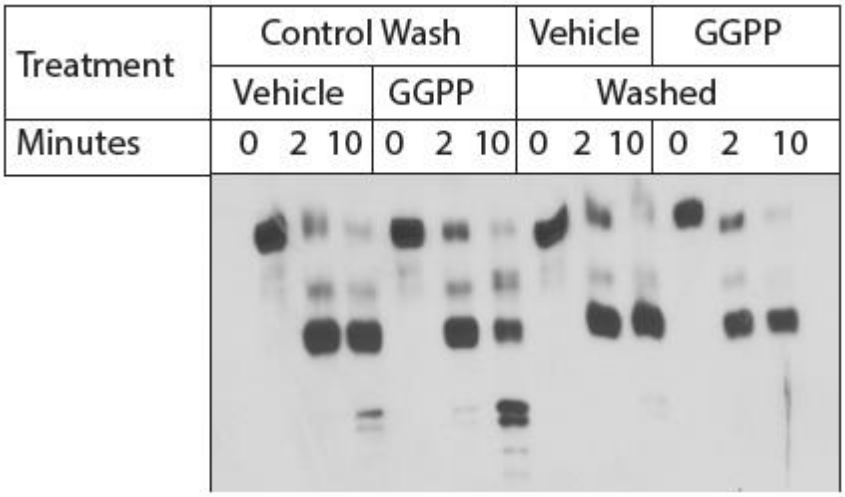

Figure 2.10. **Reversibility of GGPP treatment**
GGPP effect on Hmg2-GFP structure is fully reversible. Microsomes were washed and then treated with vehicle or GGPP (groups 1 and 2) or treated with vehicle or GGPP and then washed (groups 3 and 4). All groups were then subjected to limited proteolysis assay as described.

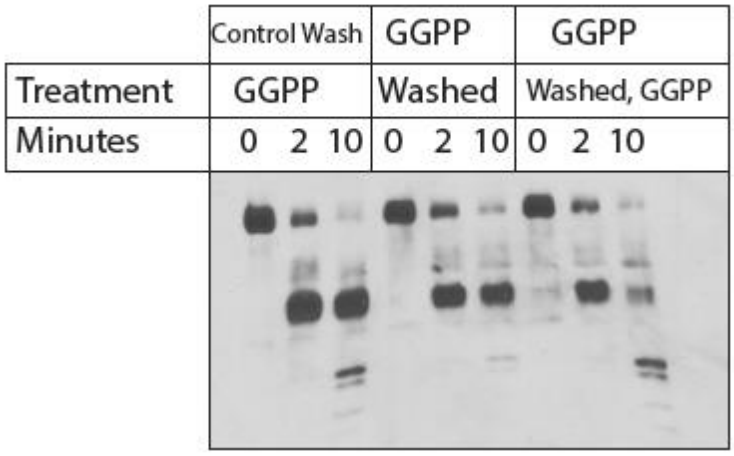

Figure 2.11. **Hmg2 responds to repeated GGPP treatment after reversal**
GGPP effect on Hmg2-GFP structure is fully reversible and effect is maintained after reversal. Microsomes that were treated with GGPP and washed maintained their ability to respond to re-addition of GGPP. Group 1 was washed then treated with GGPP. Group 2 was treated with GGPP then washed, and Group 3 were treated with GGPP, washed, then re-treated with GGPP. All samples were then subjected to limited proteolysis assay.

Antagonism of GGPP action in vitro and in vivo

The GGPP analogues 2F-GGPP and GGSPP had no ability to stimulate Hmg2-GFP degradation in vivo (Figure 2.15), nor alter Hmg2-GFP structure in the limited proteoloysis assay (Figure 2.13). The high potency and specificity of GGPP, and its ability to directly and reversibly alter the structure of Hmg2-GFP made us wonder if it acts as a ligand, causing a structural change by specific interaction with the Hmg2 transmembrane region at a particular binding site, similar to allosteric regulation of enzymes by relevant metabolites. As a test of this idea, we asked if an excess of either of the highly similar, inactive analogues might antagonize the effects of GGPP. Each was tested for an ability to block the structural effect of a low concentration of GGPP by co-incubation with an excess of analog. As expected, the test doses of either analog had no effect on myc_L-Hmg2-GFP (Figure 2.13). However, the presence of a molar excess of GGSPP clearly antagonized the structural effect of GGPP. Interestingly, only one of the analogues had this effect; the 2F-GGPP was simply inactive in an identical experiment (Figure 2.14). This is particularly important since both molecules have very similar chemistry and amphipathicity, both being developed to block the same class of enzymes (Gao et al. 2012, Lin et al. 2010). Nevertheless, only GGSPP antagonized the GGPP-induced structural effects on myc_L-Hmg2-GFP.

We further explored the antagonistic action of GGSPP by examining its effects on GGPP-induced Hmg2 degradation in vivo. Because simultaneous addition of both GGPP and GGSPP could also have interactions on the unknown influx mechanism that appears to operate in yeast, we explored the effect of the inactive analogues on the

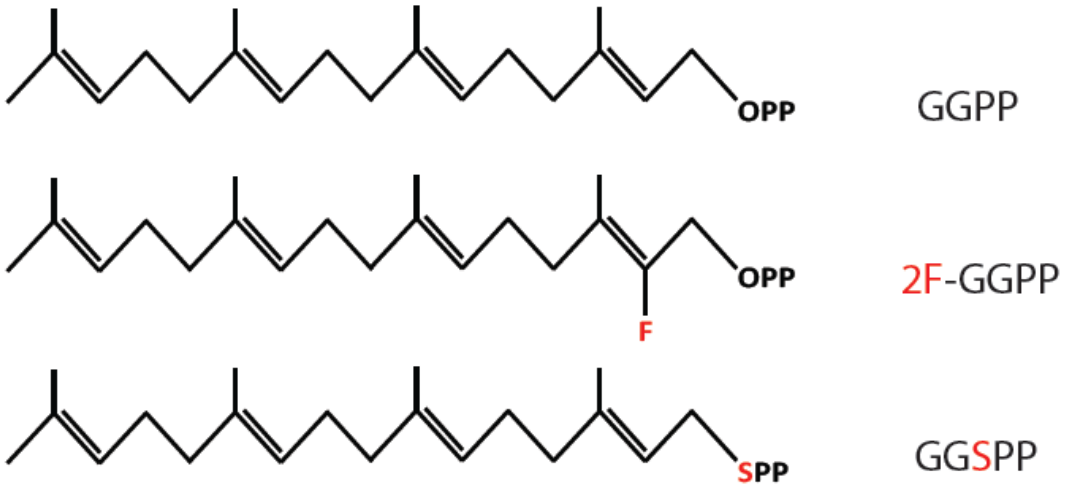

Figure 2.12. Structurally similar analogs of GGPP
Structures of GGPP, 2F-GGPP and GGSPP, tested for activity an antagonism in this figure. Note identical lipid groups of each.

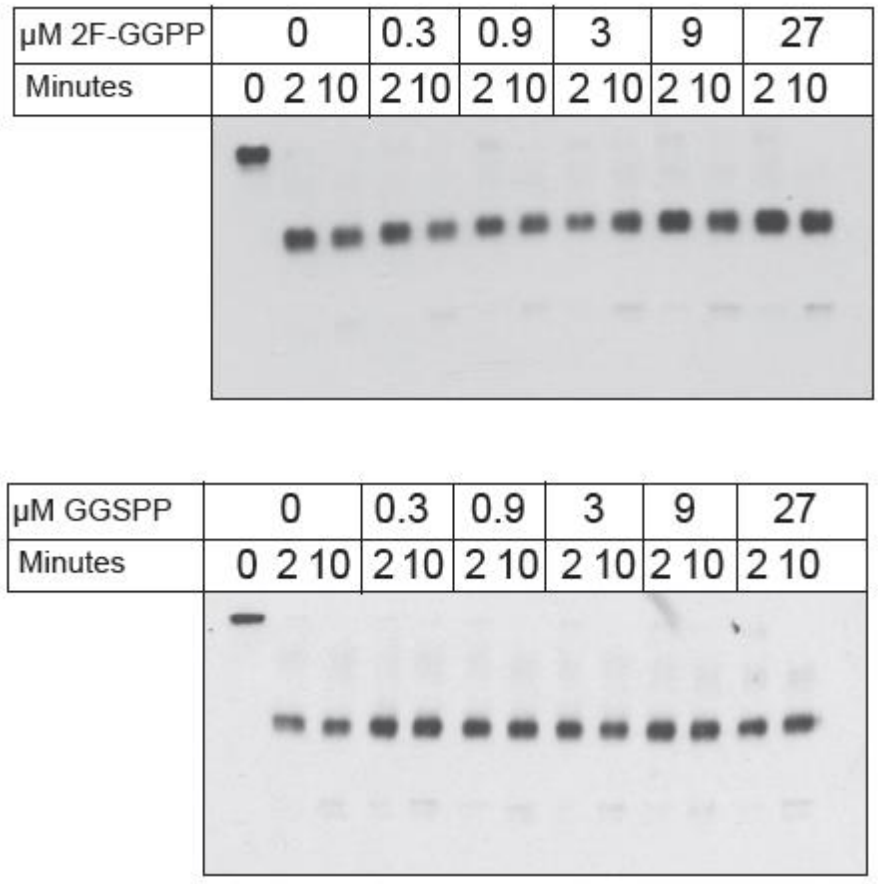

Figure 2.13. In vitro dose response of two inactive analogs of GGPP
Microsomes were incubated with the indicate concentrations of analog (top, 2F-GGPP; bottom, GGSPP) prior to proteolysis. Note neither compound has any effect even at the highest concentration tested.

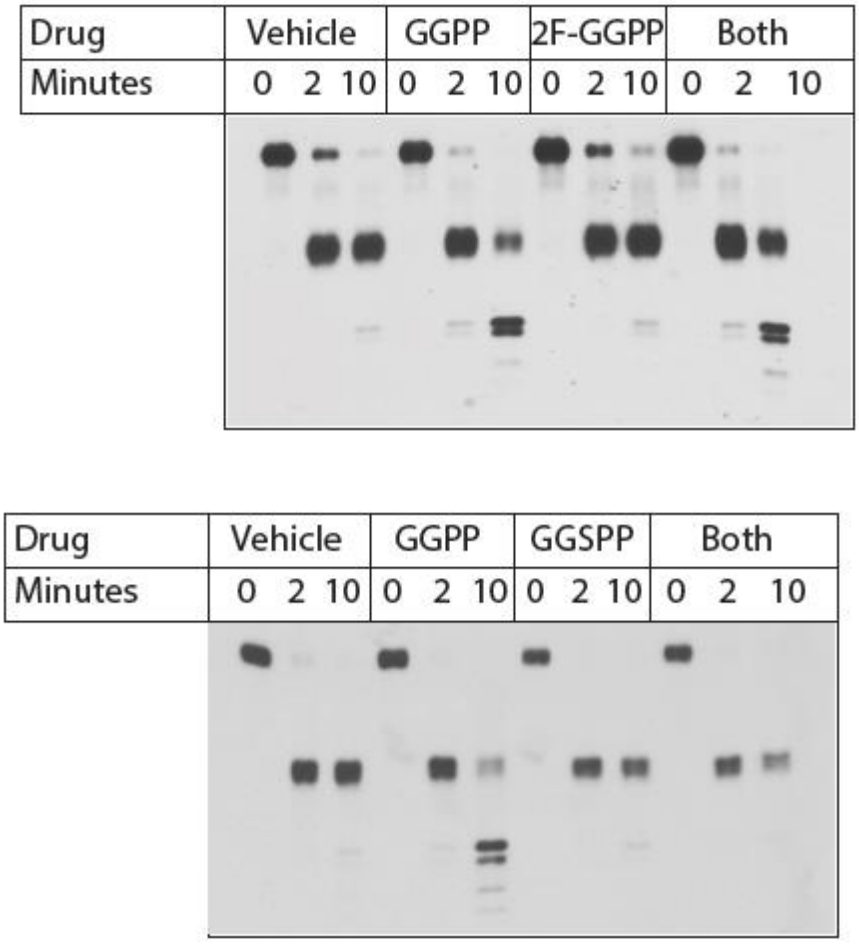

Figure 2.14. Test of antagonism by structurally similar analogs to GGPP
Test of each inactive GGPP analogue of antagonism of GGPP effect in limited proteolysis assay. On both panels, 3 μM GGPP was added where indicated, and 44 μM of indicated analogue (top, 2F-GGPP; bottom, GGSPP) was used. Microsomes were tested for effects of no addition, addition of each molecule, or the pair added together to test for antagonism. 2F-GGPP was tested on the left panel, and GGSPP was tested on the right panel. Note only GGSPP antagonized the effect of GGPP.

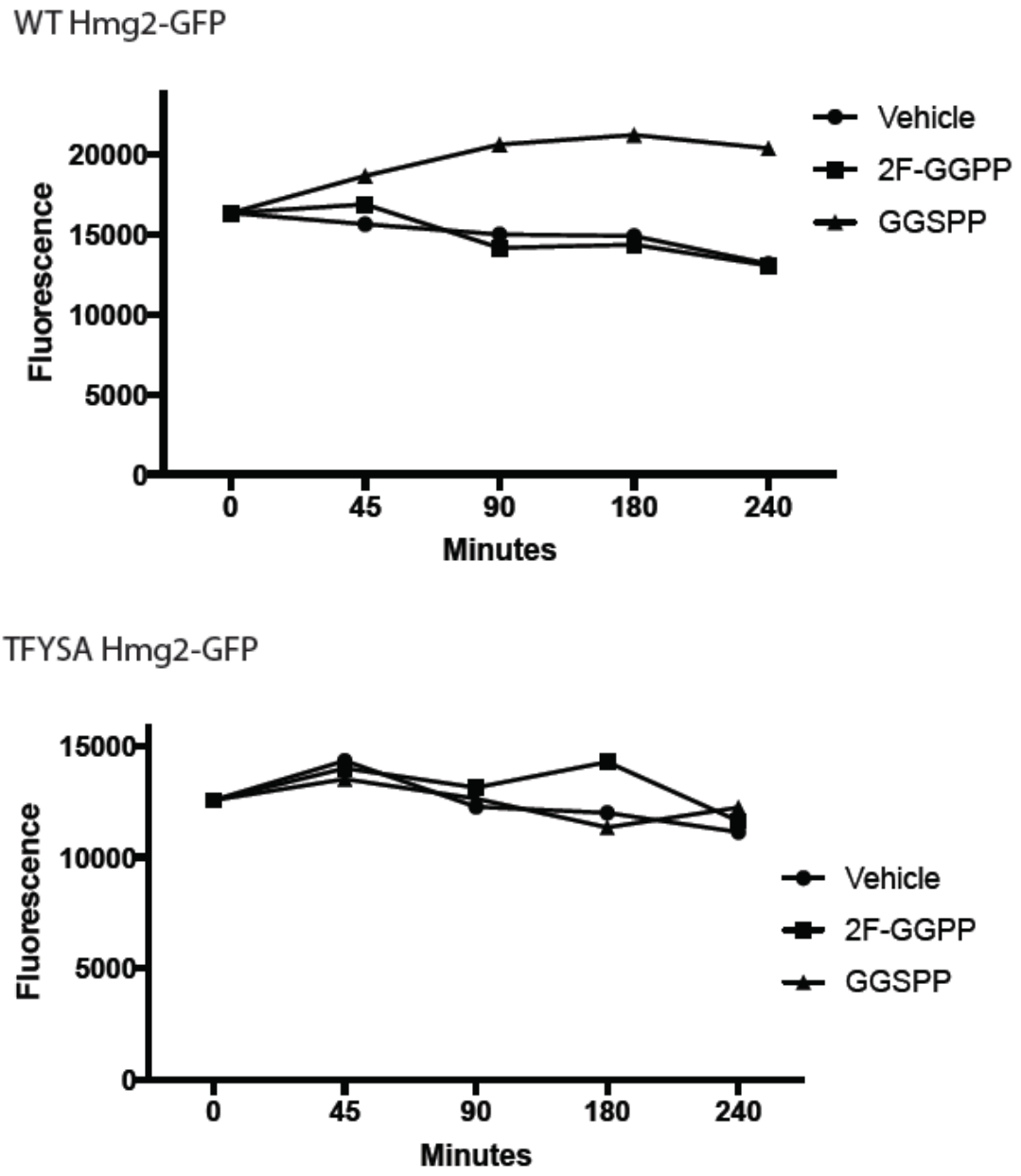

Figure 2.15. In vivo antagonism by a structurally similar analog
Effect of 2F-GGPP (non antagonist in vitro) or GGSPP (antagonist in vitro) on wild type strain with normal production of GGPP due to the sterol pathway, expressing regulated Hmg2-GFP (top) or non-regulated TYFSA mutant of Hmg2-GFP (bottom). All graphs show average fluorescence by flow cytometry of 10,000 cells.

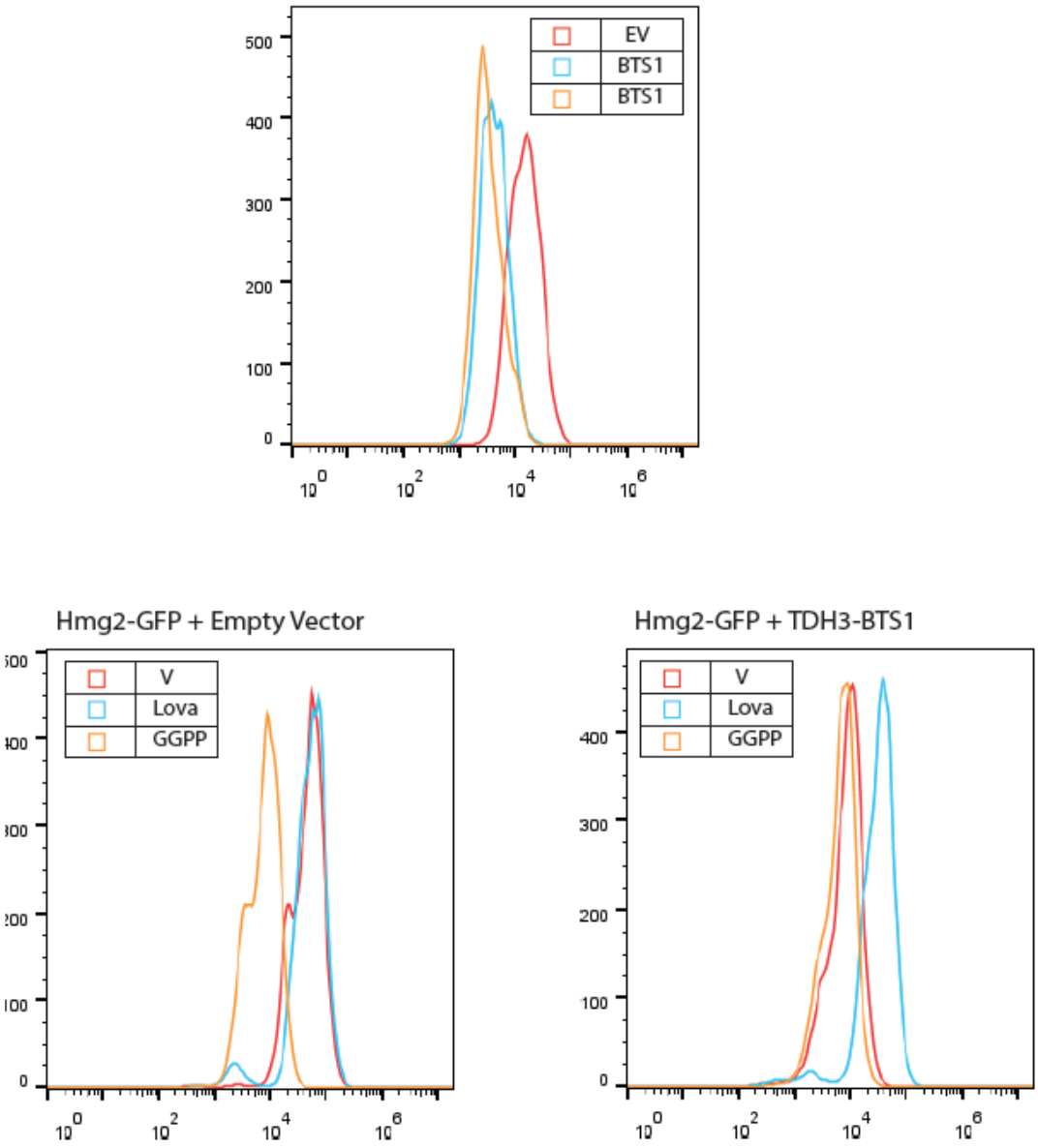

Figure 2.16. The sensitized, rapidly degrading TDH3-Bts1 strain

Strains with elevated GGPP production due to strongly expressed BTS1 gene encoding GGPP synthase. Left panel, steady-state fluorescence of strains expressing empty vector (red) or integrated BTS1 expression plasmid (blue, orange), showing strong shift in steady-state level of Hmg2-GFP fluorescence due to elevated endogenous GGPP production. Middle panel, effect of lovastatin (blue) or GGPP (orange) on Hmg2-GFP fluorescence on empty vector strain. Right panel, same experiment with a BTS1-expressing plasmid present; note addition of GGPP has little further effect and that lovastatin, that blocks GGPP production due to elevated BTS1, causes strong stabilization.

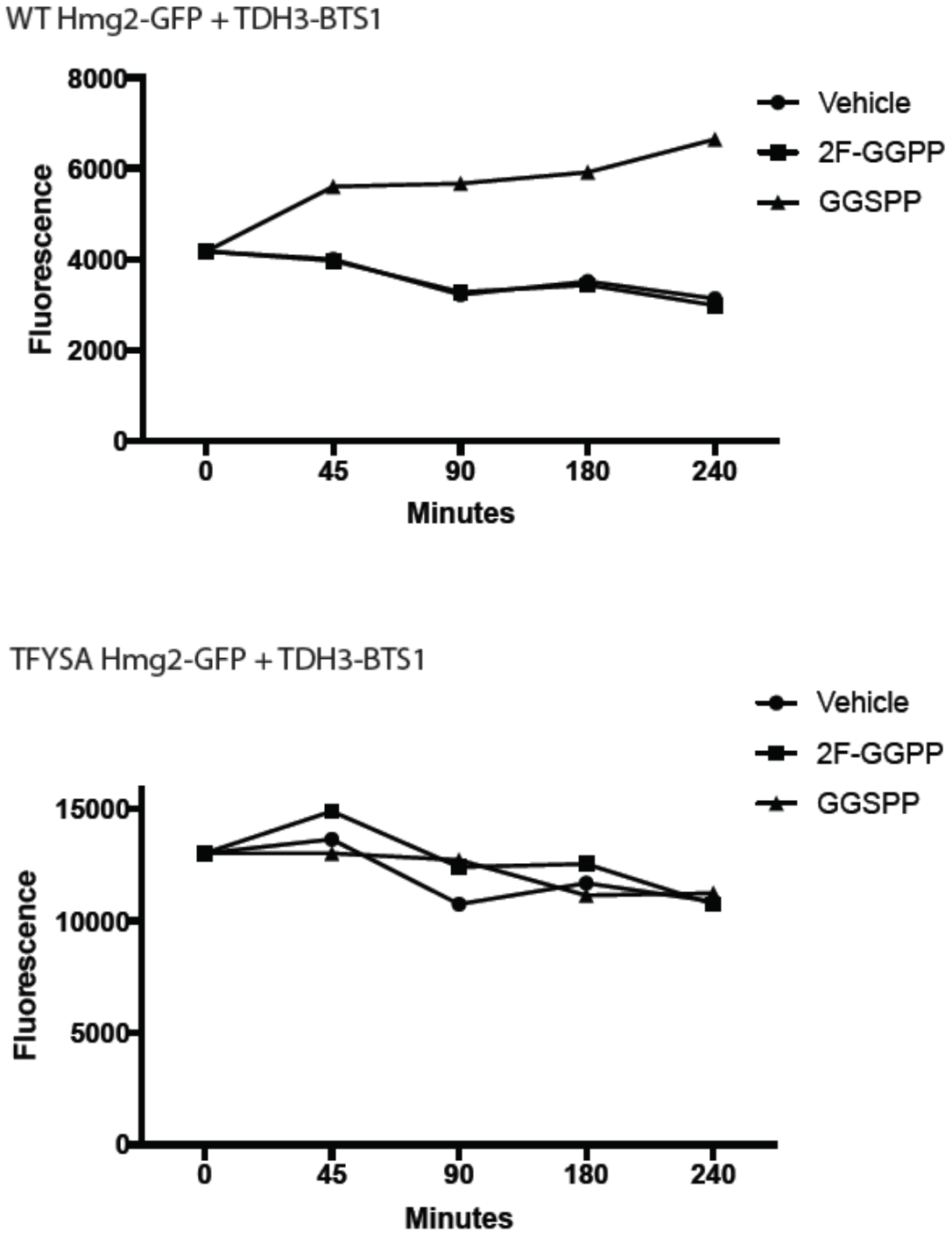

Figure 2.17. In vivo antagonism by a structurally similar analog in the sensitized Bts1 strain

Effect of GGPP analogues on Hmg2-GFP steady state levels in strains with elevated GGPP due to BTS1 expression. Same experiment in 4a, but with strains strongly expressing BTS1 to increase GGPP and Hmg2-GFP degradation rate. Left panel strain expresses normally regulated Hmg2-GFP; right panel strain expresses unregulated TYFSA mutant of Hmg2-GFP.

endogenous GGPP degradation signal, which we have extensively characterized (Gardner & Hampton 1999a, Garza et al. 2009b). We first simply added each analogue to a strain with sufficient flux through the sterol pathway to produce the needed GGPP signal for Hmg2-GFP degradation. Specifically, we examined the effect of addition of inactive analogue on the Hmg2-GFP levels during a three hours incubation period. The effects of the analogues were small, but consistent with the in vitro effects of each: 2F-GGPP had no effect, while the GGSPP caused a small but reproducible increase in Hmg2-GFP steady-state (Figure 2.15, top), implying that the added antagonist can block the degradation-stimulating effect of endogenous GGPP. Importantly, an identical experiment with the similarly degraded but unregulated TFYSA mutant of Hmg2-GFP showed no effect of the GGSPP antagonist on steady state levels, indicating that its effect was due to altering the response to GGPP signal, rather than effects on the HRD pathway itself (Figure 2.15, bottom).

To further evaluate in vivo antagonism, we developed a yeast strain that constitutively generates high levels of endogenous GGPP, ensuring continuous strong signal, and thus as high a rate of regulated Hmg2-GFP degradation possible. Although the effect of GGPP was originally discovered by direct addition to living cultures, our studies confirmed that endogenous GGPP was responsible for regulating Hmg2 stability (Garza et al. 2009b). Endogenous GGPP can be produced by several means, including through the action of the non-essential enzyme GGPP synthase, called Bts1. In our previous work, we genetically manipulated the levels of the Bts1 by expressing it from the strong galactose-inducible GAL1 promoter. Capitalizing on this mode of

GGPP generation, we made a yeast strain that constitutively expressed Bts1 from the similarly strong TDH3 promoter, to cause continuous endogenous production of high levels of GGPP. Expression of TDH3-Bts1 decreased steady state Hmg2-GFP levels by about five-fold from wild-type strains (Figure 2.16, top) and further addition of GGPP to culture media did not further decrease Hmg2-GFP (Figure 2.16, bottom right, orange curve), indicating that TDH3-Bts1 is producing maximally effective levels of GGPP. To confirm that the Bts1 was producing GGPP through the normal sterol pathway, we added the HMGR inhibitor lovastatin to block the normal production of the Bts1 substrates FPP and IPP. As expected, treatment with lovastatin increased Hmg2-GFP levels approximately six-fold (Figure 2.16, bottom right, blue curve). This constitutive high GGPP-producing strain further demonstrated the importance of GGPP in Hmg2 stability control, and allowed further testing its antagonism in vivo. Using the TDH3-Bts1 strain, we again tested the effects of direct addition of the GGPP analogues on Hmg2-GFP levels *in vivo* using flow cytometry. Consistent with the result from wild-type cells, 2F-GGPP did not change Hmg2-GFP levels, while the in vitro GGPP antagonist, GGSPP resulted in a nearly two-fold increase Hmg2-GFP steady state levels over the course of the incubation (Figure 2.17, top). The expression of additional Bts1 had no effects on the in vivo levels of the non-responding mutant TFYSA. Again, neither analog had any effects on this unregulated protein (Figure 2.17, bottom). Taken together, these results indicate that GGPP acts directly on the Hmg2 transmembrane domain, using a binding site with sufficient

structural selectivity to show high potency, stringent structure activity, and specific antagonism both in vivo and in vitro.

Testing GGPP as a ligand that promotes regulated misfolding

We have previously proposed the idea that regulated Hmg2 degradation entails a programed or regulated change to a more unfolded form, thus enhancing the probability of entry into the HRD quality control pathway (Gardner & Hampton 1999b, Shearer & Hampton 2005, Theesfeld et al. 2011). One reason we put forth the regulated misfolding model is the observed stabilization of rapidly degraded Hmg2 by the chemical chaperone glycerol. Addition of glycerol at concentrations required for chemical chaperoning (5-20%) causes rapid and reversible stabilization of Hmg2 that is undergoing in vivo degradation (Gardner & Hampton 1999a). Furthermore, the effect of glycerol is also observed in the in limited trypsinolysis assay (Shearer & Hampton 2004). We had previously shown that the effects of high concentrations of farnesol on Hmg2 were reversed by glycerol, consistent with the other evidence that this lipid causes selective misfolding of Hmg2 in a biologically relevant manner. Accordingly, we tested the ability of glycerol to antagonize the effects of the GGPP-induced structural transition. First, we confirmed glycerol's effects on Hmg2 levels *in vivo*. Addition of glycerol at concentrations required for chemical chaperoning directly to the culture medium increased Hmg2-GFP steady state levels (Figure 2.18), and slowed the degradation rate as measured by cycloheximide chase (Figure 2.18), as expected from earlier studies. We then used glycerol to evaluate the role of misfolding

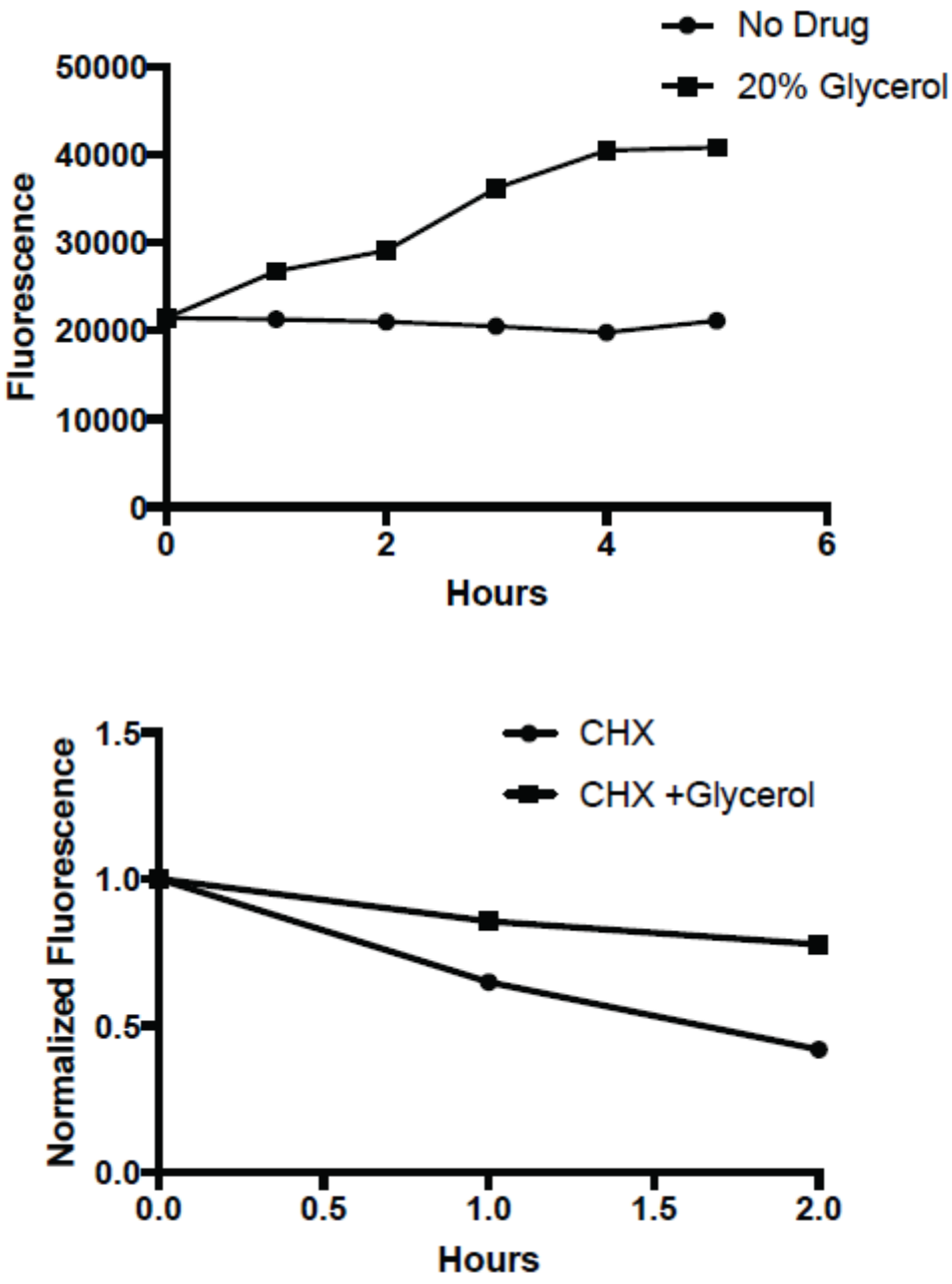

Figure 2.18. **Glycerol stabilizes Hmg2-GFP in vivo**
Effect of 20% glycerol on steady state levels of Hmg2-GFP (top) in living cells over the indicated times after addition, or the degradation rate of Hmg2-GFP (bottom) after addition of cycloheximide (CHX). In CHX chases, fluorescence is normalized to starting value at time of CHX addition.

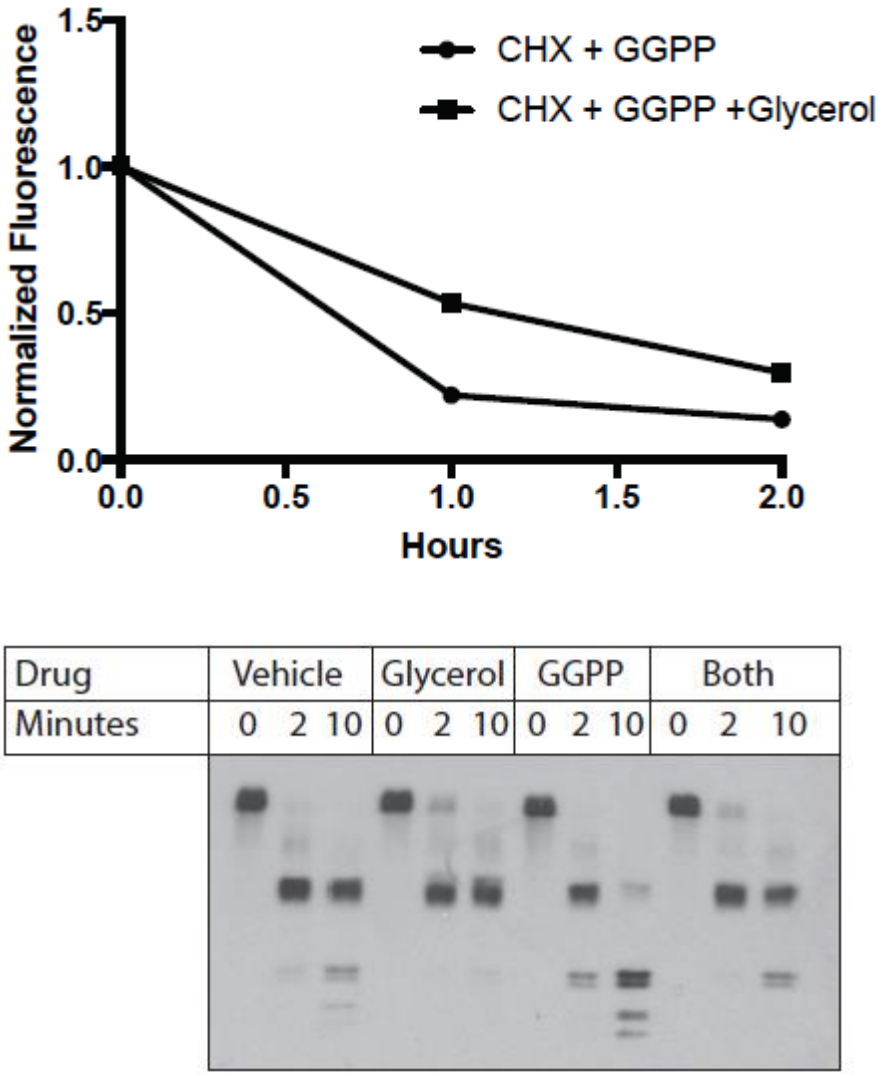

Figure 2.19. Glycerol reverses GGPP action in vivo and in vitro
Glycerol diminished the effect of added GGPP on Hmg2-GFP degradation as measured after CHX addition (top) or on Hmg2-GFP limited proteolysis due to trypisn (bottom). Glycerol was added to cells or microsomes immediately prior to the start of incubations.

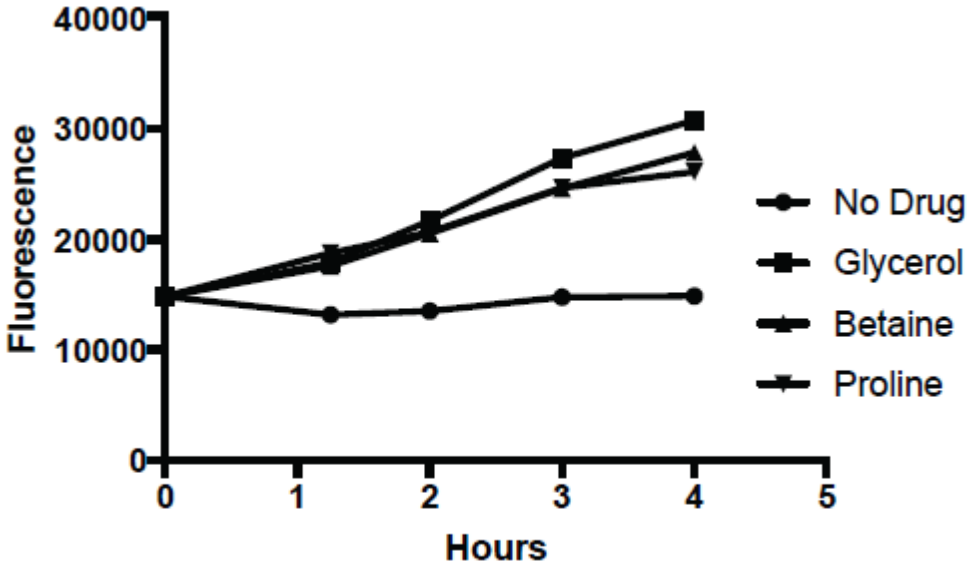

Figure 2.20. Other chemical chaperones stabilize Hmg2-GFP in vivo
Similar effect of two other chemical chaperones, betaine and proline, on Hmg2-GFP steady state in living cells..

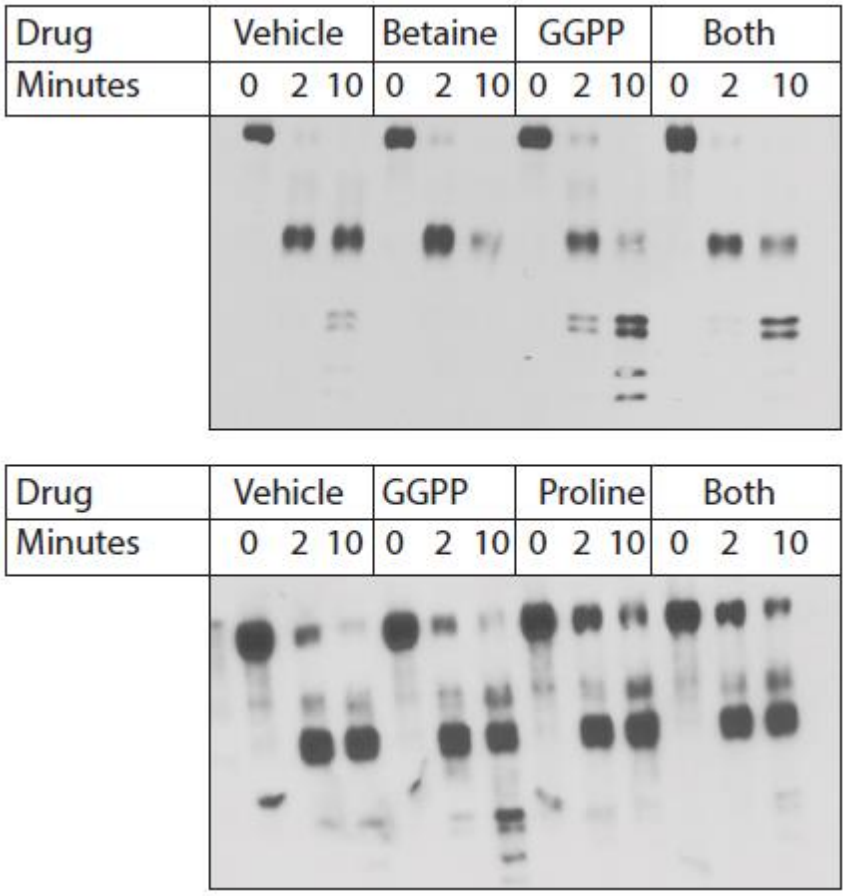

Figure 2.21. Other chemical chaperones reverse GGPP action in vitro
Similar effect of two other chemical chaperones, betaine (top) and proline (bottom), on 1myc-Hmg2-GFP limited proteolysis.

drops from 1.5 hour to approximately 30 minutes. Co-addition of glycerol partially reversed the effects of added GGPP, increasing Hmg2-GFP's half-life to over 1 hour (Figure 2.19, top). We further tested the effect of glycerol using the in vitro proteolysis assay. We treated microsomes from cells expressing myc_L-Hmg2-GFP with 20% glycerol, 27 µM GGPP, or both simultaneously. As expected from earlier work with less specific signals such as FOH (Shearer & Hampton 2005), addition of glycerol decreased the effects of added GGPP, shifting the accessibility closer to that of untreated microsomes (Figure 2.19, bottom).

These results with glycerol are consistent with GGPP causing remediable change in the folding state of Hmg2 both in vivo and in vitro. The concentrations of glycerol required for this effect are consistent with its well-known action as a chemical chaperone. To confirm this misfolding model of GGPP, we tested the effects of two entirely distinct chemical chaperones, proline and betaine. Each molecule similarly increased Hmg2-GFP levels in vivo (Figure 2.20) and reversed the effect of GGPP in vitro (Figure 2.21).

Another indicator of protein misfolding is increased susceptibility to thermal denaturation. We previously showed that treatment with high concentrations of FOH made Hmg2 more susceptible to denaturation, as indicated by the formation of low-mobility electrophoretic species during brief incubation at 70^o C (Shearer & Hampton 2005). We tested GGPP in our assay for thermal denaturation. Surprisingly, treating microsomes from a strain expressing Hmg2-GFP with GGPP at concentrations up to 20 µM did not lead to increased thermal denaturation or formation of low mobility

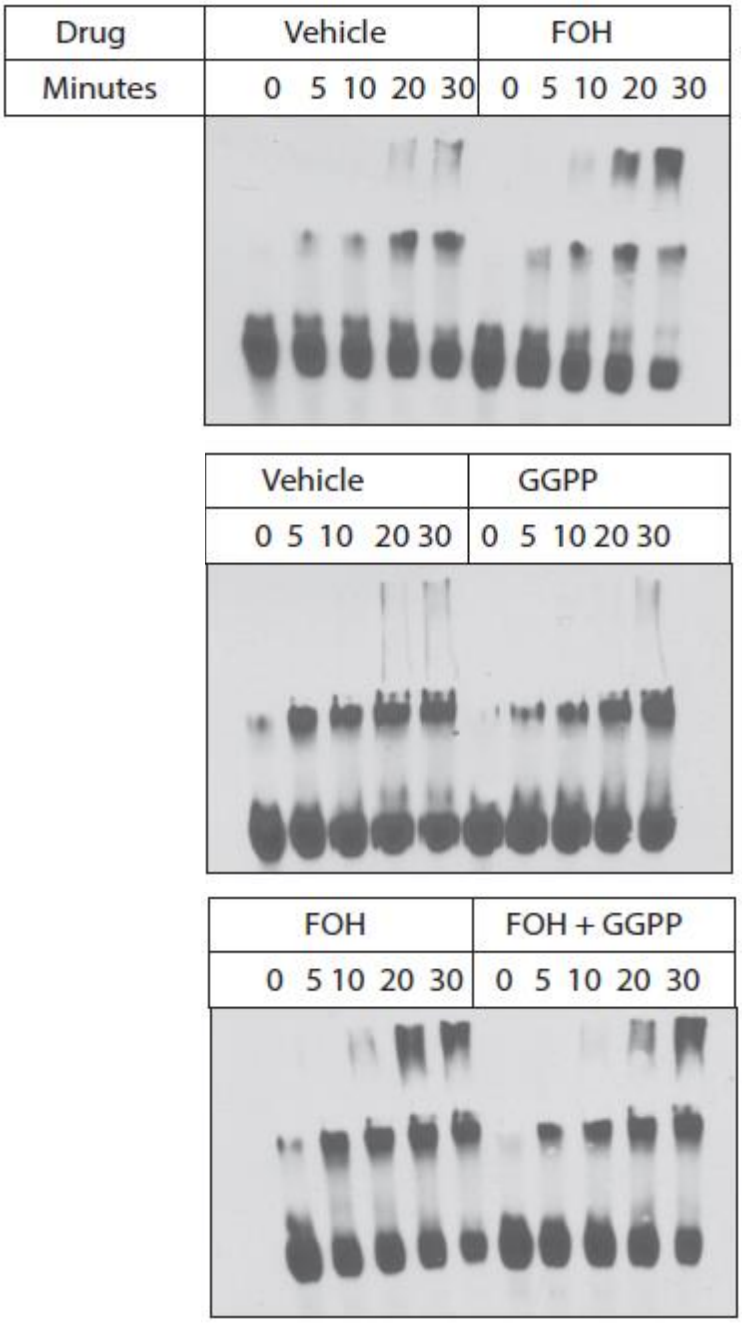

Figure 2.22. Effect of isoprenoids on thermal denaturation of Hmg2-GFP
Effect of GGPP on Hmg2-GFP thermal denaturation, in the presence and absence of FOH. Not that GGPP does not cause enhanced thermal denaturation of Hmg2-GFP, but does mildly antagonize that caused by FOH.

structures. Rather, treatment with GGPP actually slightly decreased thermal denaturation of Hmg2 compared to vehicle (Figure 2.22, middle). Furthermore, when microsomes were treated with both GGPP and FOH, GGPP slightly antagonized the FOH-induced denaturation, providing additional evidence for ligand binding (Figure 2.22, bottom). Thus, although GGPP causes an opening of the Hmg2 molecule similar to FOH, and this effect is reversed by chemical chaperone treatment, the degree of Hmg2's structural transition caused by the potent and physiological GGPP signal is clearly less extreme.

Since the GGPP-caused structural transition is reversible and antagonizable, we drew an analogy to allostery. By this model, GGPP binding to a specific site would alter the structure of Hmg2 to allow a more unfolded structure amenable to better recognition by the HRD machinery, but not gross misfolding of the protein. Although allosteric transitions are usually discussed with respect to enzyme kinetics or related protein functions, it is easily conceivable that a similar alteration in structure could render a substrate more or less susceptible to engagement of quality control machinery. Nearly all allosteric proteins are multimeric, and many require this structural feature for allostery to occur (Ascenzi et al. 2005). We tested whether Hmg2 exists as a multimer using co-immunoprecipitation, modifying our method to analyze in vivo interactions of Hmg2 and other proteins (Neal et al. 2017, Theesfeld & Hampton 2013, Vashistha et al. 2016). Specifically, we co-expressed Hmg2 tagged with GFP and Hmg2 with a myc tag in the linker domain in the same yeast strain. Co-expressing cells were subjected to non-detergent lysis and microsomes were prepared.

Microsomes were then solubilized and Hmg2-GFP was immunoprecipitated. When both tagged constructs were co-expressed in the same strain, immunoprecipitation of Hmg2-GFP caused co-precipitation of 1myc-Hmg2, demonstrating that Hmg2 forms multimeric structures (Figure 2.23). When only Hmg2-GFP or 1myc-Hmg2 was expressed in a strain, we were unable to detect the other tag in input lysates or immunoprecipitations (Figure 2.23).

We next tested whether GGPP levels affect Hmg2 multimerization. We repeated the co-immunoprecipitation experiments using cells treated with lovastatin to decrease GGPP levels *in vivo*, cells treated with added GGPP, or cells treated with only vehicle. In addition, lysis, microsome preparation, and co-immunoprecipiation from the GGPP-treated cells were all performed in the presence of added 22 μM GGPP, a concentration that maximally stimulates in vivo degradation and in vitro structural effects. In all three conditions, immunoprecipitating Hmg2-GFP pulled down the same amount of 1myc-Hmg2, suggesting that GGPP does not affect multimerization (Figure 2.24).

Taken together, these data indicate that the regulation of Hmg2 entry into the widely used and conserved HRD quality control pathway occurs by a specific and reversible interaction with the naturally produced GGPP molecule. Furthermore, the structure-activity of this interaction is stringent, to the extent that closely related structures can antagonize the effects both in vitro and in vivo. A reasonable model for these data is that this represents a form of “folding allostery” by which the GGPP

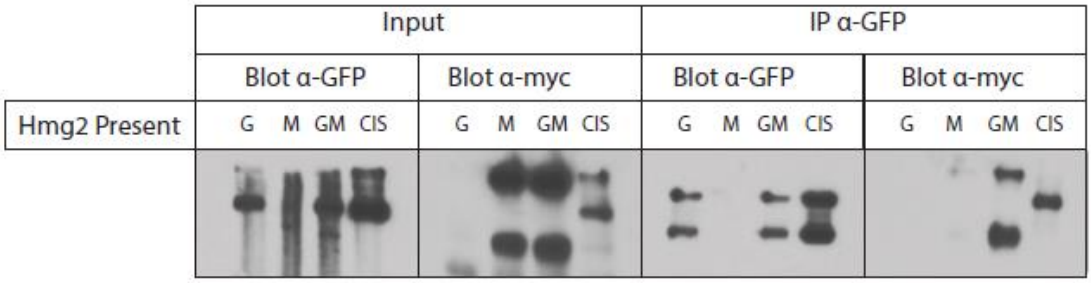

Figure 2.23. Hmg2 forms multimers in vivo

Hmg2 forms multimers. Co-immunoprecipitation of myc-tagged Hmg2 when co-expressed with Hmg2-GFP. Microsomes from strains expressing myc-Hmg2 ("M"), Hmg2-GFP ("G"), or both ("GM") were solubilized with non-denaturing detergent, and subject to GPF immunoprecipitation ("IP α-GFP") and then immunoblotted for GPF or myc as indicated. Inputs of 10% total lysates are shown in the left group ("input"). "CIS" is a strain that expresses a single myc tagged Hmg2-GFP thus putting the myc tag and GFP in cis on the same protein, as a positive control.

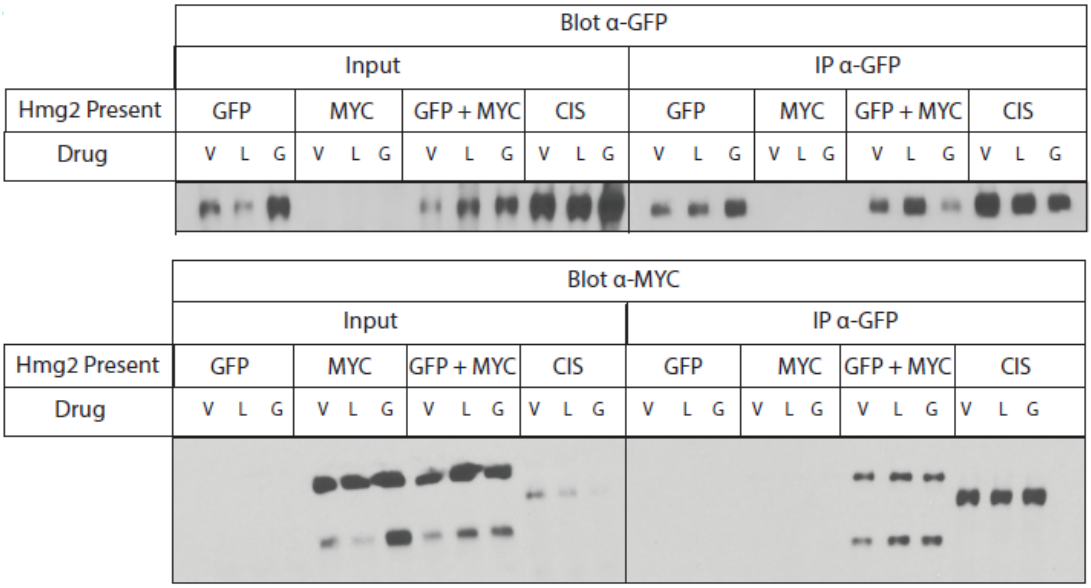

Figure 2.24. GGPP does not affect mutlimerization state of Hmg2
(Lack) of effect of changing GGPP on co-precipitation of myc immunoblot. Experiments as in 6a, but with lovastatin pretreatment (L) as described, to lower GGPP, or added GGPP prior to and during immunoprecipitation to test if altering the regulator had any effect on Hmg2 self-association.

regulator causes a subtle structural transition to a more open or less folded state to promote physiological regulation by constitutive quality control.

Discussion

In these studies we sought to understand the GGPP-mediated regulation of Hmg2 ERAD. This included a detailed study of the structure-function features of GGPP, and the effects this biological regulator had on Hmg2 itself. The emerging model is that GGPP serves as a classic allosteric regulator that, instead of reversibly changing the parameters of enzyme action, instead causes reversible changes in folding state to bring about physiological regulation. The potential of this mode of regulation both for basic understanding and translational implementation are high.

Using flow cytometry, we tested a variety of isoprenoid molecules for their ability to induce Hmg2 degradation in vivo. We also used a limited proteolysis assay of Hmg2's structure to directly examine the action of naturally occurring isoprenoids on Hmg2 structure. We found remarkable specificity for the 20-carbon isoprenoid GGPP both in vivo and in vitro. In vivo, GGPP was the only isoprenoid to induce Hmg2 degradation. In vitro, GGPP's action was both highly potent and specific. The in vitro effect of GGPP on Hmg2 could be observed at concentrations as low as 10 nM, with a half-maximum concentration in the high nanomolar range, consistent with the Km of yeast enzymes which use GGPP, and thus consistent with its role as a physiological indicator of mevalonate pathway activity. Other isoprenoids tested required concentrations orders of magnitude higher to induce changes in Hmg2 folding in the limited proteolysis assay.

Consistent with its high potency, we found that the effect of GGPP showed extreme structural specificity. Two close analogs of GGPP, 2F-GGPP and GGSPP, despite being very similar biophysically, had no effect on Hmg2 structure at any concentration tested. In fact, one of the inactive molecules GGSPP was a GGPP antagonist: GGSPP interfered with GGPP's effects on Hmg2 both in vivo and in vitro. Thus, the action of GGPP showed high potency, high specificity and was subject to inhibition by specific antagonist analog. Taken together, these observations all suggest that GGPP controls Hmg2 ERAD by binding to a specific site on the Hmg2 transmembrane region, much like an allosteric regulator of an enzyme.

We also examined the nature of Hmg2's response to GGPP. Because Hmg2 undergoes regulated entry into the HRD quality control pathway, our early studies examined whether Hmg2 undergoes regulated misfolding to make it a better HRD substrate. Consistent with this model, we showed that the chemical chaperone glycerol causes striking elevation of Hmg2 stability in vivo and drastically slows the rate of Hmg2 limited proteolysis (Shearer & Hampton 2004). Those early studies showed that the 15 carbon isoprenoid molecule farnesol (FOH) caused Hmg2 to become less folded, and this effect of FOH was not observed with mutants of Hmg2 that do not undergo regulated degradation in vivo (Shearer & Hampton 2005). The in vitro effect of FOH was antagonized by chemical chaperones, indicating that FOH causes Hmg2 misfolding (Shearer & Hampton 2005). At the time of those studies, we did not know about GGPP, and found FOHs specific but fairly impotent effects by direct tests in vitro. Accordingly, in these current studies we explored if the more potent and biologically active GGPP similarly caused programmed misfolding. Indeed, glycerol reversed the effects of GGPP

both in vivo and in vitro. We also tested two other distinct chemical chaperones—proline, betaine. These also prevent Hmg2 in vitro misfolding and in vivo degradation upon GGPP treatment. The generality of these chemical chaperones' effects suggested that Hmg2's entry into a quality control is mediated by regulated misfolding of Hmg2 in response to GGPP.

In those early studies exploring the effects of FOH on Hmg2, we also used thermal denaturation as a gauge of in vitro Hmg2 misfolding. Incubation of microsomes at 70 C induced aggregation of Hmg2 into a high molecular weight, denatured form that remains in the stacking gel of an SDS-PAGE separation, allowing straightforward assessment of time-dependent thermal denaturation by immunoblotting (Shearer & Hampton 2005). We showed that treatment of microsomes with high micromolar concentrations of farnesol increased the rate and extent of Hmg2 thermal denaturation, while mutants of Hmg2 that do not respond to FOH in the proteolysis assay also did not show effects of FOH on thermal denaturation In contrast to FOH, GGPP did not affect Hmg2 thermal denaturation, and may in fact have a slight protective effect. GGPP treatment also partially antagonized the thermal denaturation caused by farnesol. These combined results suggest that GGPP causes a subtler from of misfolding that is still remediable by chemical chaperones but not prone to enhance wholesale aggregation. In other words, GGPP action is a folding "sweet-spot", causing sufficient misfolding to enhance selective degradation the HRD machinery, but not the stress-inducing and health-compromising effects of aggregation.

Combined, these features lead us to a model of "folding state allostery", in which GGPP plays the role of an allosteric ligand. Upon interacting with GGPP, Hmg2

undergoes a conformational change to a partially misfolded state that renders it more susceptible to HRD degradation. GGPP meets the criteria for ligand-like behavior—its action is specific, potent, reversible, antagonizable, and occurs at physiologically relevant concentrations. Although usually allosteric regulators are view as “agonists” of a particular structural response, antagonizing ligands are often observable in classical enzyme allostery, and in fact can be part of the bone fide physiological control of enzyme activity in the cell. For example, AMP activates the kinase AMPK, but ATP competes to block this activation (Gu et al. 2017, Hardie 2011).

GGPP-mediated Hmg2 misfolding is sufficient to gain entry to the ERAD quality control pathway, and can be reversed by treatment with several different chemical chaperones both in vitro and in vivo. However, this misfolding is not so severe as to make Hmg2 more thermally unstable and prone to aggregation. We thus propose, with admitted poetic liberty, to call this structural effect “mallostery”- a portmanteau of the preface “mal” for misfolded or poorly structured- and allostery for the nature of this regulated and physiologically useful folding transition. While traditionally allostery has been viewed as a rigid phenomenon of highly ordered proteins, advances in structural methods have allowed for a more inclusive view. In recent years it has been more widely recognized that allosteric regulation occurs across the whole spectrum of order in proteins, including intrinsically disordered proteins. Allostery can capitalize on disorder and misfolding, with allosteric proteins undergoing disorder switching, local unfolding, or becoming partially disordered upon posttranslational modification (Liu & Nussinov 2016, Nussinov 2016).

Because most allosteric proteins are multimeric, we tested whether Hmg2 forms multimeric structures, and found that indeed it does, but making use of co-expressed, fully

regulated versions of Hmg2 with distinct epitopes. Furthermore, we found no evidence for alteration in multimerization caused by addition of even saturating concentrations of GGPP in the coprecipitation experiments. This also speaks to the idea of GGPP causing a more subtle change in structural state: full dissocation of a monomer caused by a ligand could certainly enhance recognition by the HRD pathway. However, again, it appears that the GGPP induced effects to not take things this far down the road to structural squalor. We picture the multimeric structure as allowing a fully reversible alteration of folding state that can be reversed upon removal of the GGPP ligand, thus allowing quality control regulation with minimal aggregation or denaturation.

A longstanding open question about Hmg2 has been whether its regulated degradation is due to binding of a ligand or rather due to a more global biophysical processes—for example, perturbation of the ER membrane by isoprenoid regulators. In this work, we find that GGPP causes Hmg2's structural transition at nanomolar concentrations, far below the concentrations that would be expected to alter phospholipid bilayers properties. Furthermore, highly similar molecules were unable to affect Hmg2 at concentrations hundreds of times higher: While under 100 nM GGPP had clear effects on Hmg2 structure, 40 uM 2F-GGPP, has no discernable effect on Hmg2. In the same vein, our prior work has found a similarly striking degree of specificity for Hmg2 itself. Single point mutations within Hmg2 render it stable in vivo and unable to respond to GGPP in vitro. The combination of stringent sequence specificity for Hmg2, structural specificity for ligand, and the high potency of GGPP make it unlikely that Hmg2 misfolding and degradation the result of any general biophysical perturbation of the ER membrane proteome.

Another possible explanation for GGPP's action is that, by binding to Hmg2, it presents a hydrophobic patch which the quality control machinery detects as the exposed core of misfolded protein. Such so-called "greasy patches" are the basis of a strategy for artificially engineering the degradation of target proteins (Bondeson & Crews 2017, Lai & Crews 2016). This model is at odds with two observations. One, GGPP induces not only engagement with the UPS machinery, but a structural change in vitro. Two, very similar (and with an identical hydrophobic tail) molecules did not cause any effects on Hmg2 in vitro or in vivo. Furthermore, GGSPP, which is nearly identical to GGPP, antagonizes GGPP's effects. This implies that GGSPP can bind at the same location as GGPP, but despite this it is unable to induce the structural transition or degradation. Were the hydrophobic end of GGPP the key to its action, one would not expect such a similar to behave in the opposite manner.

This model leaves several open questions. We find that GGPP's effects on Hmg2 are specific, potent, rapid, and reversible, but does GGPP bind directly to Hmg2, and if so, where? Are other ER proteins required for Hmg2 misfolding? It seems unlikely that there are unknown stoichiometric binding partners required for Hmg2 misfolding, as Hmg2 is overexpressed in our in vitro experiments, but the possibility remains. Furthermore, we find that Hmg2 can be co-immunoprecipitated with differently tagged Hmg2 constructs expressed in the same cell. If Hmg2 is a multimer, does the multimerized state influence this mode of regulation? Do members of the complex influence each other in undergoing the conformational change to the misfolded state, as in classical models of allostery, or are individual Hmg2s independent?

Thirty percent of the US population suffers from dyslipidemia; more have dyslipidemia controlled by pharmaceutical treatment (Mozaffarian et al. 2015). As the rate controlling step of the sterol pathway, HMGR is a key intervention point in metabolic disease; over 25% of adults in the US take cholesterol lowering medications, and over 20% statin drugs which target this protein (Carroll et al. 2011, Gu et al. 2003). Mammalian HMGR levels rise after statin treatment due to both increased transcription of sterol genes and stabilization of HMGR itself when sterol levels are low (Hwang et al. 2016). Key components of HMGR regulated degradation are conserved in mammals, including induction by a 20 carbon isoprenoid and ubiquitination by ER E3 ligases, including gp78 which is a Hrd1 homologue (Jo et al. 2011b, Roitelman & Shechter 1984, Sever et al. 2003a, Song et al. 2005b). Furthermore, when the mammalian HMGR and its ancillary regulatory proteins are expressed in insect cells cells, Hrd1, the same E3 ligase as in yeast, mediates sterol-regulated HMGR degradation (Faulkner et al. 2013, Nguyen et al. 2009). These extensive similarities in the system highlight the importance of a deeper understanding of the dynamics underlying HMGR's regulated quality control degradation. A greater understanding the underpinnings of HMGR stability may open up avenues for better targeting the pathway in human patients.

This phenomenon of ligand-programmed misfolding raises questions about more general pharmacological applications. Proteins without active sites for inhibitors to engage can be difficult to target pharmacologically, and has in fact been referred to as the "undruggable proteome" (Crews 2010). The UPS system has already been tapped as a tool for pharmacological targeting of these undruggable protein through regulated degradation. Two main strategies have emerged so far: targeting proteins directly to specific E3 ligases,

such as VHL (Bondeson et al. 2015), and targeting proteins with ligands fused to a long hydrophobic molecule, or "greasy patch," to mimic a misfolded protein (Bondeson & Crews 2017). Directing proteins specifically to quality control by cleaver discovery of mallosteric regulators unfolding may offer another approach for targeting the undruggable proteome, and one that nature has clearly already discovered during evolution.

Experimental Procedures

Reagents

Geranylgeranyl pyrophosphate (GGPP), geranylgeraniol (GGOH), farnesyl pyrophosphate (FPP), farnesol (FOH), geranyl pyrophosphate (GPP), isopentenyl pyrophosphate (IPP), trypsin, and cycloheximide were purchased from Sigma-Aldrich. Lovastatin was a gift from Merck & Co (Rahway NJ). S-thiolo-GGPP (GGSPP) and 2-fluoro-GGPP (2F-GGPP) were gifts from Reuben Peters (Iowa State University) and Philipp Zerbe (University of California Davis). Anti-myc 9E10 supernatant was produced from cells (CRL 1729, American Type Culture Collection) grown in RPMI1640 medium (GIBCO BRL) with 10% fetal calf serum. Living colors mouse anti-GFP monoclonal antibody was purchased from Clontech. Polyclonal rabbit anti-GFP antibody was a gift from C. Zucker (University of California San Diego). HRP-conjugated goat anti-mouse antibody was purchased from Jackson ImmunoResearch. Protein A Sepharose beads were purchased from Amersham Biosciences.

Yeast strains and plasmids

Yeast strains (Table 2.1) and plasmids (Table 2.2) were constructed by standard techniques. The integrating Bts1 overexpression construct, plasmid pRH2657 was made by replacing the SpeI-SmaI fragment of pRH2654 with the Bts1 coding region amplified from pRH2477.

Yeast strains were isogenic and derived from the S288C background. Yeast strains were grown in minimal media (Diffco yeast nitrogen base supplemented with necessary amino and nucleic acids) with 2% glucose or rich media (YPD). Strains were grown at 30^{o} C with aeration. Lumnally myc-tagged Hmg2-GFP constructs were introduced by integration of plasmid cut with *StuI* at the *ura3-52* locus. The Bts1 overexpression construct was introduced by integration of plasmid cut with *PpuMI* at the *leu2Δ* promoter.

Flow cytometry

Flow cytometry was performed as described previously (Cronin et al. 2000, Gardner & Hampton 1999a). Briefly, yeast strains were grown in minimal media into early log phase (OD_{600}<0.2) and incubated with the indicated isoprenoid molecules (naturally occurring isoprenoid concentrations as indicated; 44 μM GGSPP and 2F-GGPP unless indicated otherwise), drugs (25 μg/mL lovastatin and 50 μg/mL cycloheximide), or equal volumes of vehicle (for isoprenoid pyrophosphate molecules, 7 parts methanol to 3 parts 10 mM ammonium bicarbonate; for lovastatin, 1 part ethanol to 3 parts 20 mM Tris Base pH 8; and for cyclohexmide, GGOH, and FOH, DMSO) for the times indicated. Individual cell fluorescence for 10,000 cells was

measured using a BD Accuri C6 flow cytometer (BD Biosciences). Data were analyzed using FlowJo software (FlowJo, LLC).

Microsome preparation

Microsomes were prepared as described previously (25). Yeast strains were grown to mid-log phase in YPD. 10 OD equivalents were resuspended in 240 µL lysis buffer (0.24 M sorbitol, 1 mM EDTA, 20 mM KH2PO4/K2HPO4, pH 7.5) with PIs (2 mM phenylmethylsulfonyl fluoride and 142 mM tosylphenylalanyl chloromethyl ketone). Acid-washed glass beads were added to the meniscus and cells were lysed at 4oC on a multi-vortexer for six 1-minute intervals with 1 minute on ice in between. Lysates were cleared with 5 second pulses until no pellet remained. Microsomes were pelleted from cleared lysates by centrifugation at 14,000 x g for five minutes, washed once in XL buffer (1.2 M sorbitol, 5 mM EDTA, 0.1 M KH2PO4/K2HPO4, pH 7.5), and resuspended in XL buffer.

Limited proteolysis assay

Microsomes were subjected to limited proteolysis as described previously (Shearer & Hampton 2004). Briefly, resuspended microsomes were treated with the indicated isoprenoid molecules or equal volumes of vehicle and then incubated with trypsin at a final concentration of 15 µg/mL at 30^{o}C. Reactions were quenched at the times indicated with an equal volume of 2x urea sample buffer (USB; 8M urea, 4% SDS, 1mM DTT, 125 mM Tris base, pH 6.8). Samples were resolved by 14% SDS-

PAGE, transferred to nitrocellulose in 15% methanol, and blotted with 9E10 anti-myc antibody.

Thermal denaturation assay

The thermal denaturation assay was performed as described previously (Shearer & Hampton 2005). Briefly, resuspended microsomes were treated with the indicated isoprenoid molecules or equal volumes of vehicle and transferred to PCR tubes. Samples were placed in a thermocycler (Eppendorf Mastercycler Pro) pre-heated at 70^{o}C and incubated at 70^{o}C for the indicated times. Samples were held on ice for two minutes prior to addition of equal volumes of 2x USB. Samples were resolved by 14% SDS-PAGE, transferred to nitrocellulose in 10% methanol, and blotted with 9E10 anti-myc antibody.

Microsome preparation for co-immunoprecipitation

Microsomes were prepared for co-immunoprecipitation as described previously (Neal et al. 2017). Yeast strains were grown to mid-log phase in YPD. 10 OD equivalents were resuspended in 240 µL lysis buffer (0.24 M sorbitol, 1 mM EDTA, 20 mM KH_2PO_4/K_2HPO_4, pH 7.5) with protease inhibitors (2 mM phenylmethylsulfonyl fluoride, 100 mm leupeptin hemisulfate, 76 mM pepstatin A, and 142 mM tosylphenylalanyl chloromethyl ketone). Acid-washed glass beads were added to the meniscus and cells were lysed at 4^{o}C on a multi-vortexer for six 1-minute intervals with 1 minute on ice in between. Lysates were pelleted by

centrifugation in 5-second pulses until no pellet was apparent, with the supernatant moved to a clean tube each time. Microsomes were pelleted from cleared lysates by centrifugation at 14,000 x g for five minutes, washed once in IP buffer without detergent (500 mM NaCl, 50 mM Tris base, pH7.5), and resuspended in IP buffer with detergent (IPB; 500 mM NaCl, 50 mM Tris base, 1.5% Tween-20, pH7.5) and protease inhibitors.

Co-immunoprecipitation

Microsomes in IBP were incubated at 4^{o}C for 1 hour with rocking. Microsomes were pipetted up and down repeatedly and then solutions were cleared by centrifugation at 14,000 x g for 15 minutes. Supernatants were incubated with 15 µL polyclonal rabbit anti-GFP antibody overnight at 4^{o}C with rocking. After overnight incubation, 100 µL of 50% protein-A sepharose bead slurry swelled in IP buffer without detergent were added. Samples were incubated at 4^{o}C for two hours with rocking. Beads were then pelleted for 30 seconds at low speed and 1 minute by gravity and washed twice with IPB and once with IP wash buffer (100 mM NaCl, 10 mM Tris base, pH7.5. Beads were aspirated to dryness and resuspended in 2x USB. Samples were resolved by electrophoresis on 14% polyacrylamide gels, transferred to nitrocellulose in 12% methanol buffer, and immunoblotted with anti-GFP or anti-myc antibody as indicated.

Table 2.1. Yeast strains used in chapter 2

Strain	Genotype	Figure
RHY3970	MAT*a ade2-101 met2 his3Δ200 lys2-801 leu2Δ ura3-52::URA3::TDH3pr-HMG2-GFP*	2.4, 2.15
RHY3971	MAT*a ade2-101 met2 his3Δ200 lys2-801 leu2Δ ura3-52::URA3::TDH3pr-HMG2-GFP pdr5ΔKanMX*	
RHY7661	MAT*a ade2-101 met2 his3Δ200 lys2-801 leu2Δ ura3-52::URA3::TDH3pr-1mycHMG2-GFP*	2.6-2.11, 2.13, 2.14, 2.18-2.22
RHY7683	MAT*a ade2-101 met2 his3Δ200 lys2-801 leu2Δ ura3-52::URA3::TDH3pr-S215A-1mycHMG2-GFP*	2.7
RHY10296	MAT*a ade2-101 met2 his3Δ200 lys2-801 leu2Δ::LEU2 ura3-52::URA3::TDH3pr-HMG2-GFP pdr5ΔKanMX*	2.16
RHY10297	MAT*a ade2-101 met2 his3Δ200 lys2-801 leu2Δ::LEU2::TDH3pr-BTS1-PGK1term ura3-52::URA3::TDH3pr-HMG2-GFP pdr5ΔKanMX*	2.16, 2.17
RHY10300	MAT*a ade2-101 met2 his3Δ200 lys2-801 leu2Δ::LEU2 ura3-52::URA3::TDH3pr-TFYSA-HMG2-GFP pdr5ΔKanMX*	2.15
RHY10301	MAT*a ade2-101 met2 his3Δ200 lys2-801 leu2Δ::LEU2::TDH3pr-BTS1-PGK1term ura3-52::URA3::TDH3pr-TFYSA-HMG2-GFP pdr5ΔKanMX*	2.17
RHY11113	MAT*a ade2-101 met2 his3Δ200 lys2-801 leu2Δ ura3-52::URA3::TDH3pr-HMG2-1myc-no catalytic domain*	2.23, 2.24
RHY11114	MAT*a ade2-101 met2 his3Δ200 lys2-801 leu2Δ::LEU2::Hmg2-GFP ura3-52*	2.23, 2.24
RHY11115	MAT*a ade2-101 met2 his3Δ200 lys2-801 leu2Δ::LEU2::Hmg2-GFP ura3-52::URA3::TDH3pr-HMG2-1myc-no catalytic domain*	2.23, 2.24
RHY11116	MAT*a ade2-101 met2 his3Δ200 lys2-801 leu2Δ ura3-52::URA3::TDH3pr-1mycHMG2-GFP*	2.23, 2.24

Table 2.2. Plasmids used in chapter 2

Plasmid	Genotype
pRH312	pRS405 LEU2 YIp
pRH469	URA3::TDH3pr-HMG2-GFP YIp
pRH680	LEU2::TDH3pr-HMG2-GFP Yip
pRH1581	URA3::TDH3pr-1myc-HMG2-GFP YIp
pRH1694	URA3::TDH3pr-TFYSA-1myc-HMG2-GFP YIp
pRH2177	URA3::TDH3pr-S215A-1myc-HMG2-GFP YIp
pRH2250	URA3::TDH3pr-HMG2-1myc-no catalytic domain
pRH2477	LEU2::GAL1pr-BTS1 Yip
pRH2654	LEU2 TDH3-pr-PGK1term YIP
pRH2657	LEU2::TDH3pr-BTS1-PGK1term Yip

Acknowledgements

We thank Reuben Peters (Iowa State University) and Philipp Zerbe (University of California Davis) for providing reagents. These studies were supported by NIH grant 5R37DK051996-18 to R.Y.H. M.A.W. was supported in part by NIH CMG Training Grant 5T32GM007240-35.

Chapter Two, in full, is currently in preparation for submission for publication as: Wangeline, MA and Hampton, RY, "Ligand-regulated entry into the HRD ERAD pathway reveals the dark side of allostery." I was the principal researcher/author of this work.

CHAPTER THREE:

The SSD: A Structure Shifting Domain required for ligand-mediated misfolding

Abstract

Levels of HMG-CoA reductase (HMGR) are controlled by regulated degradation by the endoplasmic reticulum associated degradation (ERAD) quality control pathway. This degradation is keyed to levels of sterol pathway molecules and is part of feedback regulation of the sterol pathway. The yeast isozyme of HMGR, Hmg2, is degraded by the Hrd ERAD pathway in response to the 20-carbon isoprenoid geranylgeranyl pyrophosphate (GGPP). Yeast Hmg2, mammalian HMGR, and a variety of other proteins involved in sterol metabolism and regulation, contain a conserved transmembrane region called the sterol sensing domain (SSD). Mutations in this domain disrupt regulation and function in all known SSD-containing proteins, but the role of the SSD itself, as opposed to other regions of these proteins and the conserved insulin-related Insig proteins which bind some SSD proteins, remains unclear. Here we describe studies to dissect the role of Hmg2's SSD as well as other structural features of the protein. Using in vivo and in vitro methods we demonstrate an independent role for the SSD in ligand-regulated misfolding. We found that mutations in the SSD block GGPP-induced degradation and misfolding. Using in vitro structural methods and in-cis epistasis, we were able to distinguish mutations in the SSD which prevent misfolding from a mutation in a different region of Hmg2 which allows regulated misfolding but blocks ubiquitination and degradation. In in-trans experiments, we found that expression of Hmg2 with a mutated SSD interferes with regulation of wild type Hmg2 expressed in the same strain. Using a homology-based

targeted approach, we also mutated residues elsewhere in Hmg2's transmembrane region and found that the first luminal loop plays an important role in regulation.

We propose a model for the SSD as an independent module for regulated entry in to proteostasis pathways—ERAD in yeast Hmg2 and mammalian HMGR, but a variety of other quality control and trafficking pathways in the case other SSD-containing proteins.

Introduction

Regulation of sterol uptake, production, trafficking, breakdown, and export are critical processes in eukaryotic organisms. Sterol pathway molecules are essential components of biological membranes and are required for the correct processing, localization, and enzymatic function of a variety of proteins. Normal metazoan development depends upon cholesterol modification of the Hedgehog ligand. Ensuring sufficient levels of sterol pathway molecules is thus essential to the development and heath of the organism. At the same time, pathway intermediates and oxidation products compete for proteins involved in a variety of important processes. Cells must not only ensure that enough sterol end products are produced, but also tightly control the levels of a wide variety of other sterols, oxysterols, and isoprenoids in both space and time. As a result, inborn errors of sterol metabolism and trafficking lead to a variety of disorders, including deadly neurodegenerative diseases, while dyslipidemias later in life are linked to heart disease and neurodegeneration.

Many proteins involved in sterol regulation contain a conserved membrane domain called the Sterol Sensing Domain, or SSD. This domain is found in such diverse proteins as the Sterol Response Element Binding Protein (SREBP) Cleavage Activating Protein (SCAP), the Hedgehog pathway receptor Patched, the sterol trafficking protein Niemann-Pick Disease Type C 1 (NPC1), the cholesterol pathway enzyme 7-Dehydrocholesterol Reductase (DHCR7) and the rate-controlling step of the sterol pathway, HMG-CoA Reductase (HMGR), from yeast to mammals. Regulation of some of these proteins is essential for cell and whole-organism homeostasis, while mutations in others give rise to disorders such as Niemann-Pick Disease and Smith-Lemli-Opitz Syndrome and the cancer syndrome Gorlin Syndrome.

The SSD itself consists of five transmembrane-spanning segments and associated juxtamembrane regions, and is conserved between yeast and mammals (Figure 3.1 and 3.2). The domain seems to universally be involved in binding, transporting, or responding to sterols. Two prominent SSD-containing proteins, mammalian SCAP and HMGR, also bind to partner proteins called Insigs, which are required for their regulation. A key feature of SSD-containing proteins is that they are often regulated by coopting more general proteostasis pathways; for example, the SREBP/SCAP/Insig axis regulates transcription of sterol genes by coopting ER/Golgi transport, while HMGR is regulated by the ubiquitin proteasome system. The interplay of sterols, SSD proteins, Insigs, and the proteostasis machinery is complex, with some SSD proteins having no apparent requirement for Insigs while others are so intimately

involved with Insigs that it has been proposed that the SSD be renamed the Insig Binding Domain.

In brewer's yeast, the HMGR isozyme Hmg2 contains an SSD with a high degree of conservation to mammalian SCAP. Hmg2 is a normal ER transmembrane protein which is nonetheless degraded by the ubiquitin proteasome system when levels of downstream sterol pathway molecules are high. Previous work in our laboratory has shown that Hmg2 degradation is programmed primarily by the isoprenoid geranylgeranyl pyrophosphate (GGPP), and that in the presence of GGPP, Hmg2 undergoes a structural transition and takes on many of the features of a misfolded protein, allowing its detection and ubiquitination by the E3 ubiquitin ligase Hrd1. We have likened this transition to a sort of folding allostery. We have previously shown that mutations in the SSD of Hmg2 render the protein stable in vivo.

In this work, we use the yeast HMGR system to further dissect the function of the critical and conserved SSD. We find that the SSD is not only required for normal degradation of Hmg2 in vivo, but that mutations in the SSD also block GGPP-induced misfolding in in vitro assays. A mutational and in-cis epistasis analysis reveals that the SSD constitutes a structural determinant of misfolding which is separable from other features in Hmg2 required for normal regulation and degradation, while an in-trans analysis finds that lesions in the SSD are able to "poison" the misfolding of wild-type Hmg2 expressed in the same cell. SSD-programmed misfolding is autonomous of Insigs and even occurs in detergent micelles. Finally, we describe the characterization of a new region required for normal Hmg2 regulation, the first luminal loop. Taken

together, these findings suggest a model of the SSD as a misfolding module which programs entry into quality control pathways in response to a signal.

Results

The SSD is required for Hmg2 regulated misfolding

Previous work by our laboratory identified several mutations in the SSD of Hmg2 (Theesfeld et al. 2011). Surprisingly, all SSD point mutations, including the mutation S215A, shown had the effect of stabilizing Hmg2 and blocking its response to the degradation signal GGPP (Figure 3.3 and 3.4) (Theesfeld et al. 2011). We had previously seen that in addition to blocking Hmg2 degradation in vivo, the S215A mutation also blocked the response to a putative ligand, farnesol (FOH) in an in vitro assay for Hmg2 folding. In the time since that work, we have found that the bona fide signal for Hmg2 misfolding is a different molecule, geranylgeranyl pyrophosphate (GGPP), which is effective at concentrations approximately 1000 times lower than FOH (Chapter 2). Accordingly, we tested SSD mutants for misfolding with this more potent molecule.

To indirectly assay Hmg2's structural state, we used limited proteolysis. To do so, we used a version of Hmg2 with a normal transmembrane domain but with the C-terminal catalytic replaced with GFP. A myc tag present in the first luminal loop is protected by the ER membrane and allows detection of the protein after proteolytic cleavage. Importantly, this version of Hmg2, which we will call 1myc-Hmg2-GFP, is regulated normally (Shearer & Hampton 2004, 2005). When microsomes prepared

from strains expressing Hmg2 are treated with limiting concentrations of trypsin, a characteristic pattern of cleavage fragments is produced, which can be detected by blotting for the protected myc tag (Figure 3.5, left). When Hmg2's structure is more open or misfolded, such as when it is treated with the isoprenoid GGPP, it becomes more accessible to proteolytic cleavage and the smaller fragments are produced more rapidly (Figure 3.5, right). Importantly, only the rate at which the fragments are produced changes, not the pattern itself (Shearer & Hampton 2004, 2005).

We tested the S215A version of 1myc-Hmg2-GFP in this limited proteolysis assay. The S215A protein did not respond to GGPP at any concentration tested, even at concentrations 2000-fold higher than those required to stimulate misfolding in the wild type protein (Figure 3.6). We also tested the L219F mutation, which also causes stability in vivo, and found it too blocked the response to GGPP in vitro (Figure 3.7).

Insig independence

The SSD is perhaps best known for binding to proteins called Insigs. Mammalian HMGR requires Insig for its regulated degradation, and mammalian SCAP requires Insig for regulation of its trafficking from the ER to the Golgi. While in the in experiments described in this work Hmg2 is overexpressed at levels far above that of the yeast Insigs (Flury et al. 2005), we tested whether there might be any residual Insig effect by removing the yeast Insigs, Nsg1 and Nsg2.

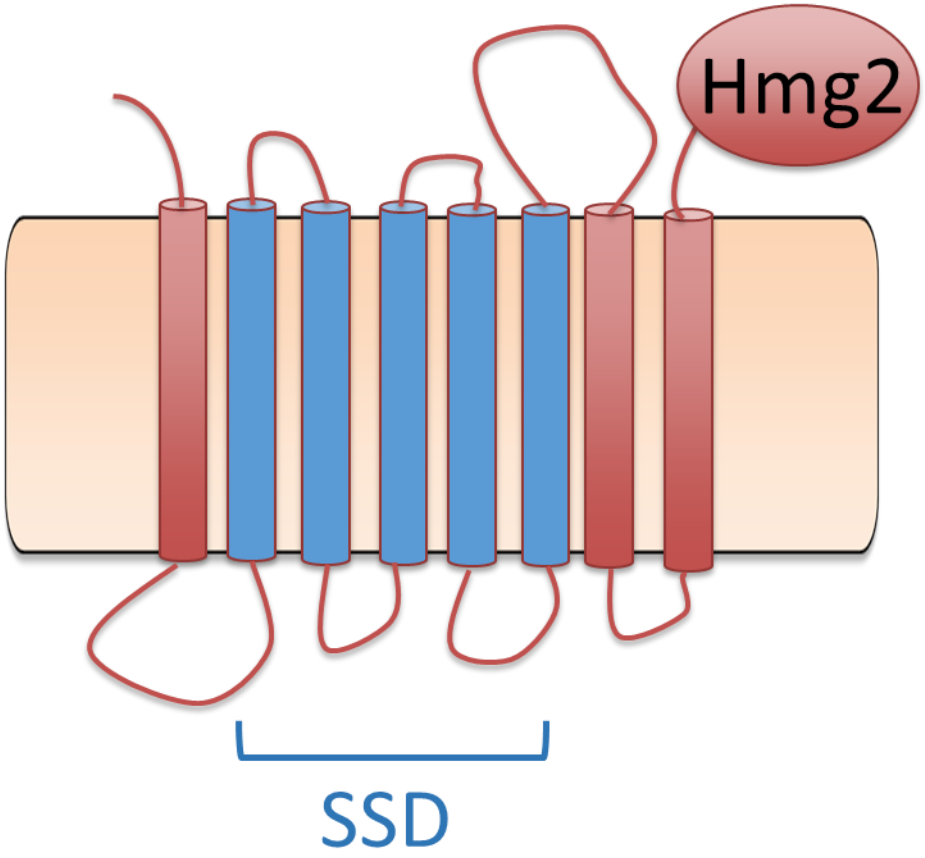

Figure 3.1. Schematic of the SSD
A schematic of the SSD of *S. cerevisiae* Hmg2. Transmembrane regions composing the SSD are highlighted in blue. The membrane is oriented with the cytosol up and the ER lumen down.

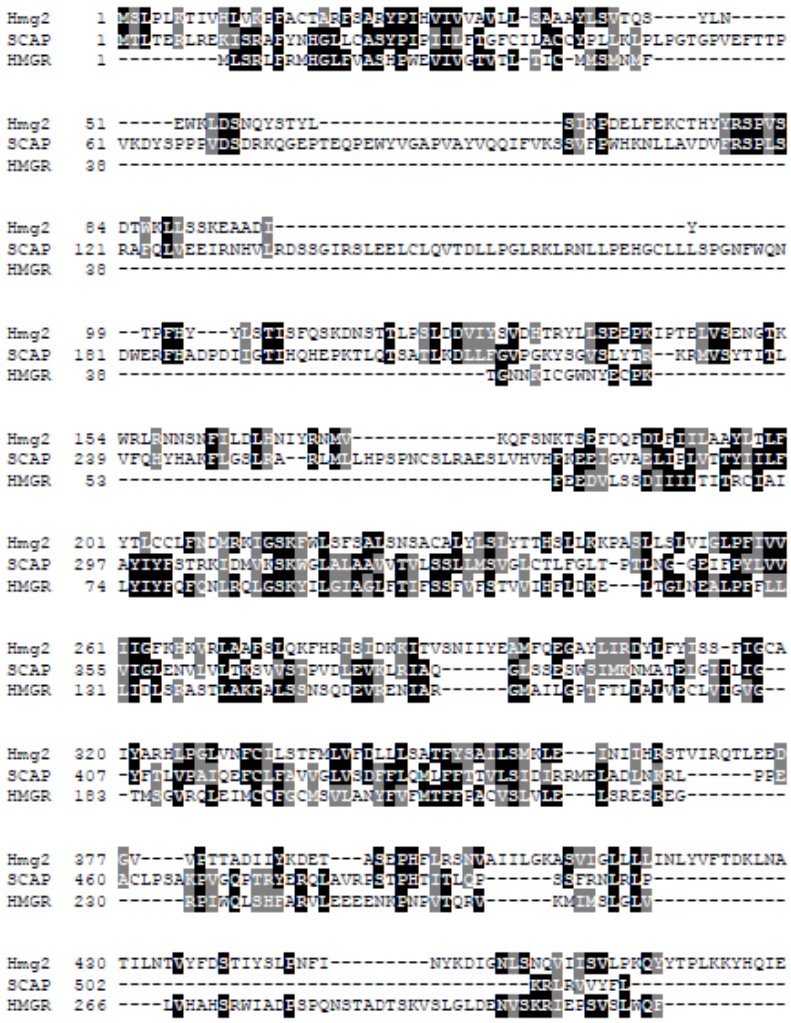

Figure 3.2. SSD sequence alignment

Sequence alignment of a *S. cerevisiae* Hmg2, *Homo sapiens* SCAP, and *Homo sapiens* HMGR containing the region of the SSD (approximately residues 189 to 354). Similar residues are highlighted in gray and identities are highlighted in black. Alignment produced using the T-Coffee alignment program (Di Tommaso et al. 2011, Notredame et al. 2000).

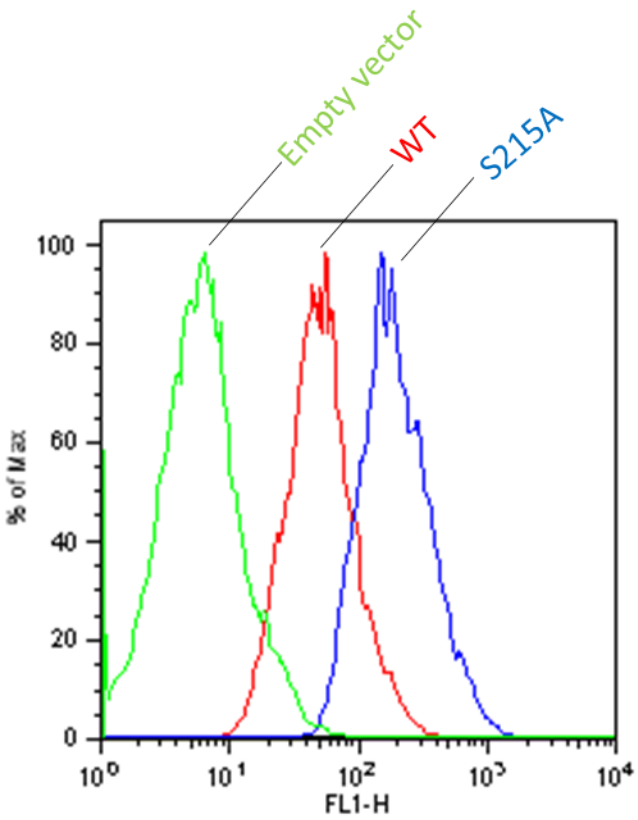

Figure 3.3. The SSD mutation S215A stabilizes Hmg2
Steady state fluorescence histograms of cells expressing wild type (red) or S215A (blue) Hmg2 fused to GFP (Hmg2-GFP) or empty vector (green) to show dynamic range. Fluorescence was measured by flow cytometry of 10,000 cells in log phase.

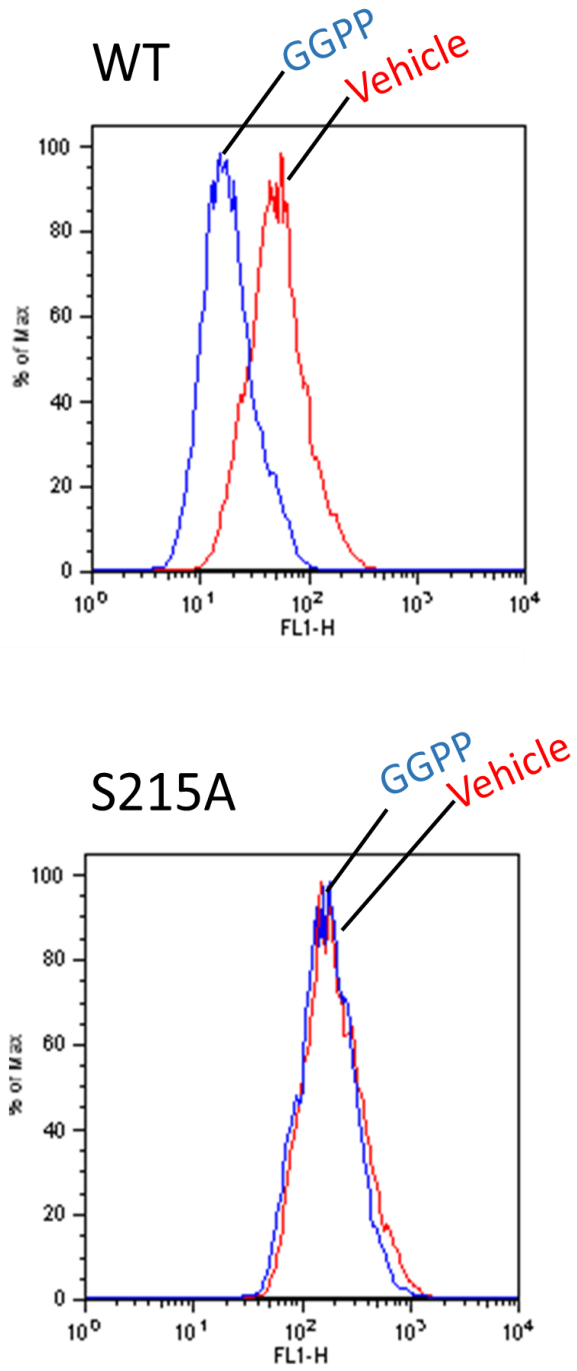

Figure 3.4. The SSD mutation S215A renders Hmg2 insensitive to isoprenoids
Steady state fluorescence histograms of cells expressing wild type (top) or S215A (bottom) Hmg2 fused to GFP (Hmg2-GFP). Cultures are treated with vehicle (red) or 22 μM GGPP (blue). Fluorescence was measured by flow cytometry of 10,000 cells in log phase.

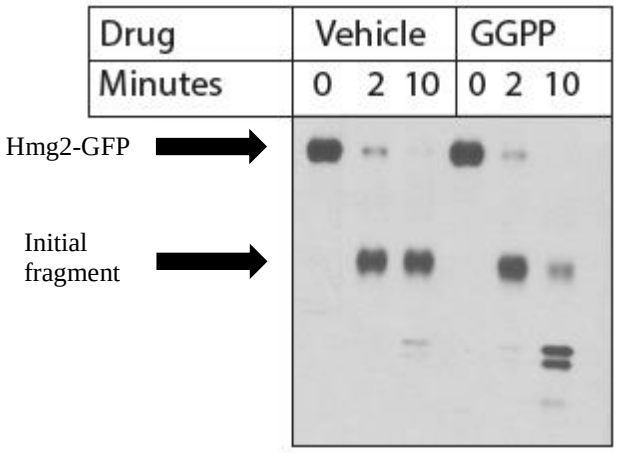

Figure 3.5. Sample limited proteolytic assay for structure of 1myc-Hmg2-GFP
Limited proteolysis performed on microsomes treated with vehicle (left) or 22 μM GGPP (right). Microsomes from cells expressing 1myc-Hmg2-GFP were incubated with trypsin for the indicated times. The initial size of 1myc-Hmg2-GFP before proteolysis is indicated with an arrow labeled "Hmg2-GFP." The size of the first fragment, which results from rapid and unregulated cleavage in the linker between the membrane domain and GFP is marked "initial fragment." This figure is reproduced from figure 2.6 in Chapter 2.

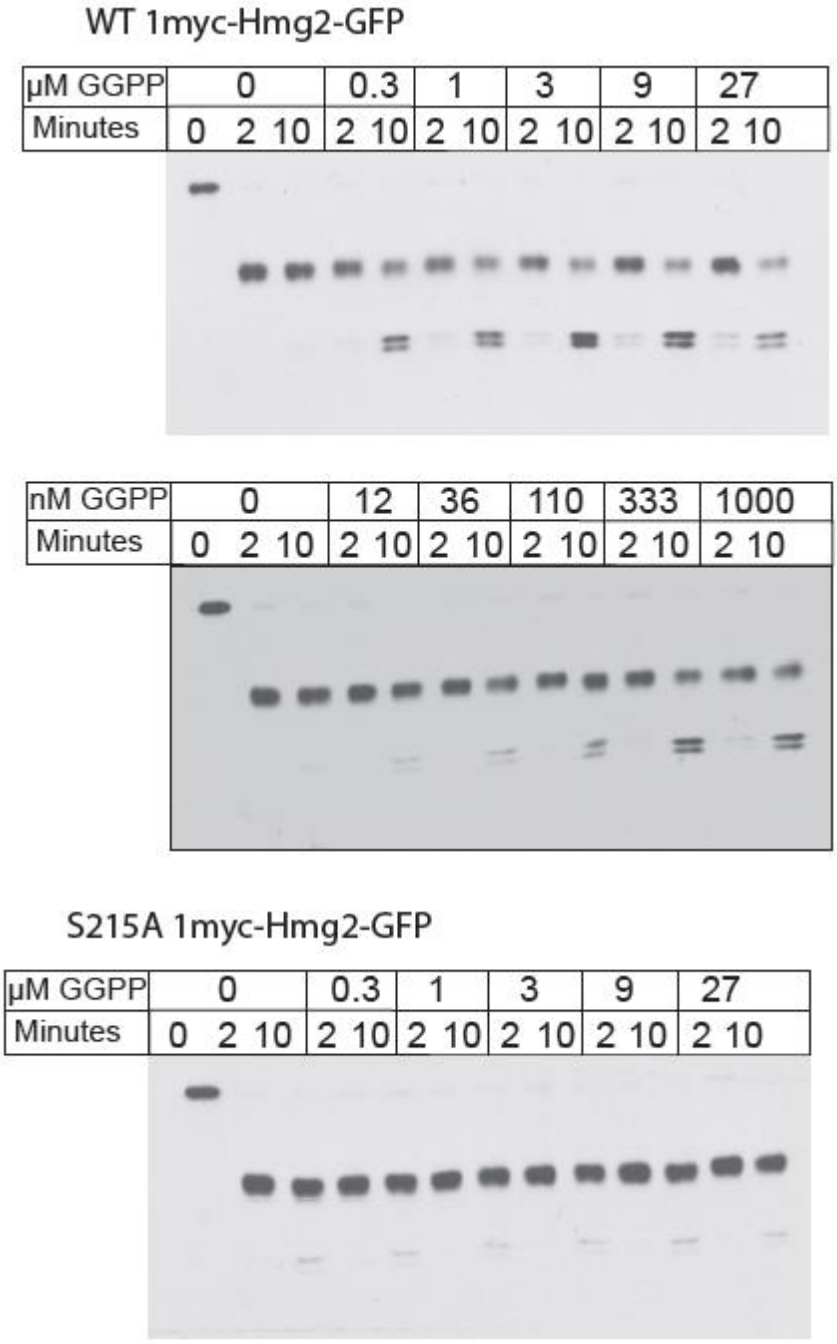

Figure 3.6. The SSD mutation S215A blocks in vitro misfolding of Hmg2
Dose response of GGPP in the limited proteolysis assay. Microsomes from cells expressing wild type (top, middle) or S215A (bottom) 1myc-Hmg2-GFP were treated with the indicated concentration of GGPP and subjected to limited proteolysis as in Figure 3.6. These panels are reproduced from Figure 2.7 in Chapter 2.

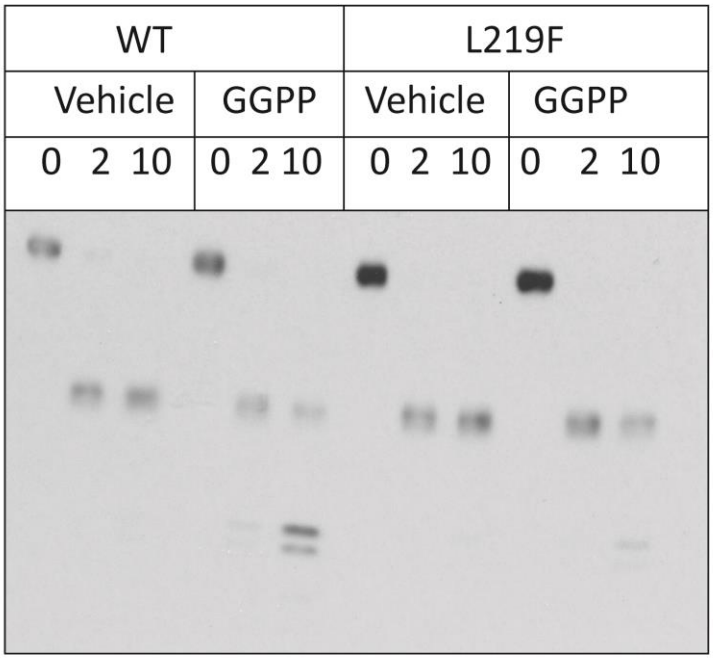

Figure 3.7. The L219F mutation blocks in vitro misfolding of Hmg2
In vitro proteolysis on wild-type and L219F 1myc-Hmg2-GFP treated with vehicle or 22 μM GGPP for 0, 2, or 10 minutes as indicated.

We asked whether Insigs were required for misfolding in vitro using the limited proteolysis assay. When 1myc-Hmg2-GFP was expressed in the nsg1Δnsg2Δ, it responded normally to GGPP in the in vitro assay (3.8). Previous work in our lab has found that Insig overexpression blocks Hmg2 misfolding (Flury et al. 2005). These data suggest a function of the SSD in Hmg2 autonomous of the Insig proteins.

Separate determinants of folding and degradation

While our laboratory has identified a huge number of stabilizing mutations in Hmg2, we have never before been able to distinguish between the various stages of Hmg2 entry into the ubiquitin proteasome pathway. Looking at the end points of ubiquitination and in vivo stability, we have been unable to distinguish between mutated proteins which cannot detect GGPP, those which cannot undergo regulated misfolding, and those which cannot be ubiquitinated. Accordingly, with the limited proteolysis assay giving us the ability to look indirectly at Hmg2 folding, we tested other stabilizing mutations that we had previously identified in Hmg2.

In our earliest studies of Hmg2, we identified two single residue requirements for Hmg2 degradation, K6 and K357 (Gardner & Hampton 1999b). Mutation of either one of these residues to arginine resulted in complete stabilization of Hmg2 by cycloheximide chase and a complete lack of response to sterol pathway signals (Gardner & Hampton 1999b, Gardner et al. 2001a, Garza et al. 2009b). As these residues

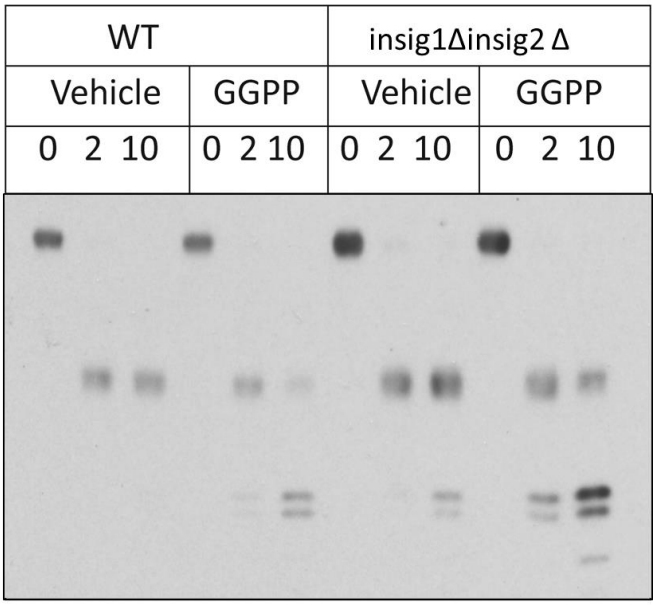

Figure 3.8. Insig deletion does not interfere with isoprenoid-induced misfolding of Hmg2

In vitro proteolysis assay on cells expressing wild type 1myc-Hmg2-GFP in either a wild type (left) or insig1 and insig2 deletion background. Microsomes were treated with vehicle or 22 μM GGPP for 0, 2, or 10 minutes as indicated.

were both lysines and both facing the cytosol, we had hypothesized that they could be ubiquitination sites.

We returned to these mutations using the in vitro proteolysis assay. The K357R version of 1myc-Hmg2-GFP behaved like the SSD mutants discussed above; it did not misfold in response to added GGPP (Figure 3.9). Surprisingly, the K6R version did respond to GGPP, and behaved identically to wild type 1myc-Hmg2-GFP in the misfolding assay. This defined for the first time two different kinds of determinants for Hmg2 degradation. We also tested these two determinants in cis by making a K6R S215A double mutant. The S215A mutation was epistatic to K6R for in vitro misfolding; the double mutant did not respond to GGPP in vitro (Figure 3.10).

Analysis of other regions of the transmembrane domain

In addition to our analysis of previously identified mutations in Hmg2, we carried out two new mutational analyses of the transmembrane region. In the first, we conducted a narrowly targeted analysis of highly conserved and partially conserved residues in the SSD and the loop and transmembrane domain immediately following it (loop 6 and transmembrane domain (TM) 7). Multiple single and combinatorial mutations in the region were made (Table 3.1). However, nearly all of these mutations had no apparent effect on Hmg2-GFP stability (Figure 3.11-3.13). Only two new amino acids were identified as requirements for regulated degradation of Hmg2, aspartate 165 (loop 1) and asparagine 401, (at the border of loop 6 and TM 7). Mutation of N401 to alanine increased Hmg2-GFP levels in vivo as assayed by flow

Table 3.1. Hmg2 mutations examined in chapter 3

Table of Hmg2 mutations newly made for this study (marked with *) or previously identified but newly examined using in vitro methods in this study. The S215A mutation, which was previously examined both in vivo and in vitro using farnesol, is included in bold for reference. Light shading indicates stability or lack of misfolding in vitro. Dark shading indicates fast degradation or high basal proteolysis in vitro. K6R, the only mutation with a separation of degradation and folding phenotype, is marked with a dagger (†). For a full list of SSD mutations previously examined in vivo, see (Theesfeld et al. 2011)

Mutation	Region	Degradation phenotype	Folding phenotype
K6R†	N-terminus	Stable, no GGPP effect	None
RYL133-135AAA*	Loop 1	Fast degradation, blunted regulation	High basal proteolysis, no GGPP effect
RYL133-135AAA S215A	Various	Slightly fast degradation, no regulation	Unknown
K6R RYL133-135AAA	Various	Slightly fast degradation, blunted regulation	Unknown
K153A*	Loop 1	None	Slight change in cleavage pattern (loss of doublet); otherwise wild-type
K153A R155A R157A*	Loop 1	Fast degradation, blunted regulation	High basal proteolysis, no GGPP effect
K153A R155A R157A S215A*	Loop 1	Slightly fast degradation, blunted regulation	Unknown
K6R K153A R155A R157A*	Loop 1	Slightly fast degradation, blunted regulation	Unknown
K6R K153A R155A R157A S215A*	Loop 1	Slightly fast degradation, no regulation	Unknown
D165A*	Loop 1	None	None
TLCC202-205AAAA	SSD	Stable, no GGPP effect	Unknown
I213T*	SSD	None	None
S215A	**SSD**	**Stable, no GGPP effect**	**No GGPP effect**
I213T K216N*	SSD	None	None
L219F	SSD	Stable, no GGPP effect	No GGPP effect
K357R	Loop 6	Stable, no GGPP effect	No GGGP effect
D384A*	Loop 6	None	None
R399A*	Loop 6 / TM7 border	None	None
S400A*	Loop 6 / TM7 border	None	None
N401A*	Loop 6 / TM7 border	Stable, no GGPP effect	No GGPP effect

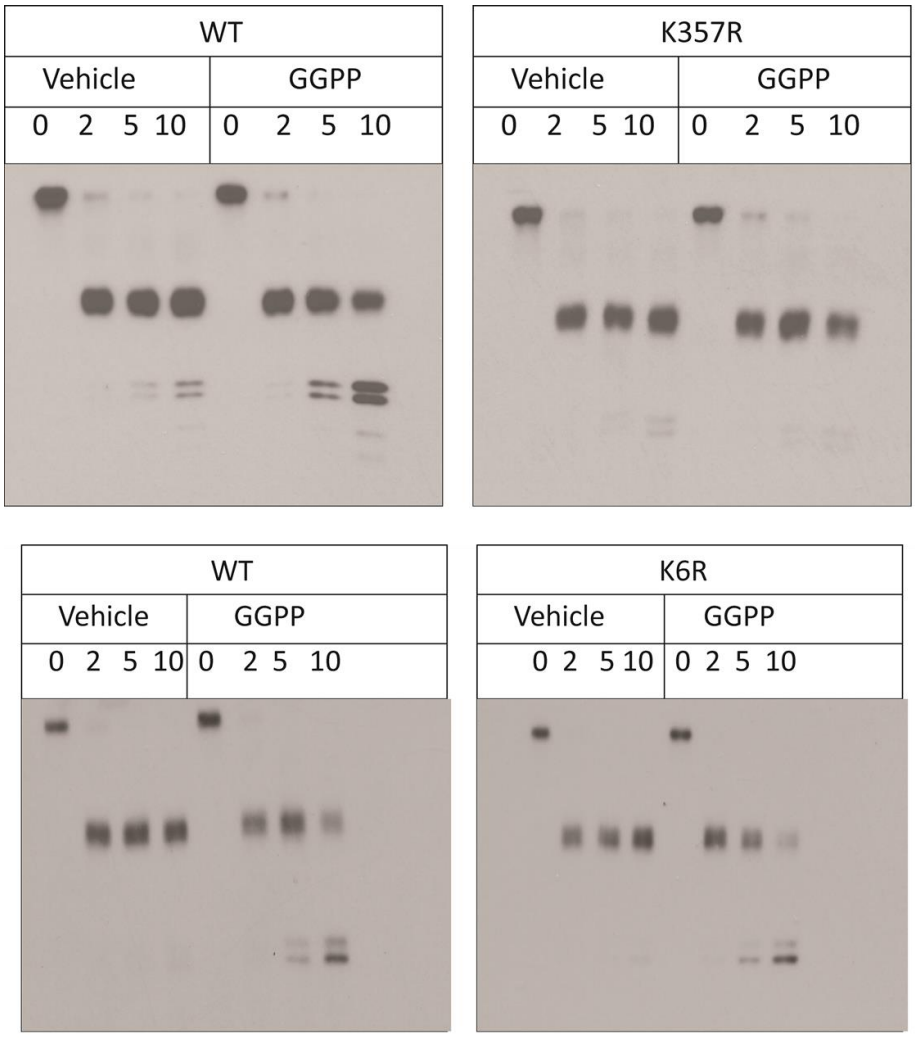

Figure 3.9. The K357R mutation, but not the K6R mutation, blocks in vitro misfolding of Hmg2

Limited proteolysis assay on microsomes from cells expressing wild type (top and bottom left panels),, K357R (top right panel), and K6R (bottom right panel) 1myc-Hmg2-GFP. Microsomes were treated with vehicle (left of each panel) or 22 μM GGPP (right) prior to proteolysis for 0, 2, 5, or 10 minutes as indicated.

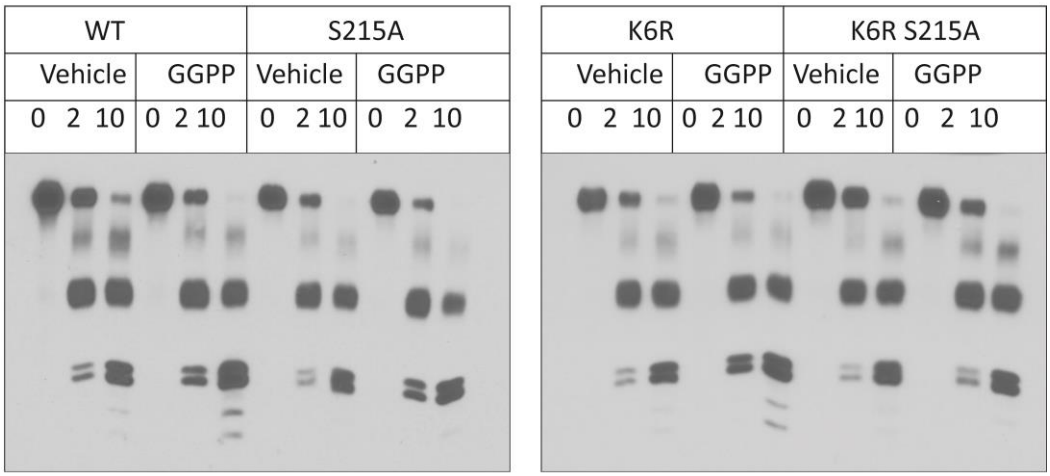

Figure 3.10. The S215A mutation is epistatic to K6R for misfolding in *cis*
Limited proteolysis assay on microsomes from cells expressing wild type (left offirst panel), S215A (right of first panel), K6R (left of second panel) or K6R S215A (right of second panel) 1myc-Hmg2-GFP for 0, 2, or 10 minutes as indicated. Microsomes were treated with vehicle or 22 μM GGPP.

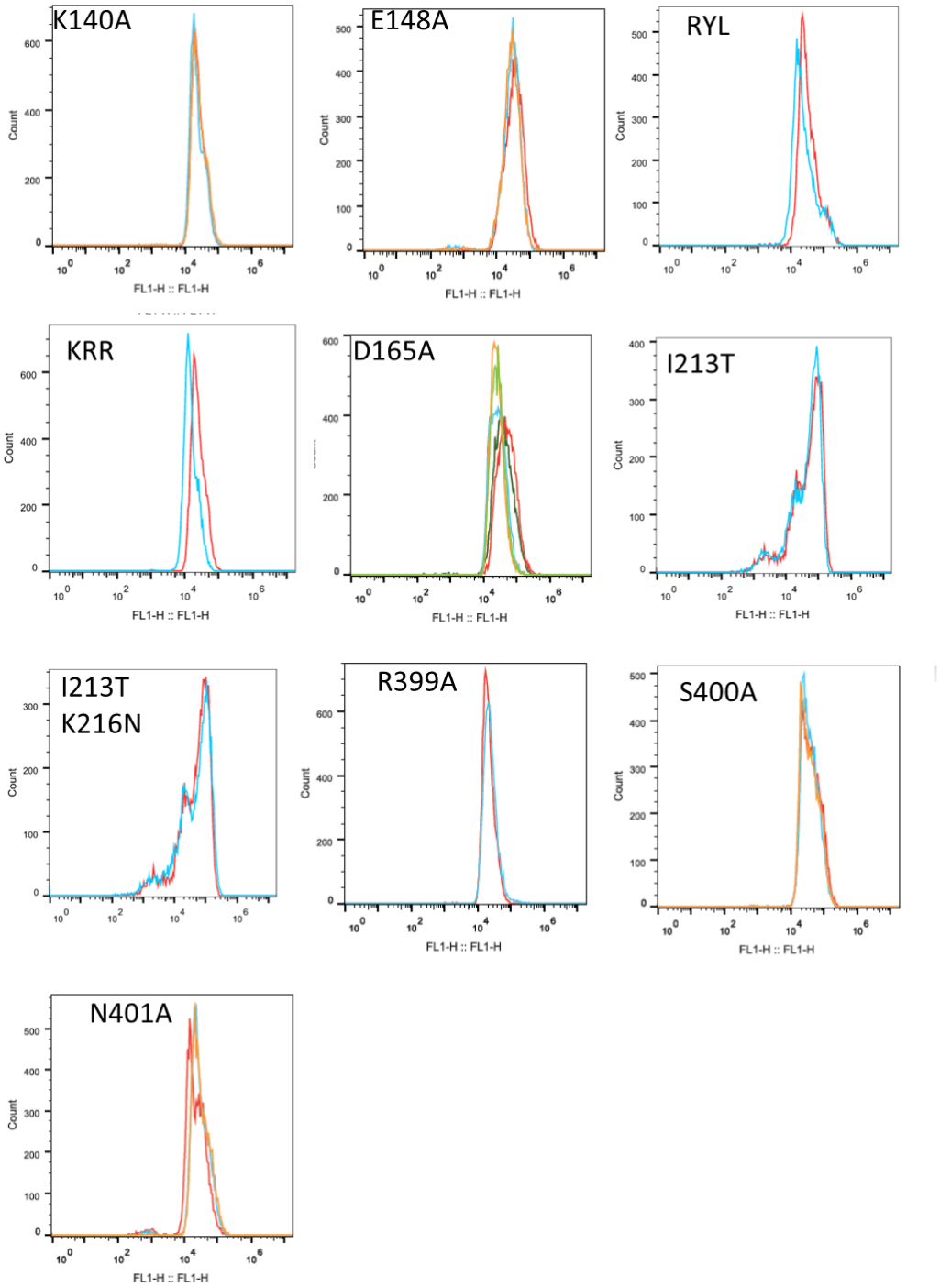

Figure 3.11. Steady state level comparisons of other mutations made in this study
Fluorescence histograms of yeast expressing the indicated mutations. Single or multiple candidates of mutated Hmg2-GFP at steady state compared to wild type in red. Readings taken in log phase on 10,000 cells. RYL stands for RYL133-135AAA. KRR stands for K153A R155A R157A. E148A, K140A, I213T, I213T K216N, R399A, and S400A have wild-type fluorescence. RYL and KRR have slightly lower fluorescence. D165A and N401A have slightly elevated fluorescence.

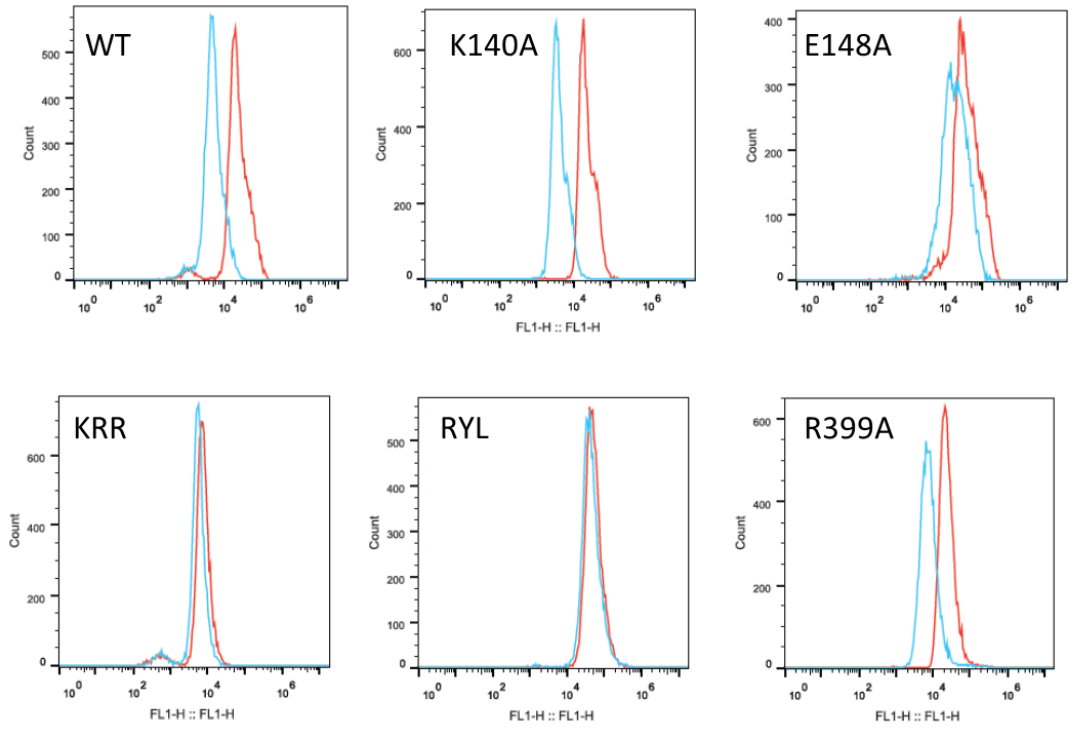

Figure 3.12. Comparison of response to GGPP by other mutations made in this study

Fluorescence histograms of yeast expressing the indicated mutations, incubated with 22μM GGPP for 1 hours. Wild-type in top left for comparison. Readings taken in log phase on 10,000 cells. RYL stands for RYL133-135AAA. KRR stands for K153A R155A R157A. K140A, E148A, and R399A respond normally. RYL and KRR have a blunted response.

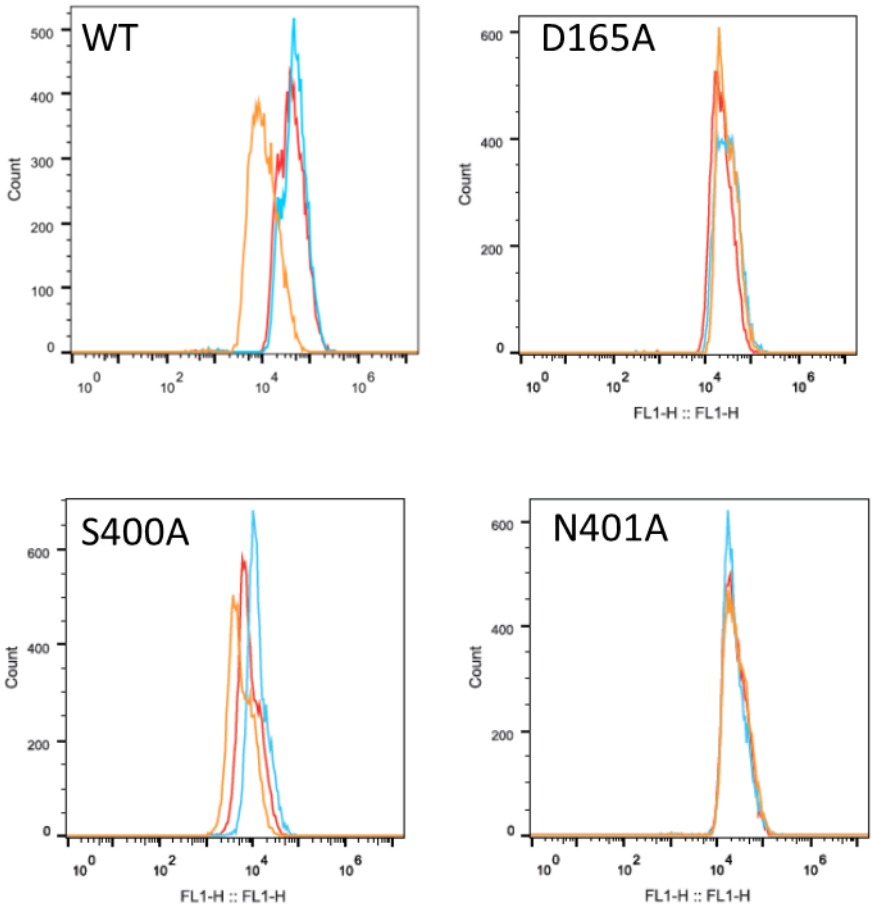

Figure 3.13. Comparison of response to GGPP and lovastatin by other mutations made in this study

Fluorescence histograms of yeast expressing the indicated mutations, incubated with 22μM GGPP for 1 hour or 25μg/mL lovastatin for 2 hours. Wild-type in top left for comparison. Readings taken in log phase on 10,000 cells. S400A responds normally. D165A has a blunted response. N401A does not respond.

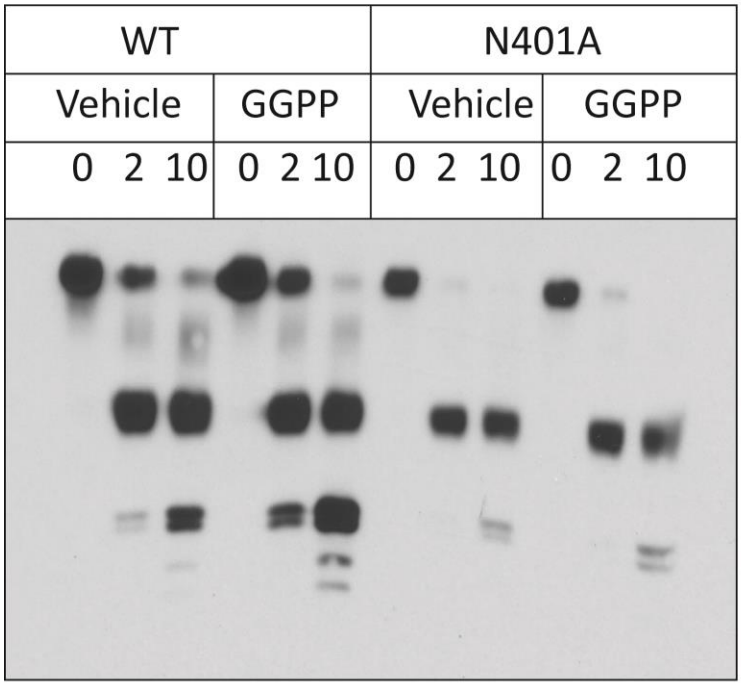

Figure 3.14. N401A mutation behaves like an SSD mutation in vitro and blocks misfolding

In vitro proteolysis on wild type or N401A 1myc-Hmg2-GFP treated with vehicle or 22 μM GGPP. Proteolysis was for 0, 2, or 10 minutes as indicated.

cytometry (Figure 3.11, 3.13). The N401A mutation also rendered 1myc-Hmg2-GFP unable to misfold in response to GGPP treatment in vitro (Figure 3.14).

The second targeted approach was based on homology. It has been reported that mammalian SCAP binds cholesterol in its first luminal loop (Motamed et al. 2011). The membrane region of Hmg2 is closely related to that of mammalian SCAP (Theesfeld et al. 2011). The classic SCAP activating mutations Y298C, L315F, and D443N, while not all identical in Hmg2, all have counterpart stabilizing mutations—TLCC202-205AAAA, L219F, and K357R—at those sites (Hughes et al. 2008, Theesfeld et al. 2011, Yabe et al. 2002). This suggests a hypothesis wherein Hmg2's first luminal loop could be involved in binding its own signal. Another analysis of homology in this loop also suggested that this hypothesis was worth testing. An alignment of the entire Hmg2 sequence with the full sequence of the GGPP-binding subunits of the type I and type II geranylgeranyltransferases (GGTases), Ram2 and Bet2, respectively, showed very little similarity outside of the catalytic region, as might be expected of these very different proteins. However, two (and only two) other regions of Hmg2 did align with both of these GGPP-binding proteins with regions of similar and identical residues—a short segment of loop 1 and a short segment of loop 7 (Figure 3.15 and 3.16). This was interesting, because SCAP loop 7 binds loop 1, which is required for trafficking of SCAP to the Golgi (Zhang et al. 2013, 2016).

We wondered whether, if loop 1 were a binding site for a signal, we could overexpress it to outcompete Hmg2. We began by making overexpression constructs

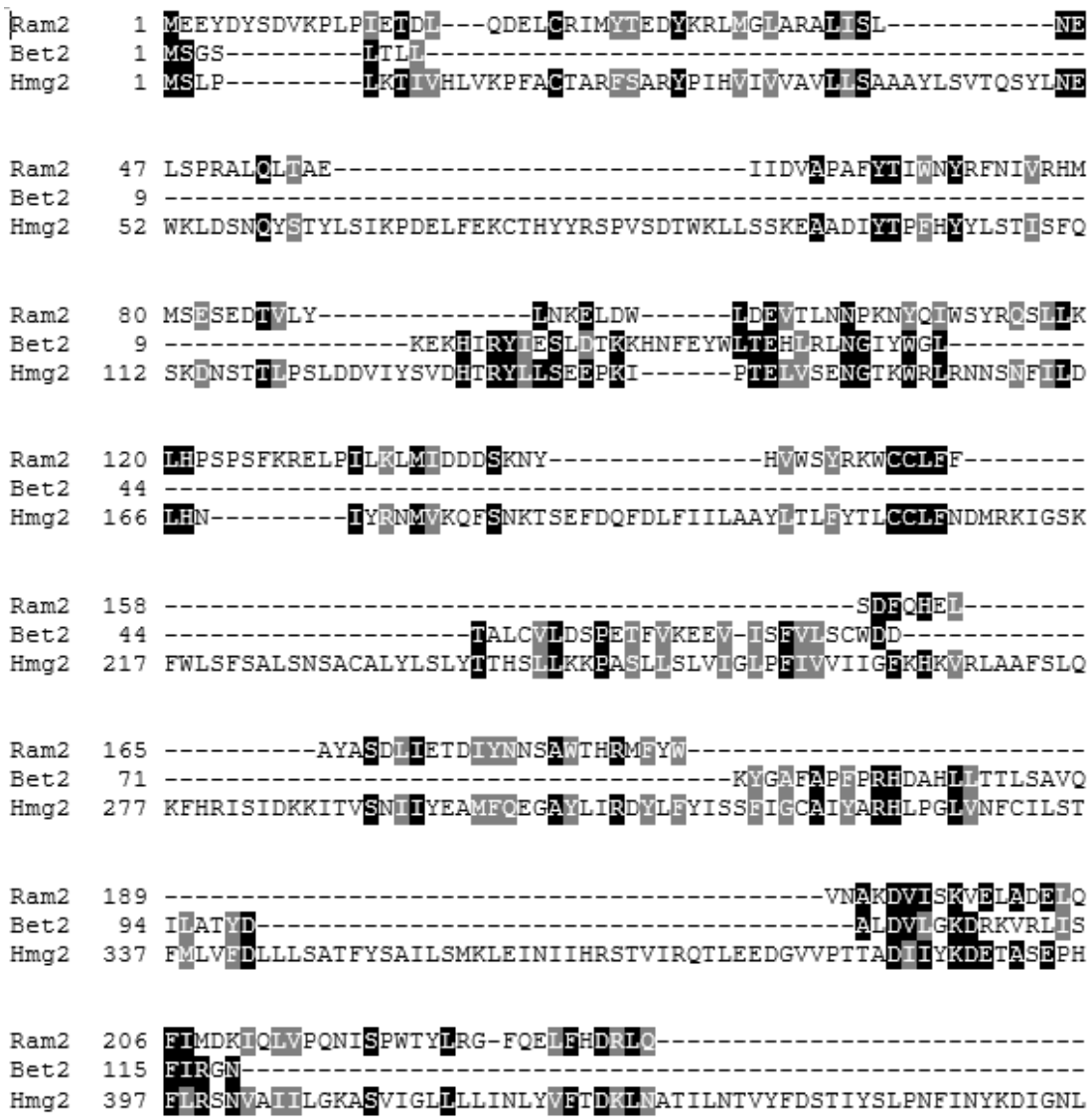

Figure 3.15. Alignment of Hmg2 with the GGPP-binding proteins Ram2 and Bet2
Sequence alignment of a *S. cerevisiae* Ram2, Bet2, and Hmg2 containing the transmembrane region. Similar residues are highlighted in gray and identities are highlighted in black. Only two regions of any overlap were found; in Hmg2 loop 1 from approximately amino acid 130 to 160 and in the loop 6/TM7/loop 7 region at approximately amino acids 380 to 420. Alignment produced using the T-Coffee alignment program (Di Tommaso et al. 2011, Notredame et al. 2000).

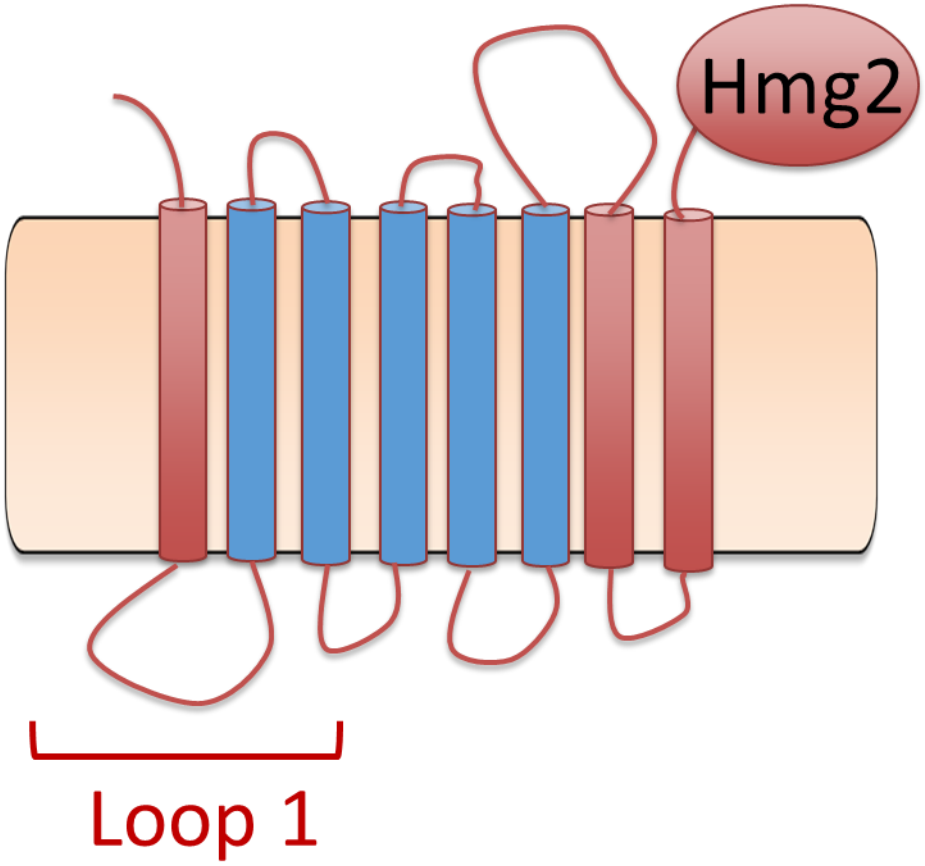

Figure 3.16. Schematic of Hmg2 with Loop 1 location
The SSD is highlighted in blue. Loop 1 is indicated with a red bracket. The cytosol is up and the ER lumen is down.

of the loop 1 region. Three constructs were made, the first containing only the loop (Loop1-only) the second containing the initial cytoplasmic segment of Hmg2, plus the first TM domain, plus the first loop (TM1-Loop1) and the second containing the TM1-Loop1 segment plus the second TM domain (TM1-Loop1-TM2) (Figure 3.17). All contain the luminal myc tag. These constructs were expressed from the constitutive TDH3 (GAPDH) promoter from a high-copy 2μM plasmid in strains also expressing Hmg2-GFP. We then treated the cells with GGPP and assayed Hmg2-GFP levels by flow cytometry.

The Loop1-only construct had no apparent effect on GGPP action. This may be because of its localization. Without the first TM domain, it is unclear whether Loop1-only is correctly localized and folded. However, the TM1-Loop1 and TM1-Loop1-TM2 constructs both had small but consistent effects on GGPP action. Expression of either, but not Loop1-only or empty vector, slightly blunted the effects of GGPP on Hmg2-GFP levels (3.18). While the effect was small, importantly the unregulated TFYSA Hmg2-GFP, which is degraded rapidly and constitutively regardless of GGPP levels, was unaffected (3.19). Immunoblotting for the myc tag contained in the TM1-Loop1 and TM1-Loop1-TM2 constructs reveals that their levels are low, and cycloheximide chase shows that they are rapidly degraded (3.20). Their low levels may be an explanation for the small effect size. These results suggests that loop 1 has a role in binding something that is important for regulation of Hmg2, and that expression of the loop apart from Hmg2 can interfere with its regulation.

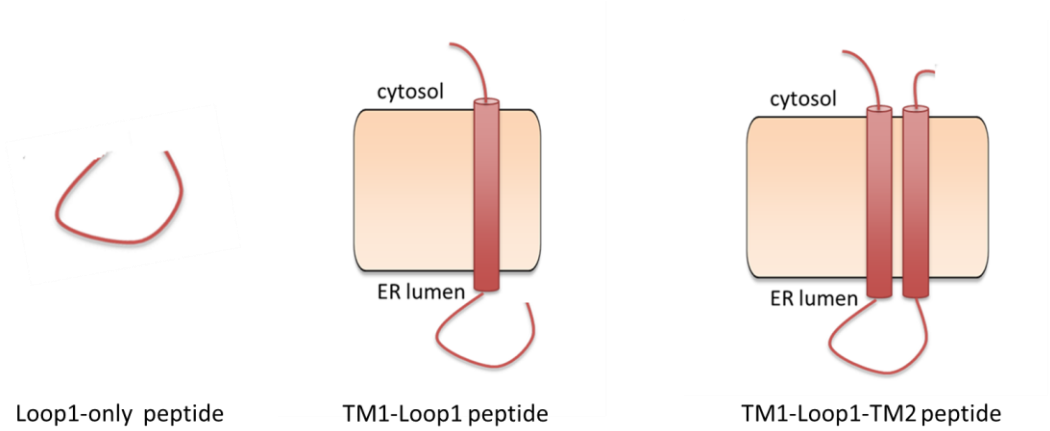

Figure 3.17. Schematic of loop 1 overexpression constructs
Schematic of the three loop1 over expression constructs. Loop1-only comprises Hmg2 amino acids E51 through D188. TM-Loop1 comprises M1 through D188. TM1-Loop1-TM2 comprises M1 through N208. The loop constructs were expressed from the GAPDH (TDH3) promoter on 2μM plasmids.

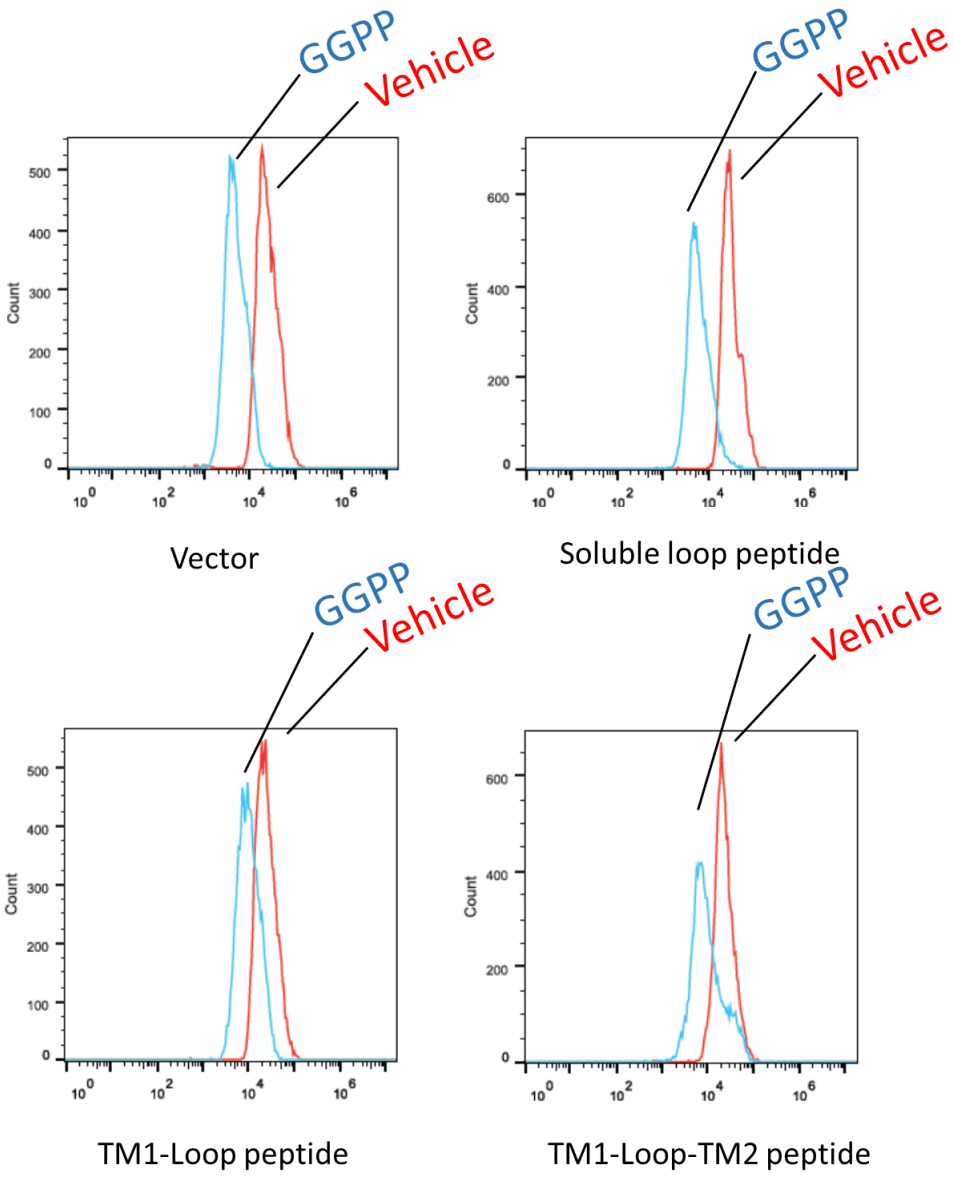

Figure 3.18. Co-expression of TM1-Loop1 and TM1-Loop1-TM2 but not Loop1-only blunts GGPP regulation

Steady state fluorescence histograms of cells expressing wild type Hmg2-GFP either with empty vector (top left) or in the presence of an overexpressed loop construct. Cells are treated with vehicle (red) or 22 μM GGPP (blue) for 45 minutes.

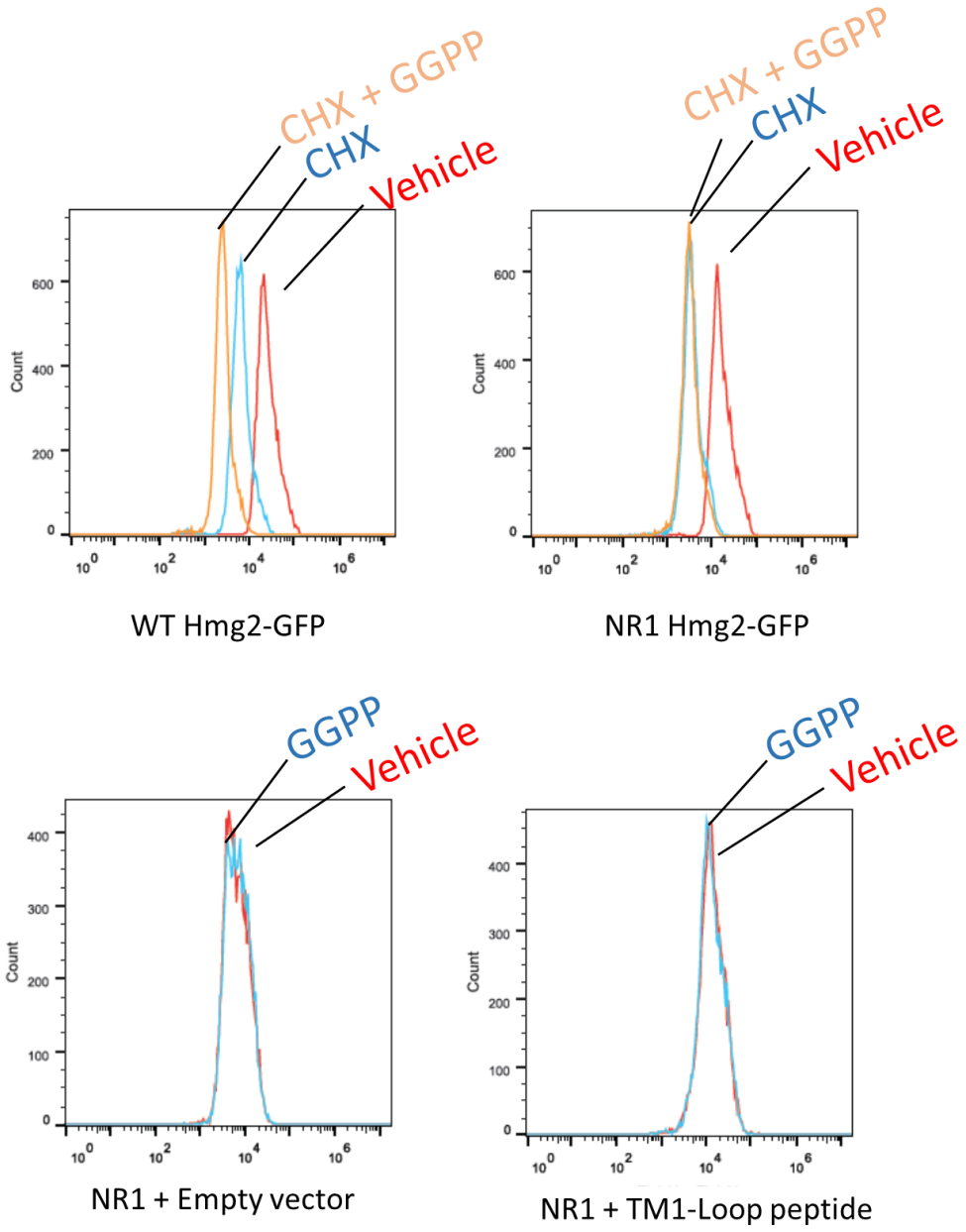

Figure 3.19. Co-expression of TM1-Loop1 does not affect NR1 TFYSA Hmg2-GFP

Steady state fluorescence histograms of cells expressing wild type wild type (top left) or the non-responding TFYSA mutation (all others) Hmg2-GFP either with empty vector or in the presence of an overexpressed loop construct. In the top two panels, cells are treated with vehicle (red), 25 µg/mL lovastatin (blue), or 22 µM GGPP (yellow) to demonstrate lack of TFYSA regulation. In the bottom two panels, cells are treated with vehicle (red) or 22 µM GGPP (blue) for 45 minutes.

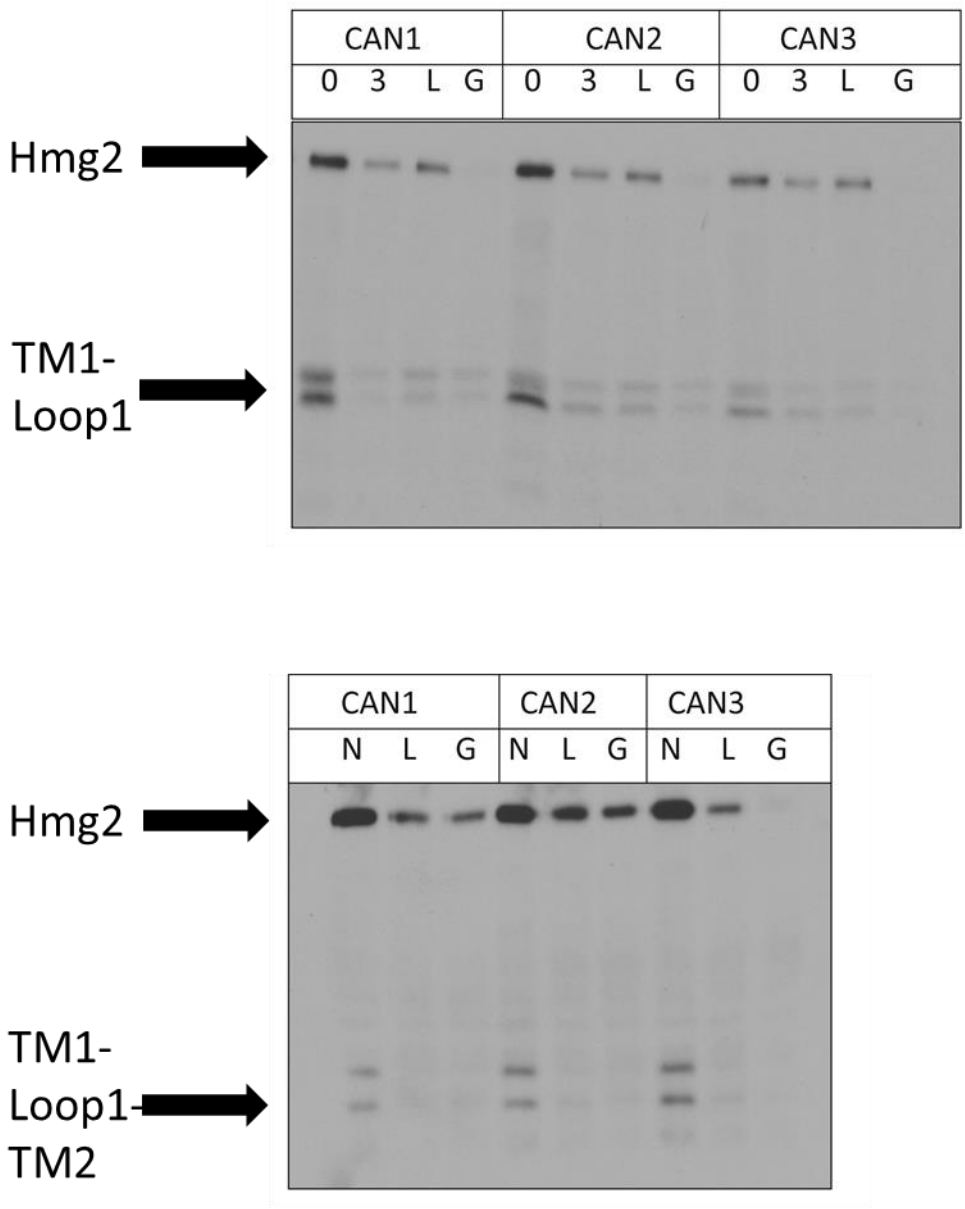

Figure 3.20. Loop 1 constructs are expressed at low levels and degraded
Anti-myc immunoblot of lysates from cells expressing both Hmg2 with a myc tag and the TM1-Loop1 (top) and TM1-Loop1-TM2 (bottom) constructs. Cells were treated with cycloheximide and vehicle (0, 3 in top panel, N in bottom panel)), 25 μg/mL lovastatin (L) or 22 μM GGPP (G) as indicated. Both the loop peptide and full-length Hmg2 are indicated with arrows. Three candidates for each overexpression strain are shown.

We then made point mutations in loop 1, beginning with residues which were conserved between Hmg2 and one or more of the GGPP-binding proteins. We prioritized regions that contained positively charged residues, on the hypothesis that they might be important for binding the negatively charged pyrophosphate moiety of GGPP. The residues RYL 133-135 were mutated to alanines. The residues K153, R155, and R157 were also mutated to alanines, K153 alone, and all in combination. K153A had no effect on Hmg2 regulation (Figure 3.25), but both the triple mutant RYL133-135AAA (RYL) and K153A R155A R157A (KRR) partially destabilized Hmg2 (Figure 3.21-3.23). We next tested these constructs in the limited proteolysis assay. As might be predicted from their in vivo instability, both RYL and KRR had a high basal level of proteolysis but did not respond to GGPP (Figure 3.24 and 3.25.

We tested these mutations for in-cis epistasis with the stabilizing mutations S215A and K6R. The addition of S215A or K6R partially stabilized RYL and KRR (Figures 3.21-3.23). The S215A mutation ablated GGPP regulation of both RYL and KRR. The double mutation further stabilized KRR, bringing its steady state levels up to those of wild-type and slowing its degradation. In addition, while the loop 1 mutations alone did not completely ablate the in vivo response to GGPP, the addition of the S215A mutation did, as expected.

Finally, we also mutated aspartate 165 to alanine. The D165A mutation slightly increased steady state levels in vivo, stabilized Hmg2, and rendered it insensitive to GGPP in a cycloheximide chase.

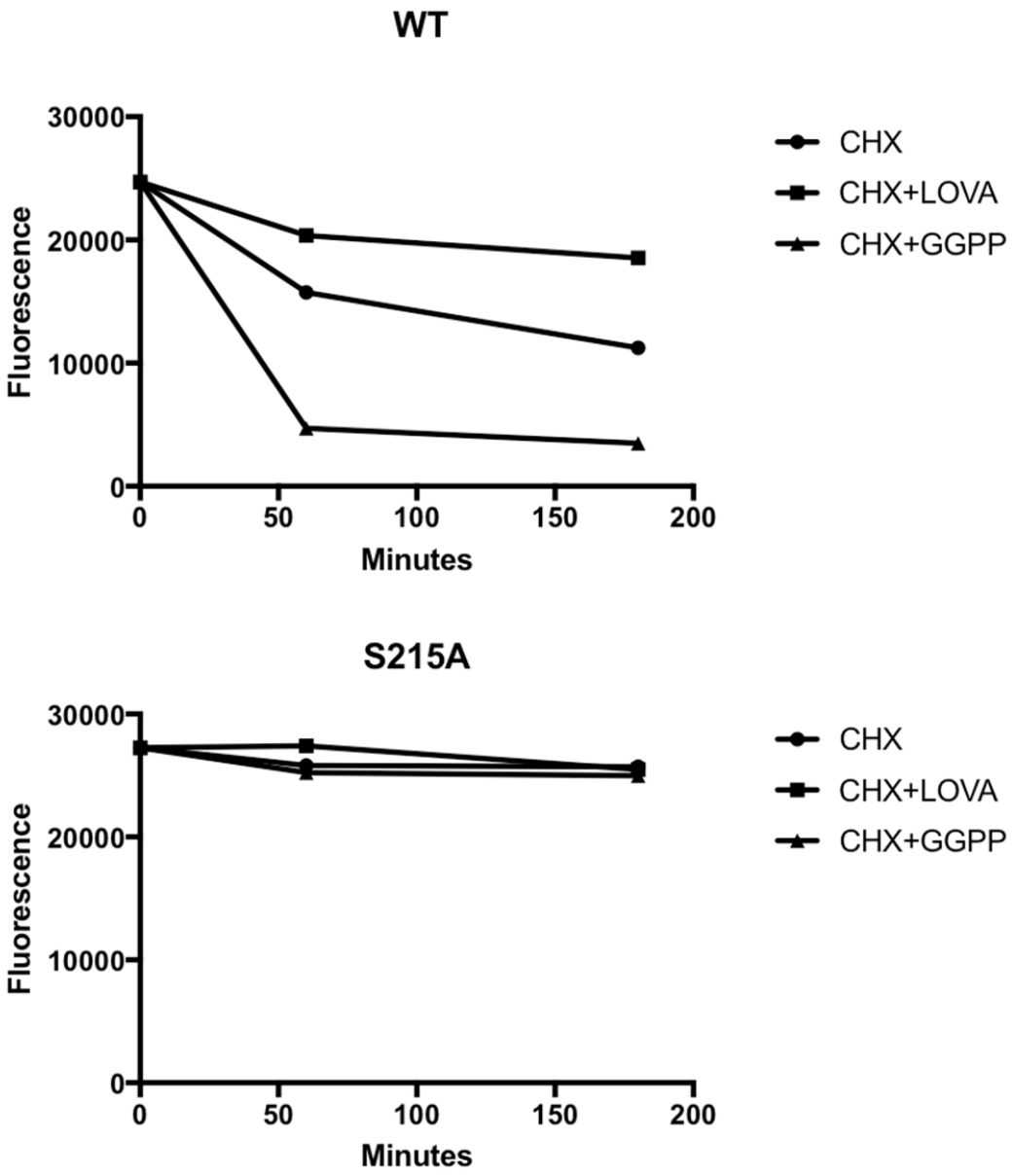

Figure 3.21. Cycloheximide chases with GGPP and lovastatin on WT and S215A Hmg2-GFP for comparison

Values are mean fluorescence of 10,000 cells treated with cycloheximide plus vehicle, 22 μM GGPP, or 25 μg/mL lovastatin.

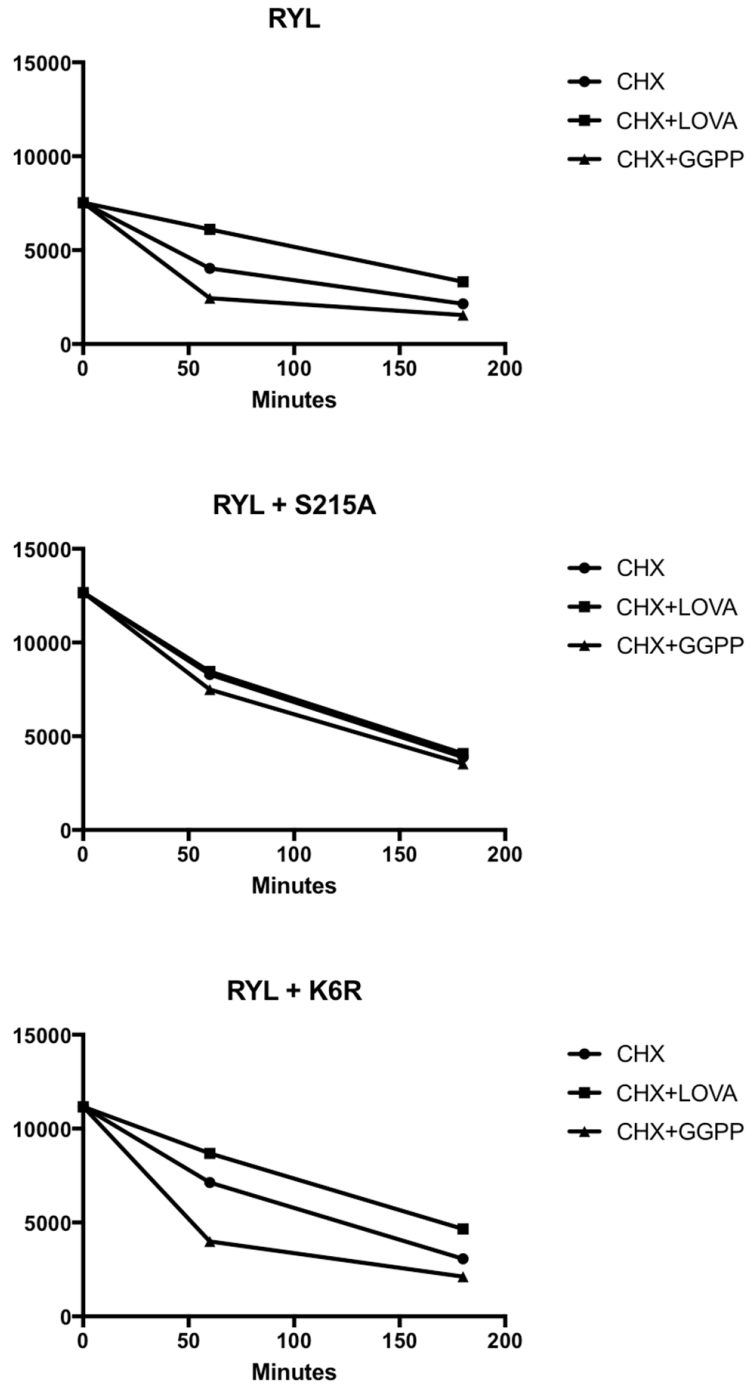

Figure 3.22. Cycloheximide chases with GGPP and lovastatin on RYL and epistasis mutations

Values are mean fluorescence of 10,000 cells treated with cycloheximide plus vehicle, 22 μM GGPP, or 25 μg/mL lovastatin. RYL is RYL133-135AAA.

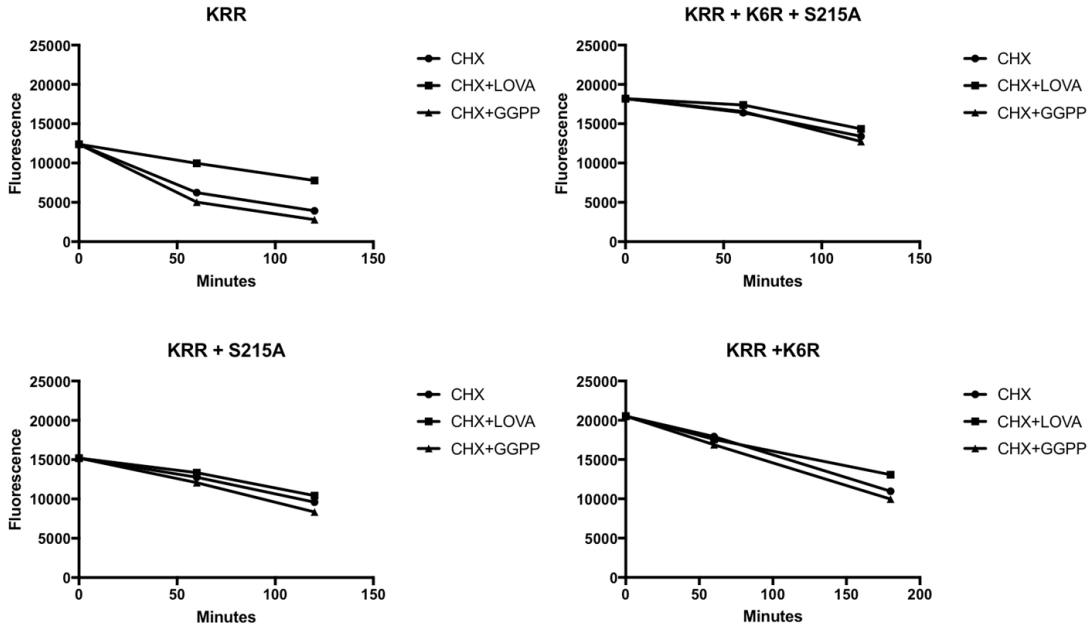

Figure 3.23. Cycloheximide chases with GGPP and lovastatin on KRR and epistasis mutations

Values are mean fluorescence of 10,000 cells treated with cycloheximide plus vehicle, 22 μM GGPP, or 25 μg/mL lovastatin. KRR is K153A R155A R157A. Note that time course on the KRR + K6R mutation differs from other graphs.

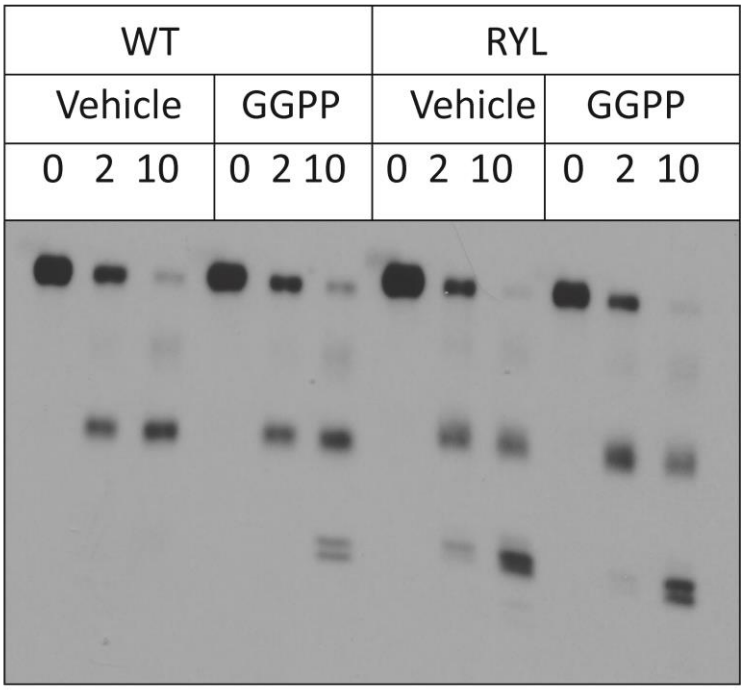

Figure 3.24. The RYL mutation causes constitutive misfolding in vitro
Limited proteolysis assay on microsomes from cells expressing WT (left) and RYL133-135AAA (RYL; right) 1myc-Hmg2-GFP. Microsomes were treated with vehicle or 22 μM GGPP prior to proteolysis.

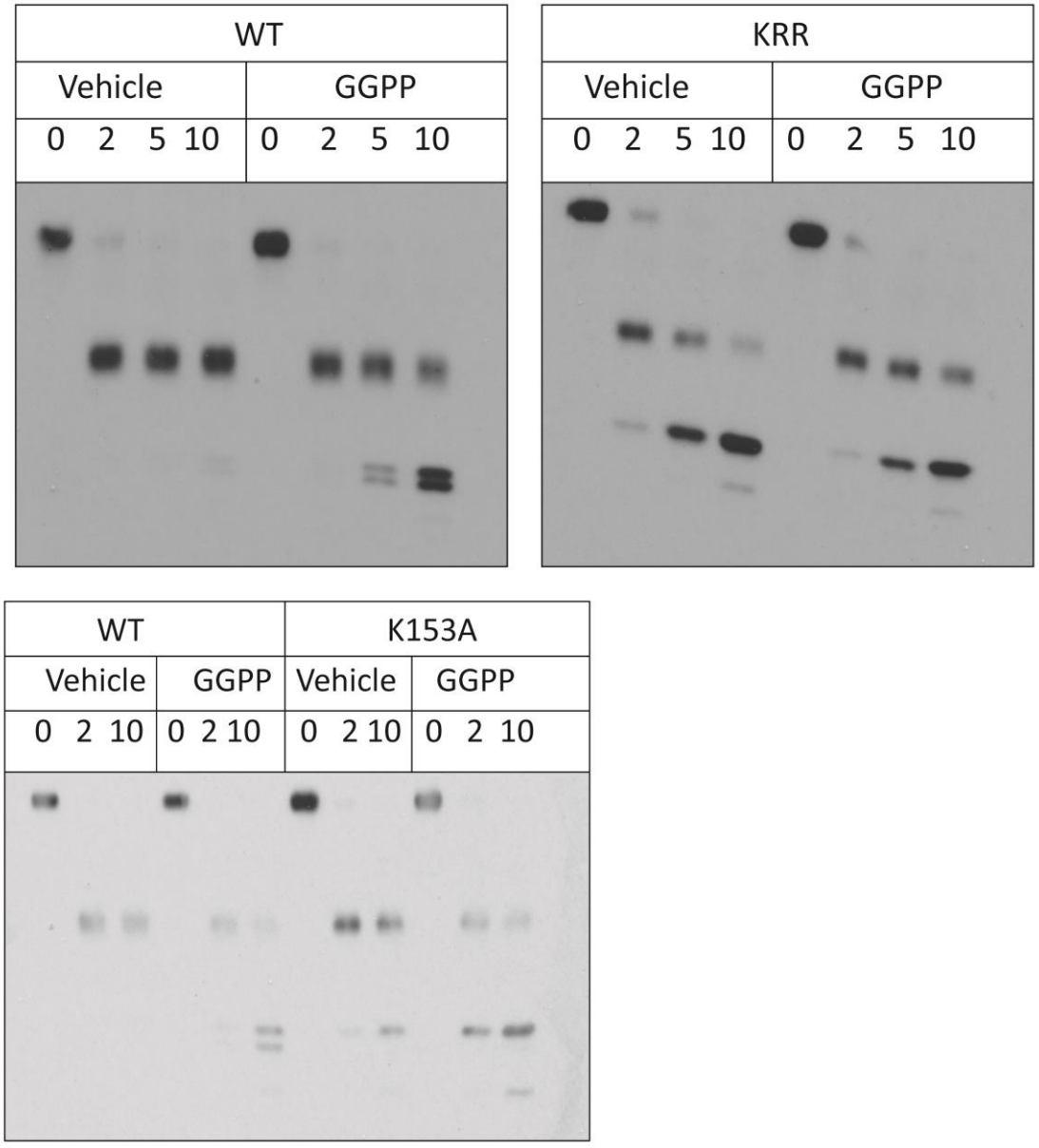

Figure 3.25. The KRR mutation but not K153A alone causes constitutive misfolding in vitro

Top: Limited proteolysis assay on microsomes from cells expressing WT (left) and K153A R155A R157A (KRR; right) 1myc-Hmg2-GFP. Microsomes were treated with vehicle or 22 μM GGPP prior to proteolysis. Bottom: WT versus the K153A single mutation, which is normally regulated.

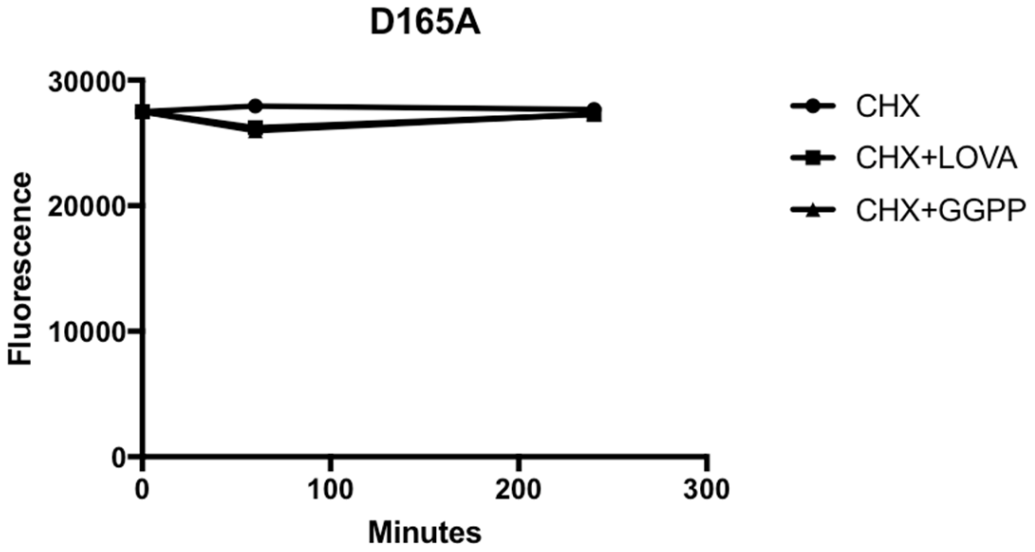

Figure 3.26. D165A is stable and does not respond to GGPP in vivo
Values are mean fluorescence of 10,000 cells treated with cycloheximide plus vehicle, 22 μM GGPP, or 25 μg/mL lovastatin.

Taken together, these data show that loop 1 plays an important role in regulating Hmg2 degradation.

Toxic subunits

We have previously shown that Hmg2 exists in a multimer by demonstrating that a myc-tagged version of Hmg2 can co-immunoprecipitate with a GFP-tagged version (see Chapter 2, Figure 2.23). Since the GFP-tagged version of Hmg2 does not have a catalytic domain, these data also suggest that the membrane domain of Hmg2 is capable of mediating this self-interaction. Given that mutations in the SSD appear to block a conformational change in Hmg2's membrane domain, and that the membrane domain appears to be in contact with the membrane domain of other Hmg2s, we hypothesized that blocking the structural transition in one Hmg2 might interfere with this conformational change in another Hmg2 in the same way that for some allosteric proteins, "toxic" subunits can "poison" a whole multimeric assembly. We tested this hypothesis by constructing yeast strain expressing differently-tagged Hmg2 proteins, one wild type and one containing the stabilizing mutation S215A.

For our in vivo experiments, we used a wild-type version tagged with GFP (Hmg2-GFP) and either a wild type or a mutated version tagged with myc (Hmg2-1myc or K357R Hmg2-1myc) so that the "background" copy would not interfere with detection of wild type Hmg2 by flow cytometry. When these two versions of Hmg2 were co-expressed, steady state fluorescence of wild type Hmg2-GFP was higher in the strain co-expressing the mutated K357R 1myc-Hmg2 than in the strain expressing

the wild type 1myc-Hmg2, implying that the mutated copy stabilized the wild type copy (Figure 3.27).

We also tested this hypothesis in vitro using limited proteolysis. For these experiments, we used the same wild type version of 1myc-Hmg2-GFP from the limited proteolysis experiments above. We then co-expressed either wild-type or S215A Hmg2-GFP with no myc tag to act as the background copy, to avoid interfering with detection of the myc tag (Figure 3.28). We also compared these strains to a strain expressing only S215A 1myc-Hmg2-GFP as a positive control. Again, we found that expression of the mutated S215A Hmg2-GFP interfered with the function of the wild type copy. Wild type 1myc-Hmg2-GFP underwent normal in vitro misfolding in response to GGPP when the background copy was wild type, but its response to GGPP was blunted when the background copy had the S215A mutation (3.18). Not only is the SSD essential for Hmg2 misfolding, but lesions in the SSD can block the function of wild type Hmg2 in *trans*.

The autonomous SSD

Finally, we tested the ability of the SSD to function removed from its normal membrane context. We prepared microsomes from the in vitro proteolysis strain expressing 1myc-Hmg2-GFP and subjected them to solubilization with a variety of detergents. Three of the detergents tested, Fos-Choline-13, Decyl Maltose Neopentyl Glycol (DMNG), and digitonin yielded soluble 1myc-Hmg2-GFP that retained its

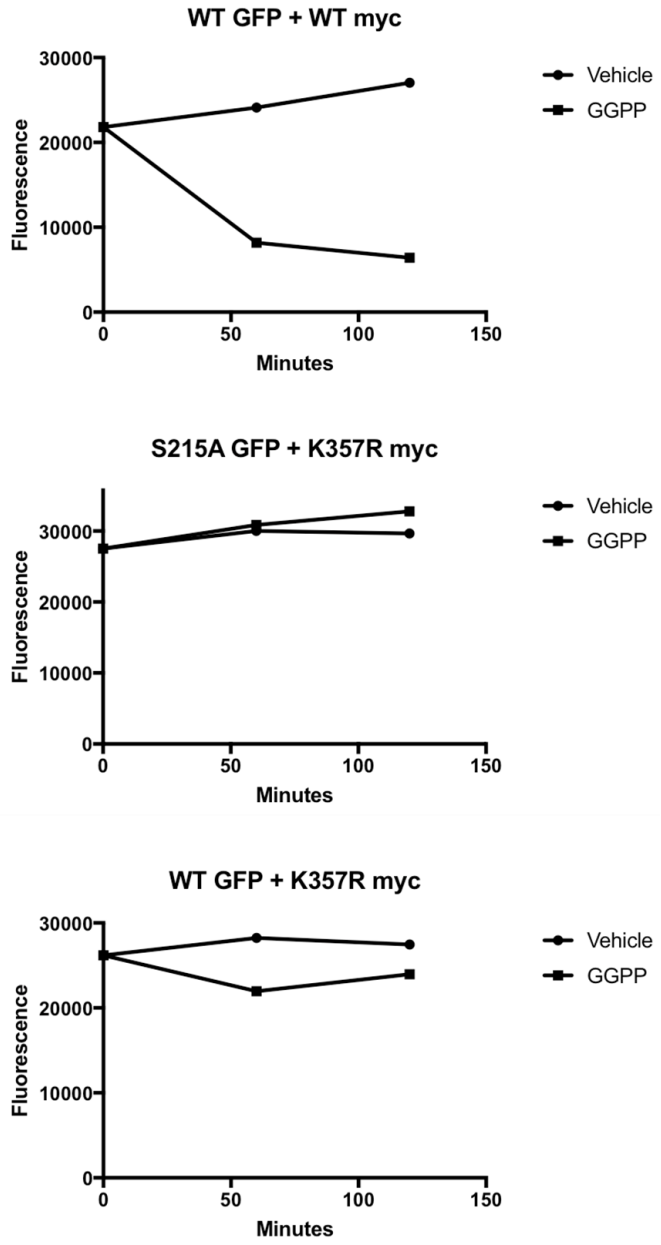

Figure 3.27. Mutated SSDs act as toxic subunits for Hmg2 degradation
Fluorescence of Hmg2-GFP over a 2 hour time course. Cells were treated with vehicle or 2 μM GGPP as indicated. Top panel shows wild type Hmg2-GFP co-expressed with a background wild type myc copy as a negative control. Middle panel shows S215A Hmg2-GFP co-expressed with a background K357R myc copy as a positive control for stability. The bottom panel shows wild type Hmg2-GFP co-expressed with the K357R Hmg2-myc in the background. Data points are the mean of 10,000 events.

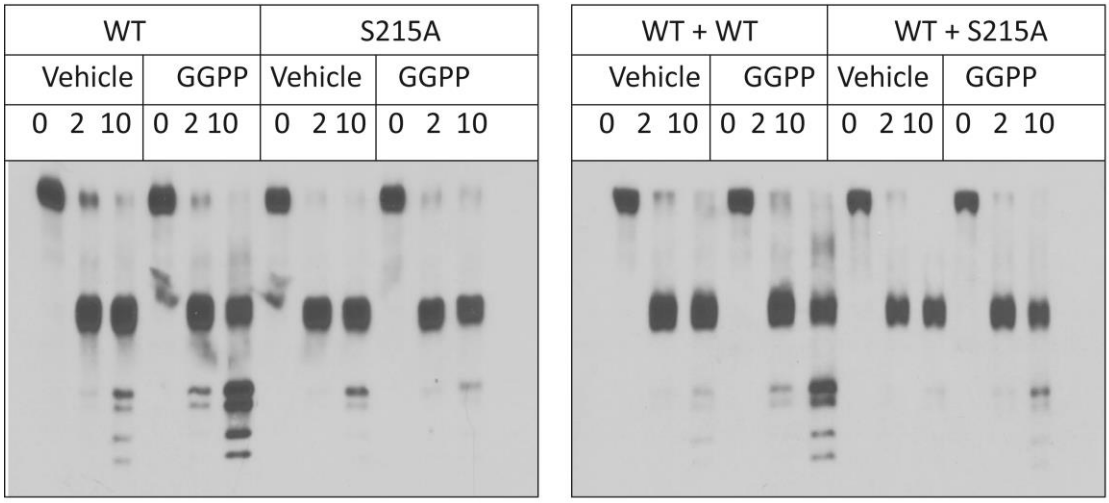

Figure 3.28. Mutated SSDs act as toxic subunits for Hmg2 misfolding
Limited proteolysis of 1myc-Hmg2-GFP. Microsomes were treated with vehicle or 2 μM GGPP as indicated. Left panel shows wild type and S215A 1myc-Hmg2-GFP expressed alone for reference. Right panel shows wild type 1myc-Hmg2-GFP co-expressed with a background wild type Hmg2-GFP copy (left) or with an S215A Hmg2-GFP copy (right). Proteolysis was for 0, 2, or 10 minutes as indicated.

normal pattern of proteolytic cleavage (Figure 3.29). This solubilized Hmg2 was, however, more sensitive to trypsin (data not shown), and lower concentrations of trypsin were used in these experiments.

Solubilized 1myc-Hmg2-GFP appeared to be constitutively more structurally open than when present in the ER membrane, with high basal rates of proteolysis. However, it retained the ability to respond to the chemical chaperone glycerol. Preparations treated with 20% glycerol were more resistant to proteolysis, just as in the normal membrane assay (Figure 3.29, third set of lanes in each panel). However, preparations made with Fos-Choline-13 and DMNG had no detectable ability to respond to GGPP, whether alone or in combination with glycerol treatment (Figure 3.29, second set of lanes in panels 1-3). Surprisingly, digitonin-solubilized preparations did respond to GGPP in the detergent limited proteolysis assay, albeit at higher concentrations than required in the membrane assay (Figure 3.29, bottom right panel). Importantly, the nonresponding TFSYA Hmg2 did not respond to GGPP in either the intact microsome or digitonin assay (Figure 3.30).

We also found that GGPP affects Hmg2's solubility in detergent. After preparing and solubilizing microsomes, we added vehicle or GGPP to the preparations and incubated for 1 hour with gentle shaking. Afterward, we separated the samples by ultracentrifugation, and found that preparations treated with GGPP had been more effectively solubilized by digitonin. Importantly, the inactive analog of GGPP, 2F-GGPP and the antagonist GGSPP, which do not stimulate Hmg2 degradation in vivo or misfolding in vitro, did not have any effect on solubility in this assay (Figure 3.31).

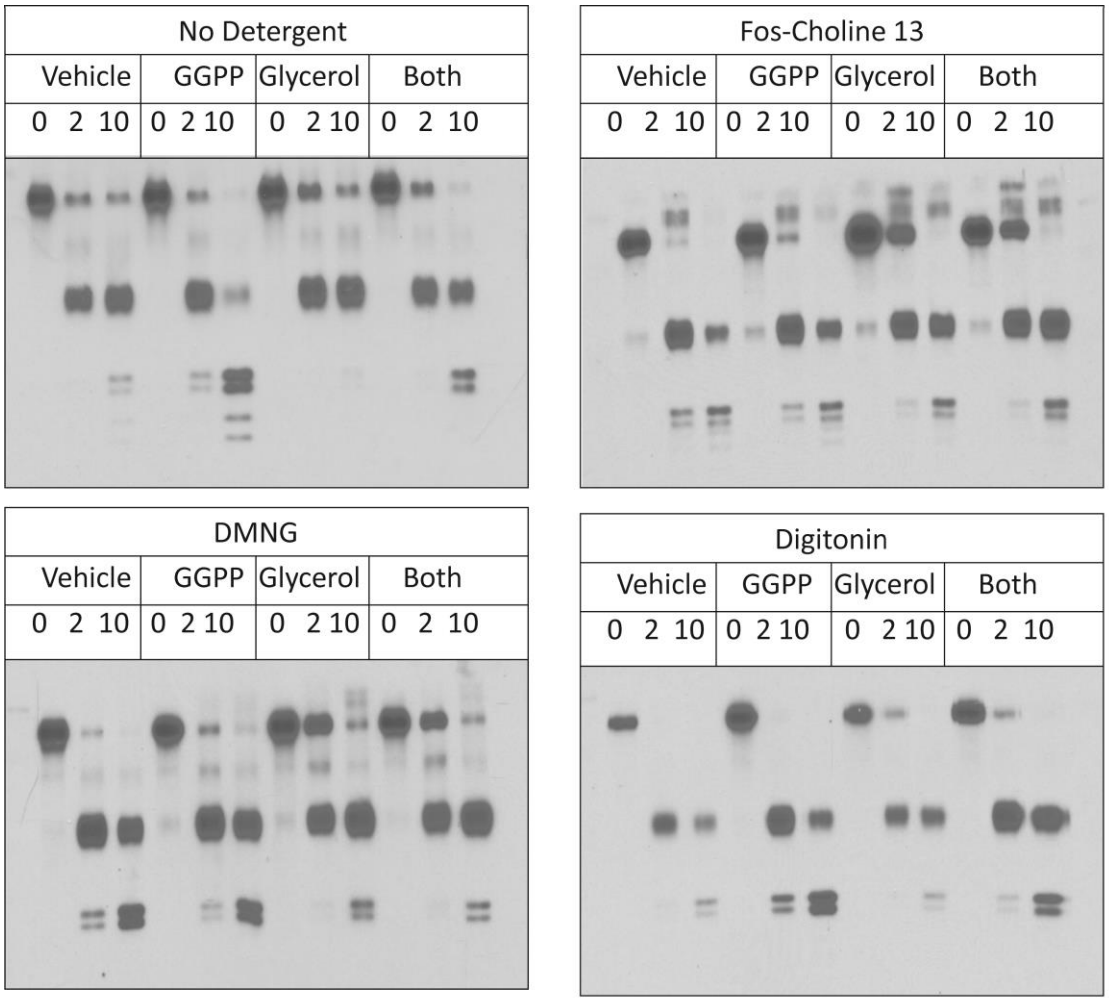

Figure 3.29. Hmg2 proteolytic pattern and misfolding are preserved in some weak detergents

Limited proteolysis on microsomes expressing 1myc-Hmg2-GFP and solubilized with the indicated detergents. Microsomes were treated with vehicle, 20% glycerol, or 22 μM GGPP. Proteolysis was for 0, 2, or 10 minutes as indicated.

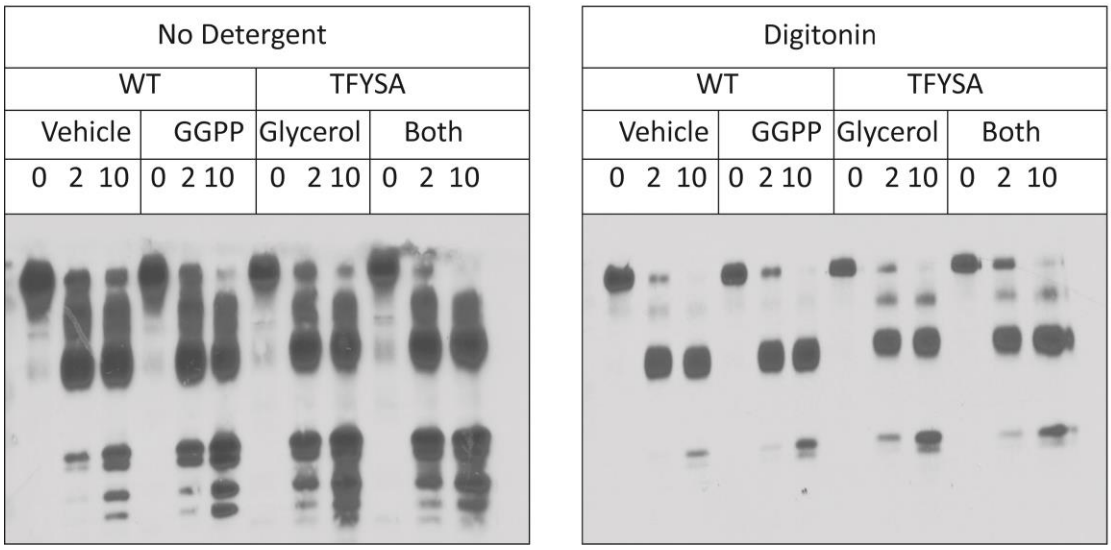

Figure 3.30. GGPP does not affect the non-responding TFYSA Hmg2 in digitonin
Limited proteolysis on microsomes expressing wild type or TFYSA 1myc-Hmg2-GFP in microsomes or solubilized with digitonin. Microsomes were treated with vehicle or 22 μM GGPP. Proteolysis was for 0, 2, or 10 minutes as indicated.

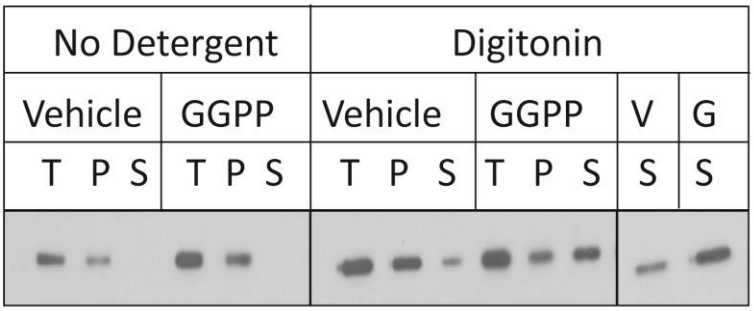

Figure 3.31. GGPP enhances Hmg2 solubility in digitonin
Total lysate (T), pellet (P), or supernatant (S) from ultracentrifugation of microsomes containing 1myc-Hmg2-GFP. Microsomes were left intact (left) or solubilized with digitonin (right) and then treated with vehicle or 22 μM GGPP. Far right shows direct comparison of digitonin supernatants treated with vehicle and GGPP; these are the same samples as in the total, pellet, and supernatant panel loaded a second time.

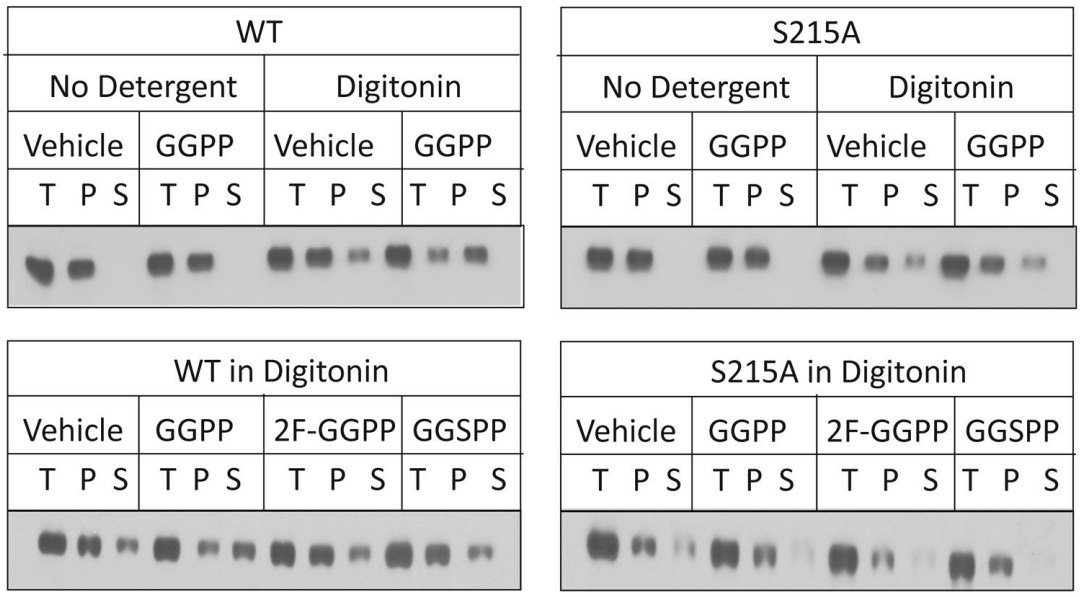

Figure 3.32. GGPP solubility enhancement is specific for active isoprenoid and the intact SSD

Total lysate (T), pellet (P), or supernatant (S) from ultracentrifugation of microsomes containing wild type or S215A 1myc-Hmg2-GFP. Top: Microsomes were left intact (left) or solubilized with digitonin (right) and then treated with vehicle or 22 μM GGPP. Far right shows direct comparison of digitonin supernatants treated with vehicle and GGPP; these are the same samples as in the total, pellet, and supernatant panel loaded a second time. Bottom: both panels show digitonin-solubilized microsomes treated with vehicle, 22 μM GGPP, 22 μM 2F-GGPP, or 22 μM GGSPP.

The stable S215A Hmg2 did not become more solubilized by GGPP in these initial experiments, indicating that this effect is specific both to the structure of GGPP and to the misfolding capability of the SSD (Figure 3.32).

These solubility experiments yielded one additional surprise. As a control, we also performed long incubations in detergent and GGPP with both wild type and S215A Hmg2. While the stable SSD mutants had not responded to GGPP in any of our other assays, we found that when incubated overnight with a high concentration of GGPP (22μM, or approximately 1000 times that required to begin to see effects in the wild type protein), S215A 1myc-Hmg2-GFP did misfold in response to signal (Figure 3.33). This effect is both structurally specific, as 2F-GGPP and GGSPP did not induce this effect in either wild type or S215A Hmg2 (Figure 3.34) and dose dependent, as lower doses of GGPP which are effective on wild type Hmg2 on a time scale of minutes did not affect S215A Hmg2 even overnight (Figure 3.35). A time course of GGPP incubation found that the response time of S215A 1myc-Hmg2-GFP is severely delayed, but that it begins to respond to GGPP by 2.5 hours of treatment with a maximal response occurring by 3.5 hours (3.36). For comparison, wild type 1myc-Hmg2-GFP responds to signal effectively immediately; even when GGPP is added at the same time as protease, there is still an effect at the first (two minute) time point. Taken together, these data indicate that the SSD is required for regulated misfolding and degradation of Hmg2. Surprisingly, as random mutation tends to interfere with normal structure and function, mutating the SSD renders Hmg2 stable. Lesions in the SSD block Hmg2 from responding to the degradation signal GGPP, preventing in vivo

degradation and in vitro misfolding. Hmg2 forms multimeric structures, and mutations in the SSD can block regulation in wild type Hmg2 in-*trans*. The SSD constitutes a separate determinant for Hmg2 regulation, and its function is autonomous of Insig proteins and partially retained even when removed from the normal context of the ER membrane. Finally, the role of the SSD appears to be kinetic, with long incubations at extremely high concentrations of signal eventually overcoming its loss. Accordingly, we propose a model wherein the SSD acts as kinetic module to induce Hmg2 misfolding. When GGPP is detected, the SSD promotes the rapid and reversible conformational change in Hmg2 to a misfolded state which can be detected by the ubiquitin proteasome pathway.

Discussion

In this work we set out to understand the role of the conserved sterol sensing domain in the regulated misfolding and ERAD of Hmg2. This included a homology-directed mutational dissection of Hmg2's transmembrane domain and an in analysis of SSD and non-SSD mutations using both in vivo and in vitro methods.

We tested SSD residues for their role in Hmg2 misfolding using flow cytometry in vivo and a limited proteolytic assay for Hmg2 structure in vitro. We found that mutations in the SSD block isoprenoid-induced misfolding of Hmg2 in vitro, meaning that the proteolysis assay can serve as an in vitro assay of SSD function. Surprisingly, all known SSD point mutations stabilize Hmg2 in vivo. No individual SSD residues were found which induced increased degradation of the

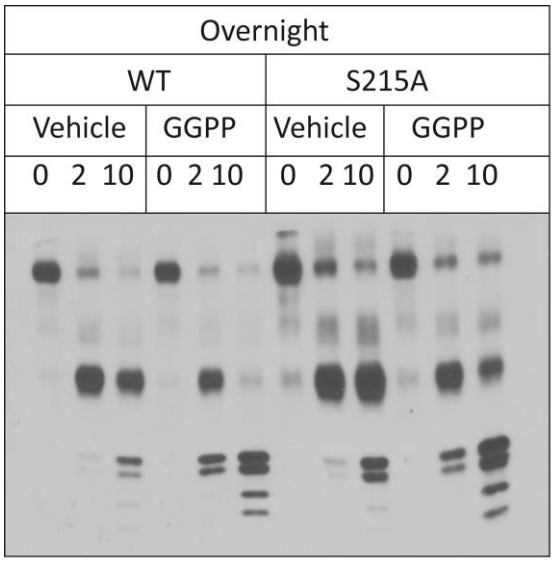

Figure 3.33. S215A Hmg2 undergoes regulated misfolding after overnight treatment with GGPP

Limited proteolysis of wild type or S215A 1myc-Hmg2-GFP treated overnight with vehicle or 22 μM GGPP. Assay was otherwise identical to the standard proteolysis assay.

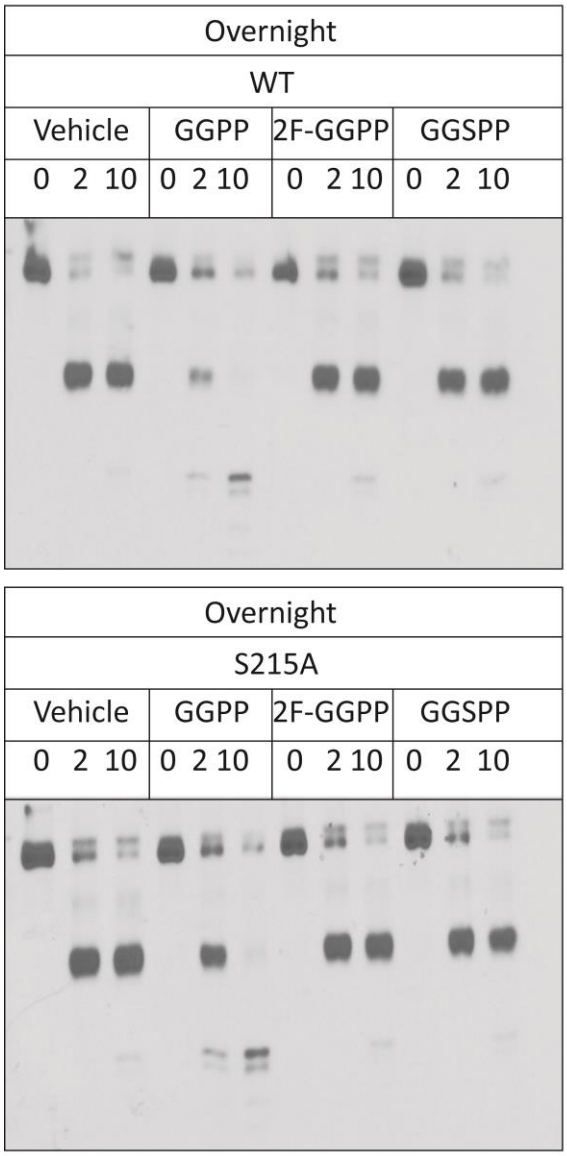

Figure 3.34. S215A misfolding is specific for active isoprenoid
Limited proteolysis of wild type or S215A 1myc-Hmg2-GFP treated overnight with vehicle or 22 μM GGPP, 2F-GGPP, or GGSPP. Assay was otherwise identical to standard proteolysis assay.

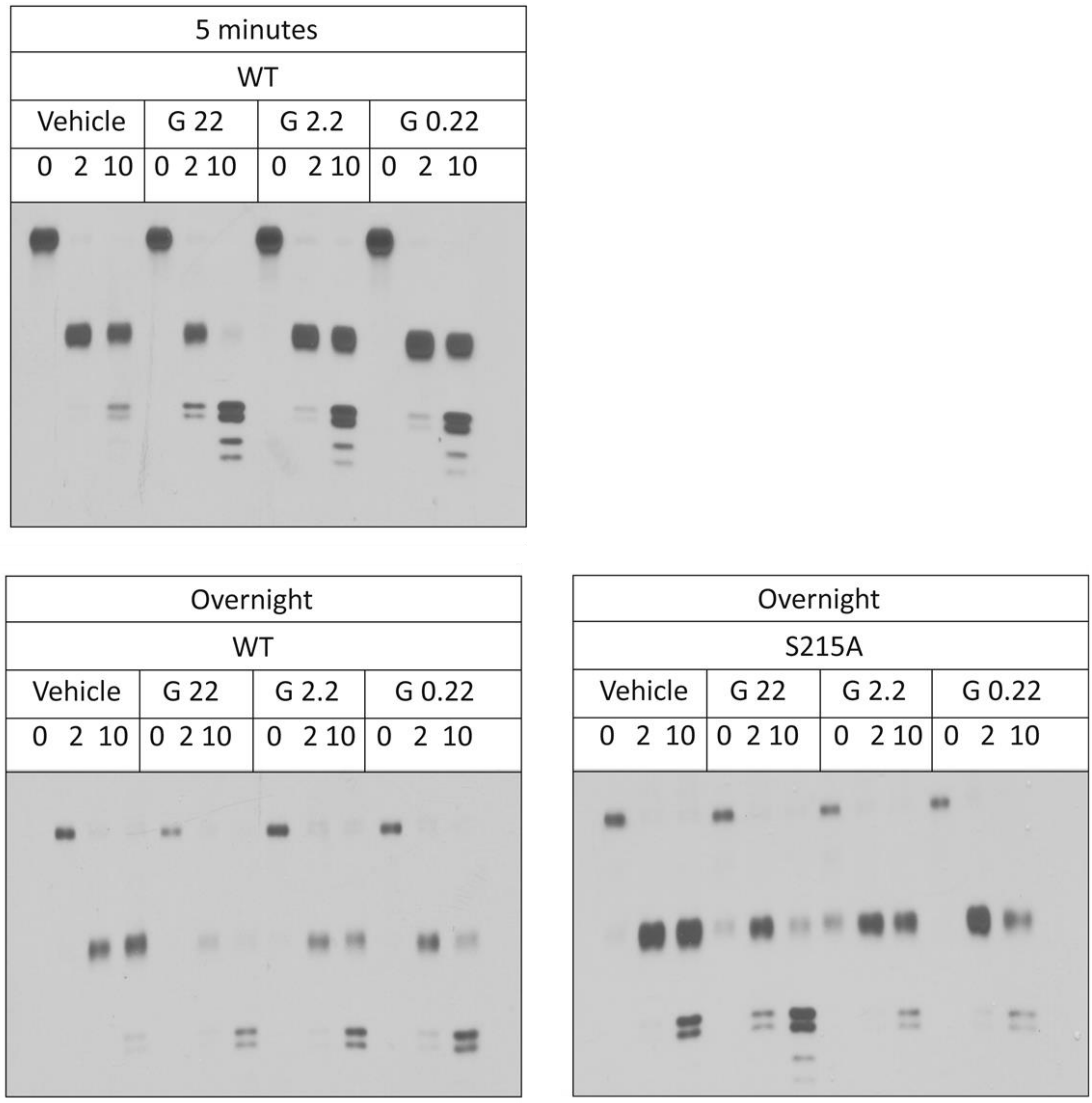

Figure 3.35. S215A misfolding is dose dependent
Limited proteolysis of wild type or S215A 1myc-Hmg2-GFP treated overnight (bottom two panels) with vehicle 10-fold dilutions of GGPP: 22 μM, 2.2 μM, and 0.22 μM. Wild type treated for five miutes is shown for comparison (top panel)

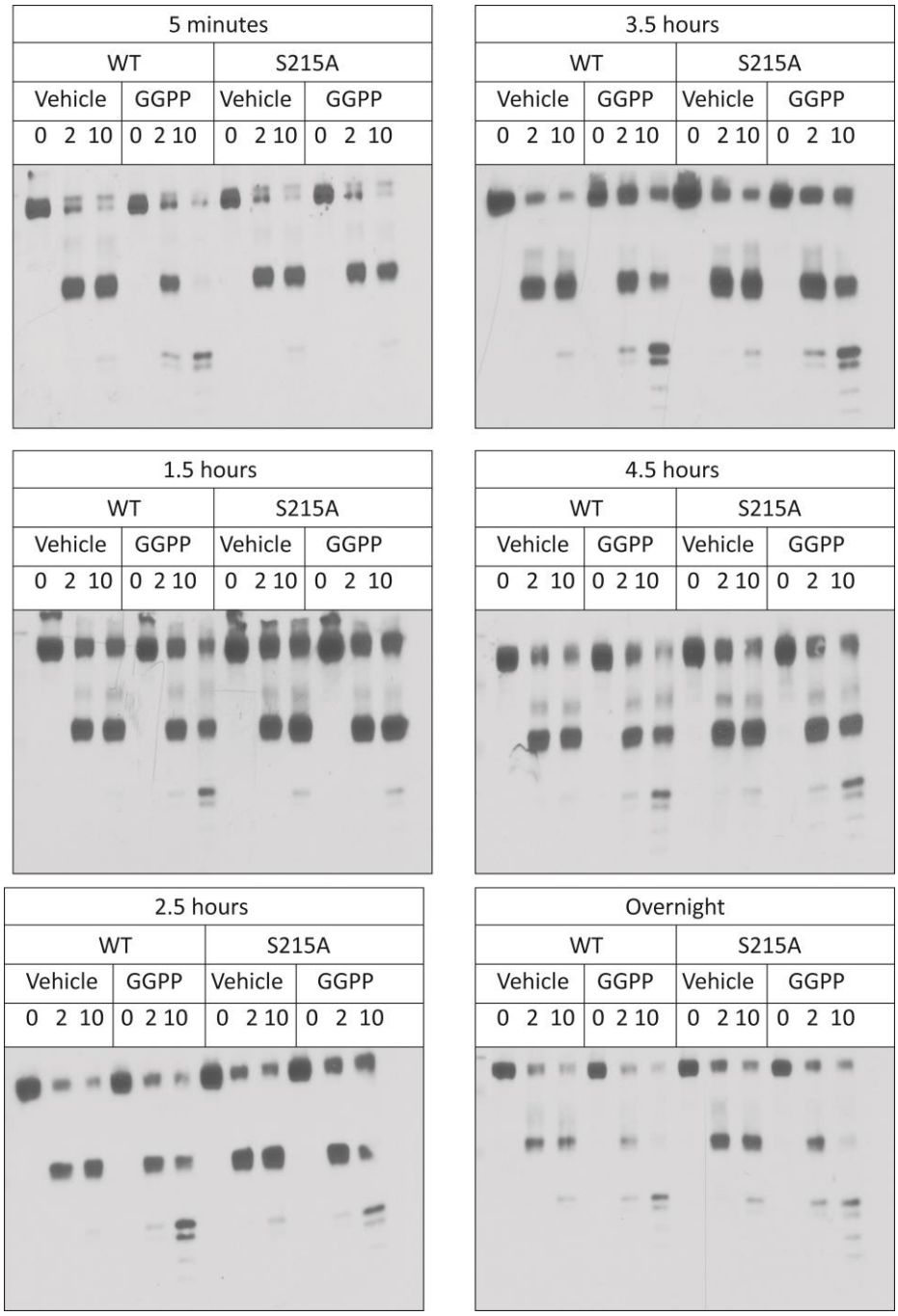

Figure 3.36. Time course of S215A misfolding

Limited proteolysis of wild type or S215A 1myc-Hmg2-GFP treated for 5 minutes, 1.5 hours, 2.5 hours, 3.5 hours, 4.5 hours, or overnight with vehicle or 22 μM GGPP as indicated. Assay was otherwise identical to the standard proteolysis assay.

protein when mutated, suggesting that the role of SSD is to undergo a conformational change which mimics misfolding. We tested whether the SSD-dependent structural change was intrinsic to the domain itself, or whether it required the SSD-binding protein Insig. Both in vivo and in vitro we found that the yeast Insigs Nsg1 and Nsg2 were not required for Hmg2 misfolding and degradation. Consistent with previous results, co-overexpressing Nsg1 alongside Hmg2 blocked regulated in vitro misfolding and in vivo degradation.

Using our structural assay for SSD function, we tested other stabilizing mutations in Hmg2. We found that while the K357R mutation does not misfold in response to GGPP, the K6R mutation responds like wild type Hmg2 in vitro. This was the first time we have identified separate regions of Hmg2 required for misfolding versus ubiquitination and degradation. Previously, all known stabilizing mutations in Hmg2 also prevented ubiquitination and vitro misfolding. Additionally, this result suggests a hypothesis wherein lysine 6, as a cytosol-facing lysine which prevents Hmg2 ubiquitination and degradation but not misfolding, may be a ubiquitination site.

We further explored the role of Hmg2's transmembrane region using in-trans co-expression experiments. Hmg2 exists as a multimer, so we tested the effects of mutations in the transmembrane region on neighboring molecules. Remarkably, we found that expressing Hmg2 with the K357R mutation, which blocks in vitro misfolding, interferes with regulation of wild type Hmg2 in *trans*. Co-expression of the mutated protein in vivo partially stabilized wild type Hmg2, while in vitro the mutated protein blunted the wild type protein's response to GGPP. This suggests a

model for Hmg2 misfolding wherein the transmembrane domains of multiple Hmg2 molecules influence each other's conformational states, similar to cooperativity and allostery.

We also performed a directed search for additional structural features involved in Hmg2 regulation. A targeted, homology-based search of the SSD and nearby residues revealed a new site, asparagine 401, required for Hmg2 degradation and misfolding. In vivo competition experiments and site-directed mutagenesis also revealed a role for the first luminal loop of Hmg2 in regulation.

Finally, we continued our analysis of the role of the SSD by pursuing further in vitro methods. We found that not only is the overall proteolytic pattern of Hmg2 preserved when solubilized in several weak detergents, but that solubilized Hmg2 can still be chaperoned by glycerol. Remarkably, in digitonin, Hmg2 still misfolds in response to GGPP. Finally, extended time courses showed that S215A Hmg2 can still respond to GGPP after long incubation times, but that its response is delayed several fold compared to the response of the wild type protein, which responds effectively immediately in vitro and begins to be degraded within minutes in vivo. Together, these finding suggest a role for the SSD as an autonomous module for promoting misfolding—or rather, a conformational change that strongly resembles misfolding—in response to a signal. In Hmg2, GGPP binding at an unknown site, potentially loop 1 and/or loop 7, causes the SSD to undergo a conformational change that exposes the protein to the ERAD quality control pathway. Lesions in the SSD block this change at physiologically relevant concentrations and time scales, and, as Hmg2 is a multimer,

even impede regulation of wild type subunits in-*trans*. This role for the SSD can be thought of in terms of a kinetic or catalytic one, as mutations in the SSD do not appear to block the conformational change absolutely so much as render it impractically slow for cellular regulation. Finally, this action of the SSD occurs independently of the yeast Insig proteins and is partially retained even in weak detergents. We propose an independent model for SSD function as a module that enables regulated entry into a variety of proteostasis pathways—ERAD in the case of yeast Hmg2 and mammalian HMGR, but also the ER-Golgi secretory pathway, retrograde transport, and the endosomal sorting complexes required for sorting (ESCRT) pathway in the case of other SSD-containing proteins.

This model of SSD function leaves several open questions. In the case of Hmg2, the most obvious of these is the question of GGPP binding. Our current in vitro approaches do not distinguish between mutations in Hmg2 which eliminate GGPP binding and those which allow binding but disable misfolding in response to binding elsewhere. Thus, the location of the GGPP binding site, if there is one, is unknown. Sequence and structural homology to SCAP and small regions of GGPP binding proteins suggest loop 1 and/or loop 7 of Hmg2 as possible locations. Indeed, this work supports a crucial role for loop 1 in Hmg2 regulation. Mutations to positively charged residues in the region of the loop which resembles the GGPP-binding proteins Ram2 and Bet2 results in dysfunctional regulation of Hmg2. The RYL133-135AAA and K153A R155A R157A mutations both result in instability and blunted GGPP regulation in vivo and high levels of basal proteolysis with no response to GGPP in

vitro. While this phenotype may on its face seem peculiar for a candidate binding site—one might predict that mutating the GGPP binding site would lead to stability that mimics that of the SSD mutations like S215A—we are not sure what a binding phenotype should look like. Mutations in loop 1 of SCAP block cholesterol binding but simultaneously cause SCAP to behave as though it is always bound to cholesterol. Thus a constitutive degradation phenotype is not decisive evidence one way or the other.

While new in vitro approaches are needed to fully evaluate candidate binding sites, one surprising result in this work may prove fruitful in intermediate studies of binding. Prolonged incubations of Hmg2 bearing the SSD mutation S215A with GGPP eventually result in in vitro misfolding of the protein. If the SSD behaves as a kinetic or "catalytic" module for promoting misfolding on useful time scales, this may distinguish it from severe lesions to a GGPP binding site. Further work is needed to evaluate whether other known SSD mutations such as TLCC202-205AAAA, L219F, FY349LA, and K357R, and SSD-like mutations, such as N401A, also respond to high concentrations of GGPP after long incubations. If known SSD mutations respond similarly to long treatments with GGPP, candidate binding regions can be tested to see whether they differ.

In addition to binding cholesterol in loop 1, SCAP requires interaction of loop 1 with loop 7 to respond to cholesterol. Mutations in loop 1 or loop 7 which prevent this binding cause SCAP to behave as though it is not bound to cholesterol, Interestingly, the newly-identified N401A mutation in Hmg2 results in stability and

lies in TM7, close to this loop. Additional mutational analyses of remaining conserved residues in loops 1 and 7 could shed further light on Hmg2 regulation outside the SSD.

Taking a longer view, studies of GGPP binding would be greatly aided by an in vitro assay for binding. Hmg2 has so far proved difficult to solubilize in many detergents, and many others appear to denature its native structure. The detergents Fos-Choline-13, decyl maltose neoptenyl glycol (DMNG), and digitonin all allow Hmg2 to retain it native structure to the extent that is proteolytic cleavage pattern is unchanged. While Fos-Choline-13 and DMNG do not appear to support regulated proteolysis and thus may not support GGPP-binding, digitonin appears to support GGPP-binding by two measures—regulated in vitro proteolysis, and an increase in solubilization when GGPP is added to preparations. While digitonin is a challenging detergent for binding studies, as it is non dialyzable, we hope that this advance in in vitro methods will prove a stepping stone to developing a binding assay in the future. Moreover, the first structures of the SSD were recently published, opening up the possibility of direct structural studies on other SSD proteins.

Proteins containing the SSD are of particular interest for their recurring roles in human disease. Roughly half of adults in the United States have dyslipidemia or control dyslipidemia with cholesterol-lowering medications such as statins and ezetimibe. SCAP is the master regulator of sterol synthesis, while HMGR, the rate-controlling step of sterol synthesis under many conditions, is the statin target and the SSD-containing intestinal cholesterol transporter NPC1L1 (Niemann-Pick Disease Type C 1 Protein Like Protein) is one of the targets of ezetimibe. Mutations in NPC1

(Niemann-Pick Disease Type C1 Protein) cause the fatal developmental and neurodegenerative disorder Niemann-Pick, while mutations in DHCR-7 (7-dehydrocholesterol reductase), the final step of cholesterol synthesis in humans, cause the developmental disorder Smith-Lemli-Opitz Syndrome. Even mutations in the more distantly related but SSD-containing Patched protein, which has the least direct role in cholesterol regulation, leads to the human cancer syndrome Gorlin Syndrome.

More strikingly, mutations in NPC1 and DHCR7, including some human disease proteins, can direct both proteins into the ERAD pathway for degradation. Treatment with chemical chaperones of NPC1 raise levels of correctly-localized NPC1 and ameliorate the sterol phenotype in mouse cells expressing human disease variants of NPC1. Moreover, even normal NPC1 appears to be regulated by ubiquitination and degradation by the endosomal sorting complex required for transport (ESCRT) pathway in response to cholesterol. A better structural and mechanistic understanding of the SSD could not only shed light on the normal workings of sterol synthesis, trafficking, and regulation, but also provide new avenues for treating human disorders.

Experimental procedures

Reagents

Geranylgeranyl pyrophosphate, cycloheximide, trypsin, and digitonin were purchased from Sigma-Aldrich. Digitonin was washed and recrystallized in ethanol 3 times according to the manufacturer's instructions. Lovastatin was a gift from Merck & Co (Rahway NJ). 2-fluoro-GGPP was a gift from Reuben Peters (Iowa State

University) and Philip Zerbe (University of California Davis). Fos-Choline-13 and Decyl Maltose Neopentyl Glycol were purchased from Anatrace. Anti-myc 9E10 supernatant was produced from cells (CRL 1729, American Type Culture Collection) grown in RPMI1640 medium (GIBCO BRL) with 10% fetal calf serum. Living colors mouse anti-GFP monoclonal antibody was purchased from Clontech. Goat anti-mouse antibody HRP-conjugated antibody was purchased from Jackson ImmunoResearch. Polyclonal rabbit anti-GFP antibody was a gift from C. Zucker (University of California San Diego). Protein A Sepharose beads were purchased from Amersham Biosciences.

Strains and plasmids

Yeast strains (Table 3.2) and plasmids (Table 3.3) were made by standard techniques. Yeast strains were isogenic and made from the S288C background. Yeast were grown in rich media (YPD) or in minimal media (Diffco Yeast Nitrogen Base with required amino acids and nucleic acids and 2% glucose) at 30^{o}C.

SSD mutation plasmids were made by splicing by overlap extension (SOEing) or site directing mutagenesis using the Life Technologies GeneArt system.

Ura3 Hmg2-GFP, 1myc-Hmg2-GFP, and Hmg2-1myc plasmids were introduced at the *ura3-52* locus by integration of plasmid cut with *StuI*. Leu2 Hmg2-GFP plasmids were introduced into the promoter of the *leu2Δ* locus by integration of plasmid cut with *PpuMI.*

Flow cytometry

Flow cytometry experiments were performed as previously described (Shearer & Hampton 2005). Yeast cultures were grown in minimal media to early log phase and incubated with the indicated molecules (22 μM GGPP, 25 μg/mL lovastatin, or 50 μg/mL cycloheximide) or equal volumes of vehicle (for GGPP, 7:3 methonol: 10 mM ammonium bicarbonate, for lovastatin 1:3 ethanol: 20 mM Tris Base pH 8, for cycloheximide, DMSO). Cell fluorescence counts were measured for 10,000 cells using a BD Accuri C6 flow cytometer (BD Biosciences). Data were analyzed using FlowJo software (FlowJo, LLC). Any averages shown are means of 10,000 ungated events.

Microsome preparation

Microsomes were prepared as described previously (Shearer & Hampton 2004, Theesfeld & Hampton 2013). Yeast were grown to mid log phase in YPD, and 10 OD equivalents were pelleted, washed in water, and resuspended in 240 μL lysis buffer (0.24 M sorbitol, 1 mM EDTA, 20 mM KH2PO4/K2HPO4, pH 7.5) with PIs (2 mM phenylmethylsulfonyl fluoride and 142 mM tosylphenylalanyl chloromethyl ketone). Acid-washed glass beads were added up to the meniscus. Cells were lysed at 4^{o} C on a multi-vortexer for six 1-minute intervals with 1 minute on ice in between. The lysates were transferred to a new tube and lysates cleared with 5 second pulses of centrifugation. Microsomes were pelleted from cleared lysates by centrifugation at

14,000 x g for five minutes, washed once in XL buffer (1.2 M sorbitol, 5 mM EDTA, 0.1 M KH2PO4/K2HPO4, pH 7.5), and resuspended in XL buffer.

Limited proteolysis assay

The limited proteolysis assay was performed as described previously (Shearer & Hampton 2004). Briefly, microsomes in XL buffer were treated with the indicated isoprenoid molecules or equal volumes of vehicle. For the S215A kinetic experiments, microsomes were pre-incubated with isoprenoids or vehicle for the indicated times. In all other cases, isoprenoids were added and then samples were immediately incubated at 30^{o} C with 15 µg/mL trypsin. Samples were quenched at the indicated times with equal volumes of 2x urea sample buffer (USB; 8M urea, 4% SDS, 1mM DTT, 125 mM Tris base, pH 6.8). Samples were resolved by SDS-PAGE on 14% gels, transferred to nitrocellulose in 15% methanol, and blotted with 9E10 anti-myc antibody.

Microsome preparation for co-immunoprecipitation

Microsomes were prepared for co-immunoprecipitation as described previously (Neal et al. 2017). Yeast strains were grown to mid-log phase in YPD and 10 OD equivalents were resuspended in 240 µL lysis buffer (0.24 M sorbitol, 1 mM EDTA, 20 mM KH_2PO_4/K_2HPO_4, pH 7.5) with protease inhibitors (2 mM phenylmethylsulfonyl fluoride, 100 mm leupeptin hemisulfate, 76 mM pepstatin A, and 142 mM tosylphenylalanyl chloromethyl ketone). Acid-washed glass beads

were added to the meniscus. Cells were lysed at 4ºC on a multi-vortexer for six 1-minute intervals with 1 minute on ice in between. Lysates were cleared by centrifugation in 5 second pulses. Microsomes were pelleted from the cleared lysates by centrifugation at 14,000 x g for 5 minutes, washed in IP buffer without detergent (500 mM NaCl, 50 mM Tris base, pH7.5), and resuspended in IP buffer with detergent (IPB; 500 mM NaCl, 50 mM Tris base, 1.5% Tween-20, pH7.5) and protease inhibitors.

Co-immunoprecipitation

Solubilized microsomes were incubated at 4º C for 1 hour with rocking. Samples were pipetted up and down and then solutions were cleared by centrifugation at 14,000 x g for 15 minutes. Then 15 µL polyclonal rabbit anti-GFP antibody was added to supernatants, which were incubated overnight at 4ºC with rocking. After incubation, 100 µL of 50% protein-A sepharose bead slurry were added. Samples were incubated at 4º C for two hours with rocking. Beads were pelleted for 30 seconds at low speed and 2 minutes by gravity. Beads were washed twice with IPB and once with IP wash buffer (100 mM NaCl, 10 mM Tris base, pH7.5. Beads were aspirated to dryness and resuspended in 100 µL 2x USB. Samples were resolved by 14% SDS-PAGE, transferred to nitrocellulose in 12% methanol, and immunoblotted with anti-GFP or anti-myc antibody as indicated.

Detergent limited proteolysis assay

The limited proteolysis assay was performed as described above with the following variations: After initial pelleting and washing of microsomes, microsomes were first thoroughly resuspended in XL buffer and then 10x the desired final concentration of detergent in XL buffer added (final concentration 0.1% Fos-Choline-13, 0.05% DMNG, 0.5% or 1% digitonin). Preparations with detergent were incubated at 4^{o} C for 1 hour with rocking and then repeatedly pipetted up and down. Finally, samples were cleared for by centrifugation in a benchtop microcentrifuge for 15 minutes at 16,000 x g. The supernatants were used for the proteolytic assay. This assay was identical to the limited proteolysis assay described above, except that a lower concentration of trypsin (3 μg/mL instead of 15) was used.

Detergent solubility assay

Microsomes were prepared as in the detergent limited proteolysis assay up to the point of detergent addition. After thorough mixing, 22 μL of GGPP, 2F-GGPP, or equal volume of vehicle were added as indicated. Microsomes were then incubated at 4^{o} C for 1 hour with rocking. Samples were again pipetted vigorously up and down and then were separated by ultracentrifugation at 89,000 RPM for 15 minutes. Pellet and supernatant were separated and incubated in USB for 10 minutes at 55^{o} C and then resolved and immunoblotted as described above.

Table 3.2. Yeast strains used in chapter 3

Strain	Genotype	Figure
RHY4990	*MATa ade2-101 met2 his3Δ200 lys2-801 leu2Δ ura3-52::URA3::HMGcd::TDH3pr1myc-HMG2-GFP L219F hmg1ΔLYS2*	3.7
RHY4991	*MATa ade2-101 met2 his3Δ200 lys2-801 leu2Δ ura3-52::URA3::HMGcd::TDH3pr1myc-HMG2-GFP TLCC202-205AAAA hmg1ΔLYS2*	3.7
RHY4992	*MATa ade2-101 met2 his3Δ200 lys2-801 leu2Δ ura3-52::URA3::HMGcd::TDH3pr1myc-HMG2-GFP FY349LS hmg1ΔLYS2*	3.7
RHY7118	*MATa ade2-101::ADE2::TDH3::YHR33c-3HA met2 his3Δ200 lys2-801 leu2Δ ura3-52::URA3::HMGcd::TDH3pr1myc-HMG2-GFP hmg1ΔLYS2*	3.8
RHY7661	MAT*a ade2-101 met2 his3Δ200 lys2-801 leu2Δ ura3-52::URA3::TDH3pr-1mycHMG2-GFP*	3.3, 3.4, 3.6, 3.9-3.13, 3.21, 3.28-3.36
RHY7683	MAT*a ade2-101 met2 his3Δ200 lys2-801 leu2Δ ura3-52::URA3::TDH3pr-S215A-1mycHMG2-GFP*	3.3, 3.6, 3.9, 3.10, 3.21, 3.28, 3.32, 3.36
RHY8624	MATa *ade2-101 met2 his3Δ200 lys2-801 leu2Δ ura3-52::URA3::prTDH3-1myc-Hmg2-GFP hmg2Δ::1MYC-HMG2*	3.8
RHY10300	MAT*a ade2-101 met2 his3Δ200 lys2-801 leu2Δ::LEU2 ura3-52::URA3::TDH3pr-TFYSA-HMG2-GFP pdr5ΔKanMX*	3.30
RHY11123	MAT*a ade2-101 met2 his3Δ200 lys2-801 leu2Δ ura3-52::URA3::TDH3pr-RYL133-135AAA-1mycHMG2-GFP*	3.11, 3.12, 3.22, 3.24
RHY11124	MAT*a ade2-101 met2 his3Δ200 lys2-801 leu2Δ ura3-52::URA3::TDH3pr-K153A-1mycHMG2-GFP*	3.11, 3.25
RHY11125	MAT*a ade2-101 met2 his3Δ200 lys2-801 leu2Δ ura3-52::URA3::TDH3pr-K153A R155A R157A-1mycHMG2-GFP*	3.11, 3.12, 3.23, 3.25
RHY11126	MAT*a ade2-101 met2 his3Δ200 lys2-801 leu2Δ ura3-52::URA3::TDH3pr-D165A-1mycHMG2-GFP*	3.11, 3.13, 3.26
RHY11127	MAT*a ade2-101 met2 his3Δ200 lys2-801 leu2Δ ura3-52::URA3::TDH3pr-K140A-1mycHMG2-GFP*	3.11, 3.12
RHY11128	MAT*a ade2-101 met2 his3Δ200 lys2-801 leu2Δ ura3-52::URA3::TDH3pr-K357R-1mycHMG2-GFP*	3.9
RHY11129	MAT*a ade2-101 met2 his3Δ200 lys2-801 leu2Δ ura3-52::URA3::TDH3pr-K6R-1mycHMG2-GFP*	3.9, 3.10
RHY11130	MAT*a ade2-101 met2 his3Δ200 lys2-801 leu2Δ ura3-52::URA3::TDH3pr-RYL133-135AAA-S215A-1mycHMG2-GFP*	3.22
RHY11131	MAT*a ade2-101 met2 his3Δ200 lys2-801 leu2Δ ura3-52::URA3::TDH3pr-K6R-RYL133-135AAA-1mycHMG2-GFP*	3.22
RHY11132	MAT*a ade2-101 met2 his3Δ200 lys2-801 leu2Δ ura3-52::URA3::TDH3pr-K153A R155A R157A-S215A-1mycHMG2-GFP*	3.23
RHY11133	MAT*a ade2-101 met2 his3Δ200 lys2-801 leu2Δ ura3-52::URA3::TDH3pr-K6R-K153A R155A R157A-1mycHMG2-GFP*	3.23
RHY11134	MAT*a ade2-101 met2 his3Δ200 lys2-801 leu2Δ ura3-52::URA3::TDH3pr-K6R-K153A R155A R157A-S215A 1mycHMG2-GFP*	3.23

Table 3.3. Plasmids used in chapter 3

Plasmid	Genotype
pRH312	pRS405 LEU2 YIp
pRH320	LEU2 2µm
pRH469	URA3::TDH3pr-HMG2-GFP YIp
pRH680	LEU2::TDH3pr-HMG2-GFP YIp
pRH1129	URA3::TDH3pr-K357R-HMG-GFP YIp
pRH1581	URA3::TDH3pr-1myc-HMG2-GFP YIp
pRH1693	URA3::TDH3pr-K357R-1myc-HMG2-GFP YIp
pRH1694	URA3::TDH3pr-TFYSA-1myc-HMG2-GFP YIp
pRH2177	URA3::TDH3pr-S215A-1myc-HMG2-GFP YIp
pRH2250	URA3::TDH3pr-HMG2-1myc-no catalytic domain
pRH2477	LEU2::GAL1pr-BTS1 Iip
pRH2654	LEU2 TDH3-pr-PGK1term YIP
pRH2657	LEU2::TDH3pr-BTS1-PGK1term YIp
pRH2903	LED2::TDH3pr-Hmg2Loop1-PGK1term 2µm
pRH2904	LED2::TDH3pr-Hmg2Start-Loop1-PGK1term 2µm
pRH2905	LED2::TDH3pr-Hmg2Start-TM2-PGK1term 2µm
pRH2906	URA3::TDH3pr-RYL133-135AAA-1myc-HMG2-GFP YIp
pRH2907	URA3::TDH3pr-K153A-1myc-HMG2-GFP YIp
pRH2908	URA3::TDH3pr-K153A R155A R157A-1myc-HMG2-GFP Yip
pRH2909	URA3::TDH3pr-D165A-1myc-HMG2-GFP Yip
pRH2910	URA3::TDH3pr-K140A-1myc-HMG2-GFP YIp
pRH2911	URA3::TDH3pr-K6R-1myc-HMG2-GFP Yip
pRH2912	URA3::TDH3pr-RYL133-135AAA-S215A-1myc-HMG2-GFP YIp
pRH2913	URA3::TDH3pr-K6R-RYL133-135AAA-1myc-HMG2-GFP YIp
pRH2914	URA3::TDH3pr-K153A R155A R157A-S215A-1myc-HMG2-GFP Yip
pRH2915	URA3::TDH3pr-K6R-K153A R155A R157A-1myc-HMG2-GFP Yip
pRH2916	URA3::TDH3prK6R--K153A R155A R157A-S215A-1myc-HMG2-GFP Yip

Acknowledgements

Thank you to Reuben Peters (Iowa State University) and Philip Zerbe (University of California Davis) for provided reagents. These studies were supported by NIH grant 5R37DK051996-18 to R.Y.H. M.A.W. was supported in part by NIH CMG Training Grant 5T32GM007240-35.

Chapter Three, in part, is currently in preparation for submission for publication of the material as: Wangeline, MA and Hampton, RY, "The SSD: A Structure Shifting Domain required for ligand-mediated misfolding." I was the principal researcher/author of this work.

CHAPTER FOUR:

Conclusions and future directions

Regulated misfolding of Hmg2: The story so far

In this work, I have described two parallel investigations into the mechanism of Hmg2 "mallosteric" misfolding. Hmg2, a normal wild-type protein, undergoes misfolding and degradation specifically under conditions of high sterol pathway flux, though this degradation is carried out by the highly general Hrd ERAD pathway. GGPP, a normal sterol pathway molecule, is the potent and specific signal for Hmg2 misfolding and degradation. At physiologically relevant concentrations, Hmg2 exposed to GGPP in vitro behaves like a misfolded protein, becoming more accessible to proteolytic cleavage and detergents in a manner reversible by several chemical chaperones. Hmg2's response GGPP is specific, potent, reversible, and antagonizable. Hmg2's regulated structural transition has the hallmarks of an allosteric conformational change, without an output of misfolding.

I have also investigated the structural features within Hmg2 required to bring about this regulated structural change, including the highly conserved sterol sensing domain (SSD). The SSD is required for the "mallosteric" misfolding of Hmg2. Mutations in the SSD stabilize Hmg2 in vivo and prevent regulated misfolding in vitro. Importantly, this role of the SSD is independent of Insigs, proteins most well-known for their role in binding and regulating SSD-containing proteins. Mutations in the SSD disrupt regulation not only in that protein itself, but also in wild type Hmg2 expressed in the same cell. The misfolding function of the SSD is not only independent of Insigs, but also persists in digitonin micelles. Finally, mutations in the

SSD do not absolutely ablate the misfolding function, but rather delay Hmg2's response to GGPP from a timescale of seconds or minutes to a time scale of hours. These findings lead to a model where the SSD works as a module to promote misfolding (or rather, a conformational change that the quality control apparatus detects as misfolding) in a rapid and reversible fashion in response to a signal. Our in vitro studies demonstrate an independent role for the SSD in inducing entry into quality control.

However, as we cannot currently detect GGPP binding, we do not know where (or if) GGPP binds to Hmg2, and thus cannot fully rule out the possibility that the SSD is instead (or additionally) a GGPP binding site. In an attempt to further investigate the possibility of GGPP binding, I performed an analysis of Loop 1 of Hmg2 based on its homology to SCAP and predicted similarity to the GGPP-binding proteins Ram2 and Bet2. Overexpression of the loop in the context of the ER, but not as a soluble and presumably cytosolic protein, blunted the response of wild type Hmg2 but not the non-responding TFYSA Hmg2 to GGPP. Mutations in the loop also disrupted Hmg2 regulation. It is unclear what the exact role of Loop 1 is, but it appears to be critical for normal Hmg2 regulation.

This work has addressed several longstanding questions about Hmg2 regulation, including: The identity of the bona fide degradation signal and the nature of its interaction with Hmg2, the looming question of whether Hmg2 misfolding was due to a specific process like ligand binding or a more general process like membrane perturbation, whether early steps in Hmg2 degradation, such as binding and

misfolding, could be genetically separated from later steps, such as ubiquitination, and the independence of SSD action.

However, there are still many open questions about how Hmg2 responds to its degradation signal and how proteins more generally are detected by the ubiquitin proteasome machinery.

Separation of binding and responding to ligands

The most obvious question with respect to Hmg2's regulation remains that of binding. Without an assay for GGPP binding, we are unable to directly determine which regions of Hmg2, if any, are responsible for binding GGPP.

Our interest in Loop 1 stemmed from the finding that Loop 1 in SCAP binds cholesterol. Mutations in the loop prevent cholesterol binding while simultaneously causing SCAP to be retained in the ER as if it is always cholesterol-bound (Motamed et al. 2011). Additionally, I performed an unbiased alignment of the entire Hmg2 coding region with those of Ram2 and Bet2, yeast proteins which bind GGPP as part of the GGTase machinery. Outside of the catalytic domain, only two regions of Hmg2 aligned with these proteins—a small stretch of Loop 1 and another stretch comprising parts of Loop 6, TM7, and Loop 7. In this work I mutated two tracts of residues in Loop 1, RYL 133-135 and K153, R155, and R157. Interestingly, these mutations caused a phenotype similar to that of the SCAP cholesterol binding mutations. Rather than rendering Hmg2 highly stable and insensitive to GGPP, which one would expect *a priori* from a GGPP-binding mutation, they destabilized Hmg2 and blunted GGPP

regulation as if the protein were always sensing some basal level of GGPP. Similarly, mutations in Loop 1 of SCAP resulted in a protein which acted as though it constantly sensed cholesterol. Perhaps neutralizing positive charges in the loop mimicked in some way an association with the negatively charged GGPP. The D165A mutation, on the other hand, stabilized Hmg2, while also blunting regulation.

The only other region of the transmembrane domain with any detectable similarity to Ram2 and Bet2 was a region comprising the C-terminal side of Loop 6, TM7, and part of Loop 7. This is intriguing, because in SCAP Loop 7 cooperates with Loop 1 in sensing cholesterol. Additionally, one of the residues in the region of similarity between Hmg2, Bet2, and Ram2 is N401. I had independently mutated this residue in earlier studies and found that the N401A mutation renders Hmg2 insensitive to GGPP, similar to S215A. Future work on the mechanism of GGPP sensing might therefore start by focusing on other residues in these regions.

While intriguing, these results are not conclusive without a way to distinguish between binding signal and responding to signal. While in the long term we hope to develop an in vitro binding assay, in the short term one way to begin addressing this question may be the surprising finding that the S215A mutation imposes a kinetic block on GGPP-induced misfolding, not an absolute one. Incubation of S215A 1myc-Hmg2-GFP with GGPP for at least 2.5 hours does eventually lead to misfolding. We do not yet know if this is true for other SSD mutations like L219F, or other mutations like N401A which are located outside the canonical SSD but currently seem to mimic the SSD phenotype. If other SSD mutations lead to the same time-delay phenotype as

S215A, we may hypothesize that there could be an additional class of mutations which never misfold. While not conclusive, this is a hypothesis that can be tested with the tools we currently have. The various tools developed and refined in this work will allow a more in-depth dissection of both new mutations presented here and old mutations we've had in the laboratory for some time.

Additionally, we are interested in better in vitro methods. In this work I described the surprising finding that in some detergents Hmg2 retains its native structure to the point that the in vitro proteolysis pattern is unchanged. Hmg2 can also be chaperoned by glycerol in these detergents. Furthermore, Hmg2 solubilized with digitonin actually retains some ability to interact with GGPP. When GGPP is added to preparations of microsomes treated with digitonin, it increases Hmg2 solubility, implying that it is able to make Hmg2 more accessible to the detergent. In addition, Hmg2 retains a partial response to GGPP in the in vitro proteolysis assay performed in digitonin-solubilized microsomes. While this response requires much higher concentrations of GGPP than the normal membrane assay, the calculated concentration of micelles is quite high at reaction conditions. As we are working far above the critical micellar concentration, using average aggregation numbers for digitonin, at 22 μM GGPP fewer than one third of micelles will contain a molecule of GGPP, even assuming that all GGPP is associated with micelles. (This assumption is unlikely to hold, as GGPP is quite soluble in water.)

While the digitonin assay is not terribly practical for larger-scale experiments due to low CMC, lack of dialyzability, and Hmg2's poor solubility, it will hopefully

provide a stepping stone toward more effective in vitro methods for binding or even structure. The first structures of an SSD were recently published (Li et al. 2016, Zhao et al. 2016), and hopefully others, including Hmg2, will follow.

This work as a platform for future small molecule studies

Several of the tools developed and refined in this work have great potential as tools for further studies of Hmg2, sterol sensing domain proteins in general, and the sterol pathway. High throughput approaches are rapidly becoming more accessible in a variety of different fields and opening up new avenues of hypothesis generation and investigation. Large chemical libraries and advances in fluorescence imaging, including in our own laboratory, make fluorescence-based chemical screens attractive for further dissecting the biochemical underpinnings of many processes.

The rapidly degrading, "sensitized" Bts1 strain presents a starting point for a high-throughput screen for molecules affecting Hmg2 stability. Hmg2-GFP expressed in this strain is rapidly degraded, due to the high level of GGPP being produced by overexpressed Bts1. Cells and colonies formed by these cells are dark on plates and in liquid culture. Thus any molecules which result in Hmg2 stabilization will cause these cells to become bright, allowing us to avoid the false-positives associated with looking for loss of fluorescence.

We expect hits to include inhibitors of Bts1, inhibitors of upstream enzymes in the sterol pathway, inhibitors of enzymes in the ubiquitin-proteasome pathway including the E1, E2, and E3 enzymes, the retrotranslocation machinery like CDC48,

and the proteasome itself, general chemical chaperones which act on Hmg2, and any molecules which can antagonize GGPP's action on Hmg2 more directly. While molecules specifically affecting Hmg2 would be greatly helpful for future studies, all of these hits are potentially useful from a clinical standpoint. Rapidly growing cells such as pathogens and cancer cells have a great need for the isoprenoid molecules produced downstream of Bts1. The fungal sterol pathway is also a target for anti-fungal drugs targeting human pathogens. And inhibitors of the ubiquitin proteasome pathway have proven effective in some cancers. Molecules specifically targeting Hmg2 might also be clinically relevant for dyslipidemia or in the variety of developmental sterol pathway disorders. Finally, chemical chaperones have potential for treating inborn disorders such as cystic fibrosis or Niemann-Pick disease. Overall, nearly any molecule which stabilizes Hmg2 in this screen would be of interest either as a tool for further studies on HMG-CoA Reductase or for investigation for clinical potential.

Ligand-mediated degradation in other systems

While this work has focused on factors involved in sterol regulation, particularly those containing a sterol sensing domain, ligand-mediated protein degradation is not a phenomenon unique to sterol biology. Several other known systems co-opt general quality control mechanisms for regulation.

The inositol triphosphate (IP_3) receptors (IP_3Rs), are critical members of various signaling pathways that converge on release of Ca^{2+} ions from the ER. They

form ligand-gated Ca^{2+} channels, and are activated by the ligand IP_3. IP_3Rs are required for such critical signaling pathways as muscle contraction and apotosis, and are downregulated in response to signaling through these and other IP_3-producing pathways. This downregulation is ubiquitin-mediated proteasomal degradation by ERAD, and requires general ERAD factors such as the p97 complex. IP_3Rs also undergo basal levels of degradation in the absence of signaling, though this degradation appears to be mediated by the lysosome and caspases, not ERAD (Wojcikiewicz 2012; Wojcikiewicz et al. 1994, 2009).

Bacteria also hijack general protein degradation machinery to achieve specific regulation. The lipid A synthesis pathway in Gram negative bacteria is essential for outer membrane formation and thus cell viability. It is a major target of antibiotic research. LpxC (UDP-3-O-N-acetylglucosamine deacetylase) catalyzes the first committed step of the pathway and is thus a target of both cellular regulation and much research in the search for new antibiotics. The pathway is controlled (in part) by the regulated degradation of LpxC by the protease FtsH. This degradation is keyed to levels of a pathway intermediate (Emiola et al. 2015, Fuhrer et al. 2006, Ogura et al. 1999). FtsH is the only essential membrane protease in *Escherichia coli*. While it is required for its role in LpxC regulation, like many quality control factors it also degrades a variety of other proteins, including unpaired subunits of integral membrane complexes (Ogura et al. 1999), making this a true case of specific metabolic regulation by a general quality control proteolytic pathway.

Ligand-mediated degradation is found in all domains of life. In addition to presenting an intriguing target for pharmacological intervention when it is found naturally, the universality of ligand-mediated degradation raises an additional question: Can we use small molecules to program the degradation of proteins not usually subject to this form of regulation?

Manipulating the stability of human disease proteins is already a subject of much study. Unstable proteins such as NPC1 and CFTR have been targeted with both general and specific chemical chaperones (Bernier et al. 2004, Ohgane et al. 2013) to restore function in cells and human patients. Other proteins have been targeted for degradation either by inducing association with a particular E3 ubiquitin ligase or through binding a ligand containing a large hydrophobic moiety or "greasy patch" (Bondeson & Crews 2017), a strategy only one step removed from the ligand-induced misfolding discussed in this work. Many proteins involved in human disease do not have active sites, and thus targeting them with the stereotypical small molecule inhibitor is not straightforward. Ligand-mediated quality control offers another strategy for targeting this "undruggable proteome," and a better understanding of ligand-induced misfolding could thus open up new avenues of intervention in human disease.

References

1. Brown, M. S. & Goldstein, J. L. Cholesterol feedback: from Schoenheimer's bottle to Scap's MELADL. *J. Lipid Res.* **50,** S15–S27 (2008).

2. Jiang, W. & Song, B.-L. Ubiquitin ligases in cholesterol metabolism. *Diabetes Metab. J.* **38,** 171–80 (2014).

3. Jo, Y. & DeBose-Boyd, R. A. Control of Cholesterol Synthesis through Regulated ER-Associated Degradation of HMG CoA Reductase. **45,** (2010).

4. Raychaudhuri, S., Young, B. P., Espenshade, P. J. & Loewen, C. J. Regulation of lipid metabolism: a tale of two yeasts. **24,** (2012).

5. Sharpe, L. J., Cook, E. C. L., Zelcer, N. & Brown, A. J. The UPS and downs of cholesterol homeostasis. *Trends Biochem. Sci.* **39,** 527–535 (2014).

6. Ye, J. & DeBose-Boyd, R. A. Regulation of Cholesterol and Fatty Acid Synthesis. *Cold Spring Harb. Perspect. Biol.* **3,** a004754–a004754 (2011).

7. Zhang, L., Reue, K., Fong, L. G., Young, S. G. & Tontonoz, P. Feedback Regulation of Cholesterol Uptake by the LXR-IDOL-LDLR Axis. *Arterioscler. Thromb. Vasc. Biol.* **32,** 2541–2546 (2012).

8. Lange, B. M., Rujan, T., Martin, W. & Croteau, R. Isoprenoid biosynthesis: the evolution of two ancient and distinct pathways across genomes. *Proc. Natl. Acad. Sci. U. S. A.* **97,** 13172–7 (2000).

9. Geelen, M. J., Gibson, D. M. & Rodwell, V. W. Hydroxymethylglutaryl-CoA reductase--the rate-limiting enzyme of cholesterol biosynthesis. A report of a meeting held at Nijenrode Castle, Breukelen, The Netherlands, August 24, 1985. *FEBS Lett.* **201,** 183–6 (1986).

10. Bloch, K. The biological synthesis of cholesterol. *Science* **150,** 19–28 (1965).

11. Infante, R. E. *et al.* NPC2 facilitates bidirectional transfer of cholesterol between NPC1 and lipid bilayers, a step in cholesterol egress from lysosomes. *Proc. Natl. Acad. Sci.* **105,** 15287–15292 (2008).

12. Ohgami, N. *et al.* Binding between the Niemann-Pick C1 protein and a photoactivatable cholesterol analog requires a functional sterol-sensing domain. *Proc. Natl. Acad. Sci. U. S. A.* **101,** 12473–8 (2004).

13. Vanier, M. T. Complex lipid trafficking in Niemann-Pick disease type C. *J. Inherit. Metab. Dis.* **38,** 187–199 (2015).

14. Abumrad, N. A. & Davidson, N. O. Role of the Gut in Lipid Homeostasis.

Physiol. Rev. **92,** 1061–1085 (2012).

15. Altmann, S. W. *et al.* Niemann-Pick C1 Like 1 Protein Is Critical for Intestinal Cholesterol Absorption. *Science (80-.).* **303,** 1201–1204 (2004).

16. Davies, J. P., Levy, B. & Ioannou, Y. A. Evidence for a Niemann–Pick C (NPC) Gene Family: Identification and Characterization of NPC1L1. *Genomics* **65,** 137–145 (2000).

17. Hussain, M. M. Intestinal lipid absorption and lipoprotein formation. *Curr. Opin. Lipidol.* **25,** 200–206 (2014).

18. Wang, L.-J. & Song, B.-L. Niemann–Pick C1-Like 1 and cholesterol uptake. *Biochim. Biophys. Acta - Mol. Cell Biol. Lipids* **1821,** 964–972 (2012).

19. Favari, E. *et al.* in *Handbook of experimental pharmacology* **224,** 181–206 (2015).

20. Jakulj, L. *et al.* Transintestinal Cholesterol Transport Is Active in Mice and Humans and Controls Ezetimibe-Induced Fecal Neutral Sterol Excretion. *Cell Metab.* **24,** 783–794 (2016).

21. Goldberg, A. L. Protein degradation and protection against misfolded or damaged proteins. *Nature* **426,** 895–899 (2003).

22. Brown, M. S. & Goldstein, J. L. Expression of the familial hypercholesterolemia gene in heterozygotes: mechanism for a dominant disorder in man. *Science* **185,** 61–3 (1974).

23. Goldstein, J. L. & Brown, M. S. Familial hypercholesterolemia: identification of a defect in the regulation of 3-hydroxy-3-methylglutaryl coenzyme A reductase activity associated with overproduction of cholesterol. *Proc. Natl. Acad. Sci. U. S. A.* **70,** 2804–8 (1973).

24. Schneider, W. J., Beisiegel, U., Goldstein, J. L. & Brown, M. S. Purification of the low density lipoprotein receptor, an acidic glycoprotein of 164,000 molecular weight. *J. Biol. Chem.* **257,** 2664–73 (1982).

25. Goldstein, J. L. & Brown, M. S. The LDL receptor. *Arterioscler. Thromb. Vasc. Biol.* **29,** 431–8 (2009).

26. Goldstein, J. L. L. & Brown, M. S. S. A Century of Cholesterol and Coronaries: From Plaques to Genes to Statins. *Cell* **161,** (2015).

27. Brown, M. S., Dana, S. E. & Goldstein, J. L. Regulation of 3-hydroxy-3-methylglutaryl coenzyme A reductase activity in human fibroblasts by lipoproteins. *Proc. Natl. Acad. Sci. U. S. A.* **70,** 2162–6 (1973).

28. Horton, J. D., Goldstein, J. L. & Brown, M. S. SREBPs: activators of the complete program of cholesterol and fatty acid synthesis in the liver. *J. Clin. Invest.* **109,** 1125–1131 (2002).

29. Osborne, T. F. & Espenshade, P. J. Evolutionary conservation and adaptation in the mechanism that regulates SREBP action: what a long, strange tRIP it's been. **23,** (2009).

30. Kuwabara, P. E. & Labouesse, M. The sterol-sensing domain: multiple families, a unique role? *Trends Genet.* **18,** 193–201 (2002).

31. Nohturfft, A., Brown, M. S. & Goldstein, J. L. Topology of SREBP cleavage-activating protein, a polytopic membrane protein with a sterol-sensing domain. *J. Biol. Chem.* **273,** 17243–50 (1998).

32. Osborne, T. F. & Rosenfeld, J. M. Related membrane domains in proteins of sterol sensing and cell signaling provide a glimpse of treasures still buried within the dynamic realm of intracellular metabolic regulation. *Curr. Opin. Lipidol.* **9,** 137–40 (1998).

33. Goldstein, J. L., DeBose-Boyd, R. A. & Brown, M. S. Protein Sensors for Membrane Sterols. *Cell* **124,** 35–46 (2006).

34. Radhakrishnan, A., Sun, L.-P., Kwon, H. J., Brown, M. S. & Goldstein, J. L. Direct Binding of Cholesterol to the Purified Membrane Region of SCAP. *Mol. Cell* **15,** 259–268 (2004).

35. Motamed, M. *et al.* Identification of Luminal Loop 1 of Scap Protein as the Sterol Sensor That Maintains Cholesterol Homeostasis. *J. Biol. Chem.* **286,** 18002–18012 (2011).

36. Yang, T. *et al.* Crucial step in cholesterol homeostasis: sterols promote binding of SCAP to INSIG-1, a membrane protein that facilitates retention of SREBPs in ER. *Cell* **110,** 489–500 (2002).

37. Burg, J. S. *et al. Insig Regulates HMG-CoA Reductase by Controlling Enzyme Phosphorylation in Fission Yeast*. *Cell Metabolism* **8,** 522–531 (2008).

38. Flury, I. *et al.* INSIG: a broadly conserved transmembrane chaperone for sterol-sensing domain proteins. *EMBO J.* **24,** 3917–26 (2005).

39. Adams, C. M., Goldstein, J. L. & Brown, M. S. Cholesterol-induced conformational change in SCAP enhanced by Insig proteins and mimicked by cationic amphiphiles. *Proc. Natl. Acad. Sci.* **100,** 10647–10652 (2003).

40. Brown, A. J., Sun, L., Feramisco, J. D., Brown, M. S. & Goldstein, J. L. Cholesterol addition to ER membranes alters conformation of SCAP, the SREBP escort protein that regulates cholesterol metabolism. *Mol. Cell* **10,** 237–

45 (2002).

41. Adams, C. M. *et al.* Cholesterol and 25-Hydroxycholesterol Inhibit Activation of SREBPs by Different Mechanisms, Both Involving SCAP and Insigs. *J. Biol. Chem.* **279,** 52772–52780 (2004).

42. Radhakrishnan, A., Ikeda, Y., Kwon, H. J., Brown, M. S. & Goldstein, J. L. Sterol-regulated transport of SREBPs from endoplasmic reticulum to Golgi: Oxysterols block transport by binding to Insig. *Proc. Natl. Acad. Sci.* **104,** 6511–6518 (2007).

43. Hausmann, G., von Mering, C. & Basler, K. The Hedgehog Signaling Pathway: Where Did It Come From? *PLoS Biol.* **7,** e1000146 (2009).

44. Ren, R. *et al.* PROTEIN STRUCTURE. Crystal structure of a mycobacterial Insig homolog provides insight into how these sensors monitor sterol levels. *Science* **349,** 187–91 (2015).

45. Hwang, S. *et al.* Contribution of accelerated degradation to feedback regulation of 3-hydroxy-3-methylglutaryl coenzyme A reductase and cholesterol metabolism in the liver. *J. Biol. Chem.* **291,** 13479–13494 (2016).

46. Beg, Z. H., Stonik, J. A. & Brewer, H. B. Phosphorylation of hepatic 3-hydroxy-3-methylglutaryl coenzyme A reductase and modulation of its enzymic activity by calcium-activated and phospholipid-dependent protein kinase. *J. Biol. Chem.* **260,** 1682–7 (1985).

47. Omkumar, R. V, Darnay, B. G. & Rodwell, V. W. Modulation of Syrian hamster 3-hydroxy-3-methylglutaryl-CoA reductase activity by phosphorylation. Role of serine 871. *J. Biol. Chem.* **269,** 6810–4 (1994).

48. Edwards, P. A., Lan, S. F. & Fogelman, A. M. Alterations in the rates of synthesis and degradation of rat liver 3-hydroxy-3-methylglutaryl coenzyme A reductase produced by cholestyramine and mevinolin. *J. Biol. Chem.* **258,** 10219–22 (1983).

49. Sever, N., Yang, T., Brown, M. S., Goldstein, J. L. & DeBose-Boyd, R. A. Accelerated degradation of HMG CoA reductase mediated by binding of insig-1 to its sterol-sensing domain. *Mol. Cell* **11,** 25–33 (2003).

50. Sever, N. *et al.* Insig-dependent Ubiquitination and Degradation of Mammalian 3-Hydroxy-3-methylglutaryl-CoA Reductase Stimulated by Sterols and Geranylgeraniol. *J. Biol. Chem.* **278,** 52479–52490 (2003).

51. Ravid, T., Doolman, R., Avner, R., Harats, D. & Roitelman, J. The Ubiquitin-Proteasome Pathway Mediates the Regulated Degradation of Mammalian 3-Hydroxy-3-methylglutaryl-coenzyme A Reductase. *J. Biol. Chem.* **275,** 35840–

35847 (2000).

52. Roitelman, J. & Simoni, R. D. Distinct sterol and nonsterol signals for the regulated degradation of 3-hydroxy-3-methylglutaryl-CoA reductase. *J. Biol. Chem.* **267,** 25264–73 (1992).

53. Amm, I., Sommer, T. & Wolf, D. H. Protein quality control and elimination of protein waste: The role of the ubiquitin–proteasome system. *Biochim. Biophys. Acta - Mol. Cell Res.* **1843,** 182–196 (2014).

54. Kleiger, G. & Mayor, T. Perilous journey: a tour of the ubiquitin-proteasome system. *Trends Cell Biol.* **24,** 352–9 (2014).

55. Jo, Y., Lee, P. C. W., Sguigna, P. V & DeBose-Boyd, R. A. Sterol-induced degradation of HMG CoA reductase depends on interplay of two Insigs and two ubiquitin ligases, gp78 and Trc8. *Proc. Natl. Acad. Sci. U. S. A.* **108,** 20503–8 (2011).

56. Song, B.-L., Javitt, N. B. & DeBose-Boyd, R. A. Insig-mediated degradation of HMG CoA reductase stimulated by lanosterol, an intermediate in the synthesis of cholesterol. *Cell Metab.* **1,** 179–189 (2005).

57. Song, B.-L., Sever, N. & DeBose-Boyd, R. A. Gp78, a Membrane-Anchored Ubiquitin Ligase, Associates with Insig-1 and Couples Sterol-Regulated Ubiquitination to Degradation of HMG CoA Reductase. *Mol. Cell* **19,** 829–840 (2005).

58. Brodsky, J. L. Cleaning Up: ER-Associated Degradation to the Rescue. *Cell* **151,** 1163–1167 (2012).

59. Hirsch, C., Gauss, R., Horn, S. C., Neuber, O. & Sommer, T. The ubiquitylation machinery of the endoplasmic reticulum. *Nature* **458,** 453–460 (2009).

60. Needham, P. G. & Brodsky, J. L. How early studies on secreted and membrane protein quality control gave rise to the ER associated degradation (ERAD) pathway: The early history of ERAD. *Biochim. Biophys. Acta - Mol. Cell Res.* **1833,** 2447–2457 (2013).

61. Lee, J. P. *et al.* TRC8, A KIDNEY CANCER-ASSOCIATED UBIQUITIN LIGASE, IS STEROL-REGULATED AND INTERACTS WITH LIPID AND PROTEIN BIOSYNTHETIC PATHWAYS. **8,** 93–106 (2010).

62. Tsai, Y. C. *et al.* Differential regulation of HMG-CoA reductase and Insig-1 by enzymes of the ubiquitin-proteasome system. **23,** (2012).

63. Lee, J. N., Song, B., DeBose-Boyd, R. A. & Ye, J. Sterol-regulated degradation of Insig-1 mediated by the membrane-bound ubiquitin ligase gp78. *J. Biol. Chem.* **281,** 39308–15 (2006).

64. Lee, J. P. *et al.* The TRC8 ubiquitin ligase is sterol regulated and interacts with lipid and protein biosynthetic pathways. *Mol. Cancer Res.* **8,** 93–106 (2010).

65. Lange, Y. *et al.* Effectors of Rapid Homeostatic Responses of Endoplasmic Reticulum Cholesterol and 3-Hydroxy-3-methylglutaryl-CoA Reductase. *J. Biol. Chem.* **283,** 1445–1455 (2008).

66. Schumacher, M. M., Elsabrouty, R., Seemann, J., Jo, Y. & DeBose-Boyd, R. A. The prenyltransferase UBIAD1 is the target of geranylgeraniol in degradation of HMG CoA reductase. *Elife* **4,** (2015).

67. Schumacher, M. M., Jun, D.-J., Jo, Y., Seemann, J. & DeBose-Boyd, R. A. Geranylgeranyl-regulated transport of the prenyltransferase UBIAD1 between membranes of the ER and Golgi. *J. Lipid Res.* **57,** 1286–1299 (2016).

68. Hampton, R. Y. & Bhakta, H. Ubiquitin-mediated regulation of 3-hydroxy-3-methylglutaryl-CoA reductase. *Proc. Natl. Acad. Sci. U. S. A.* **94,** 12944–8 (1997).

69. Hampton, R. Y., Gardner, R. G. & Rine, J. Role of 26S proteasome and HRD genes in the degradation of 3-hydroxy-3-methylglutaryl-CoA reductase, an integral endoplasmic reticulum membrane protein. *Mol. Biol. Cell* **7,** 2029–44 (1996).

70. Neal, S., Mak, R., Bennett, E. J. & Hampton, R. A Cdc48 " Retrochaperone " Function Is Required for the Solubility of Retrotranslocated, Integral Membrane Endoplasmic Reticulum-associated Degradation (ERAD-M) Substrates *. (2017). doi:10.1074/jbc.M116.770610

71. Sato, B. K., Schulz, D., Do, P. H. & Hampton, R. Y. Misfolded Membrane Proteins Are Specifically Recognized by the Transmembrane Domain of the Hrd1p Ubiquitin Ligase. *Mol. Cell* **34,** 212–222 (2009).

72. Vashistha, N., Neal, S. E., Singh, A., Carroll, S. M. & Hampton, R. Y. Direct and essential function for Hrd3 in ER-associated degradation. *Proc. Natl. Acad. Sci. U. S. A.* **113,** 5934–9 (2016).

73. Gardner, R. *et al.* Sequence determinants for regulated degradation of yeast 3-hydroxy-3-methylglutaryl-CoA reductase, an integral endoplasmic reticulum membrane protein. *Mol. Biol. Cell* **9,** 2611–26 (1998).

74. Shearer, A. G. & Hampton, R. Y. Structural Control of Endoplasmic Reticulum-associated Degradation: EFFECT OF CHEMICAL CHAPERONES ON 3-HYDROXY-3-METHYLGLUTARYL-CoA REDUCTASE. *J. Biol. Chem.* **279,** 188–196 (2004).

75. Bays, N. W., Gardner, R. G., Seelig, L. P., Joazeiro, C. A. & Hampton, R. Y.

Hrd1p/Der3p is a membrane-anchored ubiquitin ligase required for ER-associated degradation. *Nat. Cell Biol.* **3,** 24–29 (2001).

76. Gardner, R. G. *et al.* Endoplasmic reticulum degradation requires lumen to cytosol signaling. Transmembrane control of Hrd1p by Hrd3p. *J. Cell Biol.* **151,** 69–82 (2000).

77. Garza, R. M., Tran, P. N. & Hampton, R. Y. Geranylgeranyl pyrophosphate is a potent regulator of HRD-dependent 3-Hydroxy-3-methylglutaryl-CoA reductase degradation in yeast. **284,** (2009).

78. Brodsky, J. L. & Skach, W. R. Protein folding and quality control in the endoplasmic reticulum: Recent lessons from yeast and mammalian cell systems. *Curr. Opin. Cell Biol.* **23,** 464–475 (2011).

79. Koenig, P.-A. & Ploegh, H. L. Protein quality control in the endoplasmic reticulum. *F1000Prime Rep.* **6,** 49 (2014).

80. Travers, K. J. *et al.* Functional and genomic analyses reveal an essential coordination between the unfolded protein response and ER-associated degradation. *Cell* **101,** 249–58 (2000).

81. Walter, P. & Ron, D. The Unfolded Protein Response: From Stress Pathway to Homeostatic Regulation. *Science (80-.).* **334,** 1081–1086 (2011).

82. Fang, S. *et al.* The tumor autocrine motility factor receptor, gp78, is a ubiquitin protein ligase implicated in degradation from the endoplasmic reticulum. *Proc. Natl. Acad. Sci. U. S. A.* **98,** 14422 (2001).

83. Bordallo, J., Plemper, R. K., Finger, A. & Wolf, D. H. Der3p/Hrd1p is required for endoplasmic reticulum-associated degradation of misfolded lumenal and integral membrane proteins. *Mol. Biol. Cell* **9,** 209–22 (1998).

84. Vashist, S. & Ng, D. T. W. Misfolded proteins are sorted by a sequential checkpoint mechanism of ER quality control. *J. Cell Biol.* **165,** 41–52 (2004).

85. Hampton, R. Y. & Rine, J. Regulated degradation of HMG-CoA reductase, an integral membrane protein of the endoplasmic reticulum, in yeast. *J. Cell Biol.* **125,** 299–312 (1994).

86. Gardner, R. G. & Hampton, R. Y. A highly conserved signal controls degradation of 3-hydroxy-3-methylglutaryl-coenzyme A (HMG-CoA) reductase in eukaryotes. *J. Biol. Chem.* **274,** 31671–8 (1999).

87. Shearer, A. G. & Hampton, R. Y. Lipid-mediated, reversible misfolding of a sterol-sensing domain protein. *EMBO J.* **24,** 149–59 (2005).

88. Gardner, R. G., Shearer, A. G. & Hampton, R. Y. In vivo action of the HRD

ubiquitin ligase complex: mechanisms of endoplasmic reticulum quality control and sterol regulation. *Mol. Cell. Biol.* **21,** 4276–91 (2001).

89. Theesfeld, C. L., Pourmand, D., Davis, T., Garza, R. M. & Hampton, R. Y. The Sterol-sensing Domain (SSD) Directly Mediates Signal-regulated Endoplasmic Reticulum-associated Degradation (ERAD) of 3-Hydroxy-3-methylglutaryl (HMG)-CoA Reductase Isozyme Hmg2. *J. Biol. Chem.* **286,** 26298–26307 (2011).

90. Theesfeld, C. L. & Hampton, R. Y. Insulin-induced gene protein (INSIG)-dependent sterol regulation of Hmg2 endoplasmic reticulum-associated degradation (ERAD) in yeast. *J. Biol. Chem.* **288,** 8519–30 (2013).

91. Wojcikiewicz, R. J., Furuichi, T., Nakade, S., Mikoshiba, K. & Nahorski, S. R. Muscarinic receptor activation down-regulates the type I inositol 1,4,5-trisphosphate receptor by accelerating its degradation. *J. Biol. Chem.* **269,** 7963–9 (1994).

92. Wojcikiewicz, R. J. H., Pearce, M. M. P., Sliter, D. A. & Wang, Y. When worlds collide: IP(3) receptors and the ERAD pathway. *Cell Calcium* **46,** 147–53 (2009).

93. Fuhrer, F., Langklotz, S. & Narberhaus, F. The C-terminal end of LpxC is required for degradation by the FtsH protease. *Mol. Microbiol.* **59,** 1025–1036 (2006).

94. Lai, A. C. & Crews, C. M. Induced protein degradation: an emerging drug discovery paradigm. *Nat. Rev. Drug Discov.* **16,** 101–114 (2016).

95. Bernier, V., Lagacé, M., Bichet, D. G. & Bouvier, M. Pharmacological chaperones: potential treatment for conformational diseases. *Trends Endocrinol. Metab.* **15,** 222–228 (2004).

96. Leidenheimer, N. J. & Ryder, K. G. Pharmacological chaperoning: A primer on mechanism and pharmacology. *Pharmacol. Res.* **83,** 10–19 (2014).

97. Hughes, A. L., Todd, B. L. & Espenshade, P. J. SREBP Pathway Responds to Sterols and Functions as an Oxygen Sensor in Fission Yeast. *Cell* **120,** 831–842 (2005).

98. Porter, J. R., Burg, J. S., Espenshade, P. J. & Iglesias, P. A. Ergosterol regulates sterol regulatory element binding protein (SREBP) cleavage in fission yeast. *J. Biol. Chem.* **285,** 41051–61 (2010).

99. Todd, B. L., Stewart, E. V, Burg, J. S., Hughes, A. L. & Espenshade, P. J. Sterol regulatory element binding protein is a principal regulator of anaerobic gene expression in fission yeast. *Mol. Cell. Biol.* **26,** 2817–31 (2006).

100. Hughes, A. L., Stewart, E. V & Espenshade, P. J. Identification of twenty-three mutations in fission yeast Scap that constitutively activate SREBP. *J. Lipid Res.* **49,** 2001–12 (2008).

101. Lloyd, S. J.-A., Raychaudhuri, S. & Espenshade, P. J. Subunit architecture of the Golgi Dsc E3 ligase required for sterol regulatory element-binding protein (SREBP) cleavage in fission yeast. *J. Biol. Chem.* **288,** 21043–54 (2013).

102. Stewart, E. V *et al.* Yeast SREBP cleavage activation requires the Golgi Dsc E3 ligase complex. *Mol. Cell* **42,** 160–71 (2011).

103. Stewart, E. V *et al.* Yeast sterol regulatory element-binding protein (SREBP) cleavage requires Cdc48 and Dsc5, a ubiquitin regulatory X domain-containing subunit of the Golgi Dsc E3 ligase. *J. Biol. Chem.* **287,** 672–81 (2012).

104. Araki, K. & Nagata, K. Protein folding and quality control in the ER. *Cold Spring Harb. Perspect. Biol.* **3,** a007526 (2011).

105. Gidalevitz, T., Stevens, F. & Argon, Y. Orchestration of secretory protein folding by ER chaperones. *Biochim. Biophys. Acta* **1833,** 2410–24 (2013).

106. Kim, Y. E., Hipp, M. S., Bracher, A., Hayer-Hartl, M. & Ulrich Hartl, F. Molecular Chaperone Functions in Protein Folding and Proteostasis. *Annu. Rev. Biochem.* **82,** 323–355 (2013).

107. Chen, B., Retzlaff, M., Roos, T. & Frydman, J. Cellular strategies of protein quality control. *Cold Spring Harb. Perspect. Biol.* **3,** a004374 (2011).

108. Guerriero, C. J. & Brodsky, J. L. The Delicate Balance Between Secreted Protein Folding and Endoplasmic Reticulum-Associated Degradation in Human Physiology. *Physiol. Rev.* **92,** 537–576 (2012).

109. Li, X. *et al.* Structure of human Niemann–Pick C1 protein. *Proc. Natl. Acad. Sci.* **113,** 8212–8217 (2016).

110. Zhao, Y. *et al.* Structure of glycosylated NPC1 luminal domain C reveals insights into NPC2 and Ebola virus interactions. *FEBS Lett.* **590,** 605–612 (2016).

111. Vembar, S. S. & Brodsky, J. L. One step at a time: endoplasmic reticulum-associated degradation. *Nat. Rev. Mol. Cell Biol.* **9,** 944–57 (2008).

112. Stolz, A., Besser, S., Hottmann, H. & Wolf, D. H. Previously unknown role for the ubiquitin ligase Ubr1 in endoplasmic reticulum-associated protein degradation. *Proc. Natl. Acad. Sci.* **110,** 15271–15276 (2013).

113. Faulkner, R. A., Nguyen, A. D., Jo, Y. & DeBose-Boyd, R. A. Lipid-regulated degradation of HMG-CoA reductase and Insig-1 through distinct mechanisms

in insect cells. *J. Lipid Res.* **54,** 1011–22 (2013).

114. Nguyen, A. D., Lee, S. H. & DeBose-Boyd, R. A. Insig-mediated, sterol-accelerated degradation of the membrane domain of hamster 3-hydroxy-3-methylglutaryl-coenzyme A reductase in insect cells. *J. Biol. Chem.* **284,** 26778–88 (2009).

115. Gill, S., Stevenson, J., Kristiana, I. & Brown, A. J. Cholesterol-Dependent Degradation of Squalene Monooxygenase, a Control Point in Cholesterol Synthesis beyond HMG-CoA Reductase. *Cell Metab.* **13,** 260–273 (2011).

116. Foresti, O., Ruggiano, A., Hannibal-Bach, H. K., Ejsing, C. S. & Carvalho, P. Sterol homeostasis requires regulated degradation of squalene monooxygenase by the ubiquitin ligase Doa10/Teb4. *Elife* **2013,** e00953 (2013).

117. Zelcer, N. *et al.* The E3 Ubiquitin Ligase MARCH6 Degrades Squalene Monooxygenase and Affects 3-Hydroxy-3-Methyl-Glutaryl Coenzyme A Reductase and the Cholesterol Synthesis Pathway. *Mol. Cell. Biol.* **34,** 1262–1270 (2014).

118. Howe, V., Chua, N. K., Stevenson, J. & Brown, A. J. The regulatory domain of squalene monooxygenase contains a re-entrant loop and senses cholesterol via a conformational change. *J. Biol. Chem.* **290,** jbc.M115.675181 (2015).

119. Kelley, R. I. & Hennekam, R. C. The Smith-Lemli-Opitz syndrome. *J. Med. Genet.* **37,** 321–35 (2000).

120. Nowaczyk, M. J. M. & Irons, M. B. Smith-Lemli-Opitz syndrome: Phenotype, natural history, and epidemiology. *Am. J. Med. Genet. Part C Semin. Med. Genet.* **160C,** 250–262 (2012).

121. Fitzky, B. U. *et al.* Mutations in the Delta7-sterol reductase gene in patients with the Smith-Lemli-Opitz syndrome. *Proc. Natl. Acad. Sci. U. S. A.* **95,** 8181–6 (1998).

122. Wassif, C. A. *et al.* Cholesterol storage defect in RSH/Smith–Lemli–Opitz syndrome fibroblasts. *Mol. Genet. Metab.* **75,** 325–334 (2002).

123. Prabhu, A. V., Luu, W., Li, D., Sharpe, L. J. & Brown, A. J. DHCR7: A vital enzyme switch between cholesterol and vitamin D production. *Progress in Lipid Research* **64,** 138–151 (2016).

124. Zhang, J.-H. *et al.* The N-terminal Domain of NPC1L1 Protein Binds Cholesterol and Plays Essential Roles in Cholesterol Uptake. *J. Biol. Chem.* **286,** 25088–25097 (2011).

125. Skov, M., Tonnesen, C. K., Hansen, G. H. & Danielsen, E. M. Dietary cholesterol induces trafficking of intestinal Niemann-Pick Type C1 Like 1 from

the brush border to endosomes. *AJP Gastrointest. Liver Physiol.* **300,** G33–G40 (2011).

126. Infante, R. E. *et al.* NPC2 facilitates bidirectional transfer of cholesterol between NPC1 and lipid bilayers, a step in cholesterol egress from lysosomes. *Proc. Natl. Acad. Sci. U. S. A.* **105,** 15287–92 (2008).

127. Subramanian, K. & Balch, W. E. NPC1/NPC2 function as a tag team duo to mobilize cholesterol. *Proc. Natl. Acad. Sci. U. S. A.* **105,** 15223–4 (2008).

128. Liscum, L. & Sturley, S. L. Intracellular trafficking of Niemann–Pick C proteins 1 and 2: obligate components of subcellular lipid transport. *Biochim. Biophys. Acta - Mol. Cell Biol. Lipids* **1685,** 22–27 (2004).

129. Loftus, S. K. *et al.* Murine model of Niemann-Pick C disease: mutation in a cholesterol homeostasis gene. *Science* **277,** 232–5 (1997).

130. Nakasone, N. *et al.* Endoplasmic Reticulum-associated Degradation of Niemann-Pick C1. *J. Biol. Chem.* **289,** 19714–19725 (2014).

131. Schultz, M. L., Krus, K. L. & Lieberman, A. P. Lysosome and endoplasmic reticulum quality control pathways in Niemann-Pick type C disease. *Brain Res.* **1649,** 181–188 (2016).

132. Mehnert, M., Sommer, T. & Jarosch, E. ERAD ubiquitin ligases. *BioEssays* **32,** 905–913 (2010).

133. Smith, M. H., Ploegh, H. L. & Weissman, J. S. Road to Ruin: Targeting Proteins for Degradation in the Endoplasmic Reticulum. *Science (80-.).* **334,** 1086–1090 (2011).

134. Brodsky, J. L. & Wojcikiewicz, R. J. Substrate-specific mediators of ER associated degradation (ERAD). *Curr. Opin. Cell Biol.* **21,** 516–521 (2009).

135. Rosenbaum, J. C. & Gardner, R. G. How a disordered ubiquitin ligase maintains order in nuclear protein homeostasis. *Nucleus* **2,** 264–270 (2011).

136. Hampton, R. Y. & Garza, R. M. Protein Quality Control as a Strategy for Cellular Regulation: Lessons from Ubiquitin-Mediated Regulation of the Sterol Pathway. *Chem. Rev.* **109,** 1561–1574 (2009).

137. Hiller, M. M., Finger, A., Schweiger, M. & Wolf, D. H. ER degradation of a misfolded luminal protein by the cytosolic ubiquitin-proteasome pathway. *Science* **273,** 1725–8 (1996).

138. Garza, R. M., Tran, P. N. & Hampton, R. Y. Geranylgeranyl pyrophosphate is a potent regulator of HRD-dependent 3-Hydroxy-3-methylglutaryl-CoA reductase degradation in yeast. *J. Biol. Chem.* **284,** 35368–80 (2009).

139. Gardner, R. G., Shan, H., Matsuda, S. P. & Hampton, R. Y. An oxysterol-derived positive signal for 3-hydroxy- 3-methylglutaryl-CoA reductase degradation in yeast. *J. Biol. Chem.* **276,** 8681–94 (2001).

140. Kreft, S. G., Wang, L. & Hochstrasser, M. Membrane topology of the yeast endoplasmic reticulum-localized ubiquitin ligase Doa10 and comparison with its human ortholog TEB4 (MARCH-VI). *J. Biol. Chem.* **281,** 4646–53 (2006).

141. Jiang, Y., Rossi, G. & Ferro-Novick, S. Bet2p and Mad2p are components of a prenyltransferase that adds geranylgeranyl onto Ypt1p and Sec4p. *Nature* **366,** 84–86 (1993).

142. Stirtan, W. G. & Poulter, C. D. Yeast Protein Geranylgeranyltransferase Type-I: Steady-State Kinetics and Substrate Binding †. *Biochemistry* **36,** 4552–4557 (1997).

143. Witter, D. J. & Poulter, C. D. Yeast Geranylgeranyltransferase Type-II: Steady State Kinetic Studies of the Recombinant Enzyme †. *Biochemistry* **35,** 10454–10463 (1996).

144. Gao, Y., Honzatko, R. B. & Peters, R. J. Terpenoid synthase structures: a so far incomplete view of complex catalysis. *Nat. Prod. Rep.* **29,** 1153–75 (2012).

145. Lin, F.-Y. *et al.* Mechanism of action and inhibition of dehydrosqualene synthase. *Proc. Natl. Acad. Sci.* **107,** 21337–21342 (2010).

146. Gardner, R. G. & Hampton, R. Y. A 'distributed degron' allows regulated entry into the ER degradation pathway. *EMBO J.* **18,** 5994–6004 (1999).

147. Ascenzi, P. *et al.* Allosteric modulation of monomeric proteins. *Biochem. Mol. Biol. Educ.* **33,** 169–176 (2005).

148. Gu, X. *et al.* Deconvoluting AMP-activated protein kinase (AMPK) adenine nucleotide binding and sensing. *J. Biol. Chem.* **292,** 12653–12666 (2017).

149. Hardie, D. G. AMP-activated protein kinase: an energy sensor that regulates all aspects of cell function. *Genes Dev.* **25,** 1895–908 (2011).

150. Liu, J. & Nussinov, R. Allostery: An Overview of Its History, Concepts, Methods, and Applications. *PLOS Comput. Biol.* **12,** e1004966 (2016).

151. Nussinov, R. Introduction to Protein Ensembles and Allostery. *Chem. Rev.* **116,** 6263–6266 (2016).

152. Bondeson, D. P. & Crews, C. M. Targeted Protein Degradation by Small Molecules. *Annu. Rev. Pharmacol. Toxicol.* **57,** 107–123 (2017).

153. Mozaffarian, D. *et al.* Heart Disease and Stroke Statistics—2015 Update.

Circulation **131,** e29–e322 (2015).

154. Carroll, M. D., Fryar, C. D. & Kit, B. K. Total and High-density Lipoprotein Cholesterol in Adults: United States, 2011–2014 Key findings Data from the National Health and Nutrition Examination Survey. (2011).

155. Gu, Q., Paulose-Ram, R., Burt, V. L. & Kit, B. K. Prescription Cholesterol-lowering Medication Use in Adults Aged 40 and Over: United States, 2003–2012 Key findings Data from the National Health and Nutrition Examination Survey. (2003).

156. Jo, Y., Lee, P. C. W., Sguigna, P. V. & DeBose-Boyd, R. A. Sterol-induced degradation of HMG CoA reductase depends on interplay of two Insigs and two ubiquitin ligases, gp78 and Trc8. **108,** (2011).

157. Roitelman, J. & Shechter, I. Regulation of rat liver 3-hydroxy-3-methylglutaryl coenzyme A reductase. Evidence for thiol-dependent allosteric modulation of enzyme activity. *J. Biol. Chem.* **259,** 870–7 (1984).

158. Crews, C. M. Targeting the Undruggable Proteome: The Small Molecules of My Dreams. *Chem. Biol.* **17,** 551–555 (2010).

159. Bondeson, D. P. *et al.* Catalytic in vivo protein knockdown by small-molecule PROTACs. *Nat. Chem. Biol.* **11,** 611–617 (2015).

160. Cronin, S. R., Khoury, A., Ferry, D. K. & Hampton, R. Y. Regulation of HMG-CoA reductase degradation requires the P-type ATPase Cod1p/Spf1p. *J. Cell Biol.* **148,** 915–24 (2000).

161. Di Tommaso, P. *et al.* T-Coffee: a web server for the multiple sequence alignment of protein and RNA sequences using structural information and homology extension. *Nucleic Acids Res.* **39,** W13–W17 (2011).

162. Notredame, C., Higgins, D. G. & Heringa, J. T-coffee: a novel method for fast and accurate multiple sequence alignment 1 1Edited by J. Thornton. *J. Mol. Biol.* **302,** 205–217 (2000).

163. Yabe, D., Xia, Z.-P., Adams, C. M. & Rawson, R. B. Three mutations in sterol-sensing domain of SCAP block interaction with insig and render SREBP cleavage insensitive to sterols. *Proc. Natl. Acad. Sci. U. S. A.* **99,** 16672–7 (2002).

164. Zhang, Y., Motamed, M., Seemann, J., Brown, M. S. & Goldstein, J. L. Point Mutation in Luminal Loop 7 of Scap Protein Blocks Interaction with Loop 1 and Abolishes Movement to Golgi. *J. Biol. Chem.* **288,** 14059–14067 (2013).

165. Zhang, Y. *et al.* Direct Demonstration That Loop1 of Scap Binds to Loop7. *J. Biol. Chem.* **291,** 12888–12896 (2016).

166. Wojcikiewicz, R. J. H. Inositol 1,4,5-trisphosphate receptor degradation pathways. *Wiley Interdiscip. Rev. Membr. Transp. Signal.* **1,** 126–135 (2012).

167. Emiola, A., George, J. & Andrews, S. S. A Complete Pathway Model for Lipid A Biosynthesis in Escherichia coli. *PLoS One* **10,** e0121216 (2015).

168. Ogura, T. *et al.* Balanced biosynthesis of major membrane components through regulated degradation of the committed enzyme of lipid A biosynthesis by the AAA protease FtsH (HflB) in Escherichia coli. *Mol. Microbiol.* **31,** 833–44 (1999).

169. Ohgane, K., Karaki, F., Dodo, K. & Hashimoto, Y. Discovery of Oxysterol-Derived Pharmacological Chaperones for NPC1: Implication for the Existence of Second Sterol-Binding Site. *Chem. Biol.* **20,** 391–402 (2013).